Hard probes of the quark-gluon plasma

Simon Caron Huot

Ph.D. candidate

Department of Physics

McGill University

Montréal, Québec

July 2009

A Thesis submitted to McGill University in partial fulfillment of the requirements of the degree of Doctor of Philosophy

DEDICATION

À mes parents, et à Valérie.

ACKNOWLEDGEMENTS

Cette thèse, ainsi que la conspiration de conditions favorables qui y ont mené, n'aurait pu voir le jour sans toute l'affection et le soutien indéfectif au fil des années de mes parents et de ma compagne de vie. Merci. My advisor Guy Moore also played a crucial role in it, which he may or may not recognize. I thank him.

The very idea of doing a Ph. D. would make little sense without the many enlightening discussions that occur during it. My deepest thanks (in arbitrary order) go to Alex Maloney, Charles Gales, Keshav Dasgupta, Sangyong Jeon, Robert Brandenberger, Omid Saremi, Nima Lashkari, Mohammed Mia and everyone else here at McGill, for the several discussions which I had the chance to enjoy with them. Also my deepest thanks to Mikko Laine and Aleksi Vuorinen for very enjoyable discussions at Bielefeld.

ABSTRACT

Relativistic heavy ion collisions aim to study the quark-gluon plasma, a hot and dense state of matter in which quarks and gluons, which are the elementary constituents of nuclei, are set free from the forces that normally confine them. Because of the very short lifetime of the produced plasmas, to study them it is necessary to use probes produced by the collisions themselves. Particles carrying exceptionally large energies, so-called hard probes, are promising candidates to allow a precise reconstruction of the complete history and properties of the evolving plasma. In this thesis, by extending to next-to-leading order at weak coupling the calculation of scattering rates of high-energy jets, we identify an important source of theoretical uncertainties in existing models of their propagation through the medium, and we discuss how this could be improved in the near future. Considering energy loss of heavy quarks, we propose a novel nonperturbative method for quantifying it in the large mass limit, using numerical lattice simulations. Finally, we consider the prospects that hard processes in supersymmetric theories could enjoy a simplified description compared to the non-supersymmetric case, thus making these theories into useful mathematical tools.

ABRÉGÉ

Les collisions ultrarelativistes d'ions lourds visent à étudier le plasma de quarks et gluons, un état extrêment dense et chaud de la matière dans lequel les quarks et les gluons, les constituants élémentaires des noyaux atomiques, sont libérés des forces qui les confinent habituellement. Les plasmas produits ont une durée de vie très brève et doivent être étudiés à l'aide des particules produites lors de la collision elle-même. Les particles exceptionellement énergétiques, ou sondes dures, offrent la possibilité de reconstruire de façon précise l'évolution du plasma. Dans cette thèse, en étendant au second ordre perturbatif le calcul du taux de collision pour un jet de haute énergie, nous identifieront une source importante d'incertitude dans les théories existantes concernant la propagation des jets, et nous discuterons de possibles améliorations à moyen terme. Considérant l'énergie perdue par des quarks lourds, nous proposerons une méthode non-perturbative pour quantifier leur perte d'énergie dans la limite de grande masse, au moyen de simulations numériques en théorie de jauge sur réseau. Finallement, nous considérerons la possibilité que les processus durs à température finie dans les théories supersymétriques bénéficient d'une description simplifiée, par rapport au cas non supersymétrique, ce qui leur conférerait un intérêt mathématique accru.

CONTRIBUTIONS OF AUTHORS

Material contained in chapter 2 is original to this thesis. Chapter 3 contains a rewritten and expanded version of the material covered in section III of the publication [132], which is a single-authored publication by the present author. Chapter 4 contains a duplication of the remainder of the article [132].

Chapter 5 contains a duplication of the paper [133] which was written in collaboration with G. D. Moore and M. Laine. The present author significantly contributed to the main ideas of the paper, which are presented in section 5.2, including the definition (5.9) of the momentum diffusion coefficient, its Euclidean version (5.32) involving insertions of electric fields along the Polyakov loop, and the formal proof of the non-renormalization of the correlator (5.18) in question. He also significantly contributed to the writing of that section, especially of subsection 5.2.1. Sections 5.3 and 5.4 were largely constructed by the other collaborators.

Chapter 6 contains a duplication of the single-authored paper [134], which was written by the present author.

The introduction and conclusion to the thesis never appeared before.

TABLE OF CONTENTS

LIST OF TABLES

LIST OF FIGURES

CHAPTER 1
Introduction

1.1 Brief historical review

The physical world, in our present understanding, involves four, more or less independent, known forces through which its known constituents interact: the gravitational force, the electromagnetic force, the weak nuclear force and the strong nuclear force. Remarkably, the electromagnetic and weak nuclear forces are known to unify at very high energies, or short distances of order 10^{-16} cm, where they become entangled aspects of the "electroweak" interaction, but the other forces do not unify under any known regime and are naturally studied in isolation.

The modern understanding of the strong nuclear force was assembled throughout the twentieth century. A major and fundamental step was undoubtedly the very discovery by Rutherford and collaborators in 1911 of nuclei lying at the center of every atom. The discovery by Chadwick in 1932 of the neutron as a partner to the proton brought another fundamental step. In 1935, Yukawa theorized the existence of a new set of light particles which would mediate the strong force between nucleons (the protons and neutrons), thereby accounting for their binding together into nuclei. Remarkably, these particles were discovered experimentally in the late 1940's; we now refer to them as pions. This was shortly after the immense power of the strong force had irreversibly and permanently forced its way into History. Yet, a full understanding of this force remained elusive, as the discovery of a complete and unexpected spectrum of strongly interacting particles proceeded during the 1950's and 1960's. The constituent quark model, proposed independently by Gell-Mann and Zweig in 1964, could organize this complex spectroscopy in terms of the bound states of elementary constituent quarks, but it was plagued by a fundamental puzzle: the elementary quarks in question had never (and still have not) been observed in isolation. This was the so-called *confinement* problem.

A fully fledged theory of the dynamics of the quarks and of their interactions eventually emerged in 1973 after much work, under the name of Quantum Chromodynamics (QCD). QCD possesses the key property of *asymptotic freedom*, which was discovered in theoretical work by Gross, Politzer and Wilzcek [1, 2] (who shared the Nobel Prize for this discovery in 2004), and which reconciles apparently contradictory facets of the strong interactions. For one thing, and as was suggested by the high-energy experiments which took place at Geneva's CERN and at Stanford SLAC's during the sixties, at high energies the constituents of hadrons behave much like free, non-interacting particles: the quarks and the gluons. On the other hand, confinement requires interactions to become very strong as quarks are taken to large separations, so as to forbid their separation. Asymptotic freedom is that property of the effective interaction strength of a theory – which in quantum field theory, as in generic multi-scale systems, generally depends on the scale of interest – to become weaker and weaker at shorter distances. At short distances the "strong" force is intrinsically *weak*, and its strength builds up as larger and larger distance scales are allowed to cooperate, until it eventually becomes very strong and confinement dynamics sets in (at distances of order $\Lambda_{\rm QCD}^{-1} \sim (400\,{\rm GeV})^{-1}$)[1] .

The known hadrons find their places in QCD as the bound states of quarks and gluons, each of which carry an elementary SU(3) "color" charge; confinement means that they always bind into overall color-neutral objects. The pions, which Yukawa originally proposed to be the mediators of the strong force, are the mediators of only a (still strong) residual interaction between such color-neutral objects. There is nowadays overwhelming evidence for QCD accurately describing the strong force, and the confinement problem has evolved into an enduring *mathematical* problem, of proving rigorously that, and understanding how, confinement is actually realized within the theory of QCD.

Asymptotic freedom means, as was soon realized by Collins and Perry in 1976 [3], that if quarks and gluons could be packed sufficiently densely in a region of space (as is believed to have happened in the early history of the Universe, and which could occur in the core of certain neutron stars), the interaction between them would have no room to grow strong and confinement would be lost. As a function of density QCD thus experiences a *deconfinement* phase transition over which the relevant degrees of freedom turn from color-neutral bound states to streaming quarks and gluons. At asymptotically high temperatures (and thus densities), the interaction strength will be weak and due to formal similarities between weakly coupled QCD and electromagnetism this state of matter is expected to behave much like a plasma.

[1] We work in units in which $\hbar = c = 1$.

Hot and deconfined QCD matter is thus referred to as a quark-gluon plasma (QGP) [4].

An experimental program was launched in the 1980s with the aim of producing and studying this state of matter through the collisions of relativistic heavy ions. This was pursued at several locations, which included Berkeley's Bevalac, Brookhaven's Alternating Gradient Synchrotron (AGS), CERN's Super Proton Synchrotron (SPS), and Brookhaven's Relativistic Heavy Ion Collider (RHIC), which was commissioned in year 2000. For the first time at RHIC, evidence has begun to accumulate, in gold-gold collisions with center-of-mass energy of 200 GeV per nucleon, showing that a new state of matter is being produced [5, 6, 7, 8]. The commissioning of the heavy ion program at CERN's Large Hadron Collider (LHC) near Geneva, in the near future, will provide access to even higher energies and temperatures.

1.2 Relativistic heavy ion collisions

The unfolding of a heavy ion collision goes as in the following [9]. Two nuclei collide head on with each other and a dense region is created in the intersecting region. The produced matter interacts with itself, and the inertia of the outer crusts acts like a wall exerting a pressure onto the inner crusts, thereby slowing down their expansion; this is why large nuclei are used. The very large pressure of the matter drives its expansion until it eventually cools down to temperatures below the deconfinement transition. At that point the quark-gluon plasma is converted to a gas of hadrons, which ultimately stream to the experimental detectors where their properties are measured. The lifetime of the dense matter (as measured in its local rest frame) is relatively modest, estimated (from hydrodynamics model) to be of

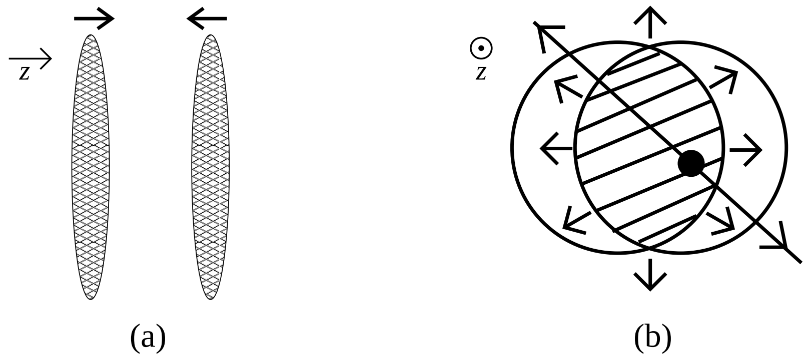

Figure 1–1: Cartoon of a heavy ion collision: (a) two Lorentz-contracted nuclei ("pancakes") collide forming (b) a dense, expanding matter in the intersecting region. Some hard particles, represented by longer arrows, are produced in the initial collision and have a finite probability of escaping the plasma.

order $5 \div 10$ fm/c ($\sim 2 \div 3 \times 10^{-23}$ s), depending on the impact parameter of the colliding nuclei. Heavy ion collisions are thus sometimes referred to as "little bangs". A cartoon of a heavy ion collision is depicted in Fig. 1–1.

A most remarkable finding at RHIC was the success of ideal hydrodynamics to describe global observables (overall momentum distributions) [5, 6, 7, 8]. This is indicative that local thermal equilibrium is achieved, with very short mean free paths compared to the lifetime of the medium. In fact the viscous corrections to ideal hydrodynamics are very well constrained [10], suggesting even that the quark-gluon plasma created at RHIC behaves very nearly like a perfect, viscosity-free, liquid.

To study any state of matter one needs some kind of probe. The accessible quark-gluon plasmas are too small and too short-lived for any external probe to be used, and *internally produced* probes must be used. The vast majority of the thousands of particles which come out of a collision are soft particles, which carry momenta $p_{\mathrm{T}} \lesssim 1$ GeV in the directions perpendicular to the beam axis. Since the medium is optically thick to them, these particles only retain information about the latest stages of the fireball evolution, at which local kinetic and chemical equilibrium are lost (kinetic and chemical *freezeout*). It is from these particles that the low viscosity is inferred.

To constrain better the history of the fireball, in particular the early, thermalization, stages, probes having less interactions are required. Good candidates are photons, which interact only electromagnetically, as well as high-energy partons (*jets*) or heavy quarks (charm and bottom). These are known collectively as *hard probes*.

This thesis will be devoted to studying and developing the theory of the latter two types of hard probes, high-energy jets and heavy quarks, in interaction with a locally thermalized quark-gluon plasma.

1.3 Organization of the thesis

The organization of this thesis is the following. In chapter 2 we begin with a review of the general formalism relevant for studying thermalized quantum field theories, with special emphasis on the quark-gluon plasma at weak coupling. In chapter 3 we introduce a novel mathematical technique for dealing with correlation functions along lightlike trajectories, which is based on ideas of Euclidean field theory. This will be applied in chapter 4 to the calculation, for the first time, of the next-to-leading order corrections to the elastic collision rate felt by a ultrarelativistic particle. This elastic rate will be related to that of bremsstrahlung energy loss.

In chapter 5 we review the description of heavy quark dynamics, at small velocities, in terms of a Langevin model. We will establish rigorously for the first time how to extract the relevant transport coefficient, the momentum diffusion coefficient, from nonperturbative lattice simulations of QCD from which the heavy quarks have been integrated out. In chapter 6 we investigate the factorization of hard processes at nonzero temperature in terms of a perturbatively calculable hard part, times a soft, temperature-dependent, part. More specifically, we will investigate the question of whether supersymmetry, if present in the zero-temperature theory, will be preserved in the hard sector.

CHAPTER 2
Finite temperature field theory

In finite temperature (quantum) field theory one has to study expectation values of operators in thermal ensembles,

$$\begin{aligned}\langle \mathcal{O}_1(x_1)\cdots\mathcal{O}_n(x_n)\rangle_\beta &\equiv \frac{1}{Z}\mathrm{Tr}\left[e^{-\beta H}\mathcal{O}_1(x_1)\cdots\mathcal{O}_n(x_n)\right] \\ &\equiv \frac{1}{Z}\sum_n e^{-\beta E_n}\langle n|\mathcal{O}_1(x_1)\cdots\mathcal{O}_n(x_n)|n\rangle, \end{aligned} \tag{2.1}$$

where $\beta = 1/T$ is the inverse temperature of the ensemble and $Z = \mathrm{Tr}\, e^{-\beta H}$ is its partition function; the states $|n\rangle$ span a basis of energy eigenstates of the theory. Throughout this thesis we set chemical potentials to zero, since the quark-gluon plasma created at RHIC can be considered, in a first approximation, to be charge-neutral. In this technical chapter, we review the general formalism relevant for studying Eq. (2.1).

We assume basic knowledge of quantum field theory and of QCD at zero temperature at the level of [11, 12]. Unless expressly stated otherwise, we ignore the massive quarks and study QCD with $N_\mathrm{f} = 3$ flavors of massless quarks. The QCD action is[1]

$$S = -\int d^4x \left[\frac{G^a_{\mu\nu}G^{\mu\nu\,a}}{4g_\mathrm{s}^2} + \sum_{i=1}^{N_\mathrm{f}} \bar\psi_i(\gamma^\mu D_\mu)\psi_i\right], \tag{2.2}$$

[1] We use $(-,+,+,+)$ metric signature.

where

$$G^a_{\mu\nu} = \partial_\mu A^a_\nu - \partial_\nu A^a_\mu + f^{abc} A^b_\mu A^c_\nu \tag{2.3}$$

is the field-strength tensor of the gauge field A^a_μ, which takes value in the adjoint representation of the SU(3) gauge group. The ψ_i are N_f Dirac fermions in the fundamental representation of SU(3) with

$$D_\mu \psi_i = (\partial_\mu - i A^a_\mu t^a)\psi_i, \tag{2.4}$$

the SU(3) generators t^a being normalized to $\mathrm{Tr}\, t^a t^b = \frac{1}{2}\delta^{ab}$. Real QCD has N_c=3 colors, but it is useful to consider also the slight generalization in which the gauge group is replaced with SU(N_c).

Textbook presentations of thermal field theory can be found in [13, 14], the first of these references also introducing the quark-gluon plasma. Review articles dealing specifically with the dynamics of the weakly coupled quark-gluon plasma are [15, 16].

2.1 Real-time formalism

The operators entering Eq. (2.1) are in the Heisenberg representation,

$$\mathcal{O}_i(t_i, \vec{x}_i) \equiv e^{iHt_i}\mathcal{O}_i(t{=}0, \vec{x}_i)e^{-iHt_i}, \tag{2.5}$$

so inspection of Eq. (2.1) reveals that any correlator of unequal-time operators will contain at least one forward and one backward time evolution operator. This is the key difference with conventional vacuum time-ordered amplitudes, for which only forward time evolution is needed (since then the final state vacuum resides at $t = +\infty$): here one has to go back to the initial time.

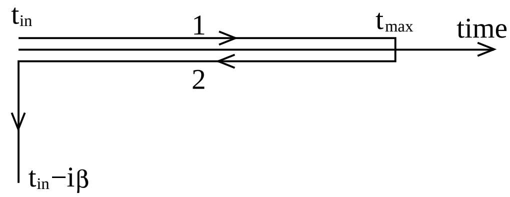

Figure 2–1: Schwinger-Keldysh contour, with $t_{\text{in}} \to -\infty$ and $t_{\text{max}} \to \infty$ in the end.

In a path-integral formulation, the forward time evolution operator e^{-iHt} is represented by a path-integral of $e^{i\int dtL}$, L the Lagrangian, over paths (field configurations) spanning the time interval t. Its inverse e^{iHt} is similarly represented by a path-integral of $e^{i\int dtL}$ over the same fields, with the sign of dt reversed as if the paths were moving backward in time. The density matrix $e^{-\beta H}$ is represented by a path integral going an amount $-i\beta$ in the imaginary time direction. Thus the minimal contour $\mathcal{C}$ needed to compute Eq. (2.1), depicted in Fig. 2–1, contains two horizontal components and one vertical component. $\mathcal{C}$ is called the *Schwinger-Keldysh contour* [17]. Bosonic fields are periodically identified at the endpoints of the contour, and fermionic fields are anti-periodically identified.

The fields on the different branches on the contour are just integration variables in a path integral, but being distinct they need distinct labels to avoid confusion. Thus we formally distinguish operators inserted on the two horizontal branches using the superscripts 1 and 2, respectively, as in $\mathcal{O}^1$ and $\mathcal{O}^2$.

The path integral over the contour $\mathcal{C}$ generates $\mathcal{C}$-ordered correlation functions, meaning time-ordered for the 1- fields and anti-time-ordered for the 2- fields:

$$\begin{aligned}\langle \mathcal{O}_1^1 \cdots \mathcal{O}_m^1 \mathcal{O}_{m+1}^2 \cdots \mathcal{O}_n^2 \rangle_{\mathcal{C}} &\equiv \frac{1}{Z} \int [\mathcal{D}\phi(x \in \mathcal{C})]\, e^{i \int_{\mathcal{C}} dt L} \\ &\quad \times \left[\mathcal{O}_1^1 \cdots \mathcal{O}_m^1 \mathcal{O}_{m+1}^2 \cdots \mathcal{O}_n^2 \right] \\ &= \langle \left[\overline{\mathcal{T}} \mathcal{O}_{m+1} \cdots \mathcal{O}_n \right] \left[\mathcal{T} \mathcal{O}_1 \cdots \mathcal{O}_m \right] \rangle_\beta, \end{aligned} \tag{2.6}$$

with the space-time arguments suppressed for clarity; $\mathcal{T}$ ($\overline{\mathcal{T}}$) is the (anti-) time-ordering symbol.

In perturbation theory vertices are generated in every part of the contour and propagators connecting different branches are needed; the vertical part of the contour can be moved to time $t_{\rm in} = -\infty$ and ignored for any practical purpose [18] (except for computing the partition function), in which case one is left with a propagator which is a 2×2 matrix involving the 1- and 2- fields (see also, [19]).

Cyclic invariance of the trace applied to Eq. (2.1) leads to identities, known as Kubo-Martin-Schwinger (KMS) or fluctuation-dissipation relations [13, 14], which hold in thermal equilibrium. They relate amplitudes with different operator orderings, and in particular they relate all two-point amplitudes to the retarded one

$$\begin{pmatrix} G_{ij}^{11}(p) & G_{ij}^{12}(p) \\ G_{ij}^{21}(p) & G_{ij}^{22}(p) \end{pmatrix} = \begin{pmatrix} G_{ij}^{\rm R}(p) \pm n(p)\rho_{ij}(p) & \pm n(p)\rho_{ij}(p) \\ (1 \pm n(p))\rho_{ij}(p) & -G_{ij}^{\rm R}(p) + (1 \pm n(p))\rho_{ij}(p) \end{pmatrix} \tag{2.7}$$

where

$$\rho_{ij}(p) \equiv G_{ij}^{12}(p) - G_{ij}^{21}(p) = G_{ij}^{\rm R}(p) - G_{ij}^{\rm A}(p) \tag{2.8}$$

is the spectral density, and the different signs refer to bosons and fermions, in which case $n(p) \equiv 1/(e^{\beta p^0} \mp 1)$ stands, respectively, for the Bose-Einstein distribution $n_{\rm B}$ or the Fermi-Dirac distribution $n_{\rm F}$. The retarded two-point function is defined as

$$\begin{aligned} G^{\rm R}_{ij}(x-y) &\equiv \langle [\mathcal{O}_i(x), \mathcal{O}_j(y)] \rangle_\beta \theta(x^0-y^0) \\ &= G^{11}_{ij}(x-y) - G^{12}_{ij}(x-y) \\ &= G^{21}_{ij}(x-y) - G^{22}_{ij}(x-y), \end{aligned} \tag{2.9}$$

where θ is the step function. The advanced function is defined as $G^{\rm A}_{ij}(x-y) \equiv G^{\rm R}_{ji}(y-x)$. For the autocorrelator of bosonic operators, we record that $G^{\rm A}_{ii}(p) = -G^{{\rm R}*}_{ii}(p)$ and $\rho_{ii}(p) = 2{\rm Re}\, G^{\rm R}_{ii}(p)$, in momentum space.

It is useful to bring retarded amplitudes to the forefront of one's formulation. Heuristically, since the Schwinger-Keldysh formalism makes causality manifest by requiring only initial data to be specified, working with explicitly causal quantities at intermediate steps can rightfully be expected to lead to simplification. In agreement with this logic, the retarded propagators are those which take the simplest form at nonzero temperature; for instance, for a free scalar field at any temperature,

$$G^{\rm R}_{(0)}(p) = \frac{i}{(p^0+i\epsilon)^2 - \vec{p}^2}, \quad \rho_{(0)}(p) = 2\pi\delta(p_0^2 - \vec{p}^2)\,{\rm sgn}(p^0), \tag{2.10}$$

which differs from the vacuum time-ordered propagator only through the $i\epsilon$ prescription (the same being true of any free-field propagator in general). This should be contrasted with the more complicated expression for the time-ordered propagator, G^{11}, given in (2.7). Furthermore, retarded amplitudes possess natural and immediate physical interpretations in terms of response theory, to be given in the next section, whereas the physical significance of time-ordered functions, familiar at $T = 0$, becomes far less immediate at $T \neq 0$. For all these reasons, the so-called *Keldysh basis* is particularly useful. It is defined by the field relabelling

$$\phi^r = \frac{1}{2}(\phi^1 + \phi^2), \quad \phi^a = \phi^1 - \phi^2 \tag{2.11}$$

in which the equilibrium propagator becomes the 2 by 2 matrix

$$\begin{pmatrix} G^{rr}(p) & G^{ra}(p) \\ G^{ar}(p) & G^{aa}(p) \end{pmatrix} = \begin{pmatrix} (\frac{1}{2} \pm n(p))\rho(p) & G^{\mathrm{R}}(p) \\ G^{\mathrm{A}}(p) & 0 \end{pmatrix}. \tag{2.12}$$

A review of this formulation, in which the transformed interaction vertices can also be found, is given in [20]; a brief overview is in [21]. In this thesis our use of this particular formalism will be limited to the tree-level in perturbation theory.

2.2 Euclidean formalism and retarded amplitudes

In zero-temperature quantum field theory, much information is contained in the Euclidean amplitudes. In fact, they are known to encode the full content of the Lorentzian theory [22]. A similar situation holds at non-zero temperature. In the Euclidean description of a thermal system, the Euclidean time becomes periodic with period β, just like the vertical component of the contour $\mathcal{C}$. The Euclidean frequencies are correspondingly quantized,

$$\omega_n = 2\pi n T, \quad \text{bosons}, \quad \omega_n = 2\pi(n+\frac{1}{2})T, \quad \text{fermions}, \tag{2.13}$$

and frequency integrals in perturbation theory turn into frequency sums:

$$\int \frac{d^4p}{(2\pi)^4} \to T \sum_{\omega_n} \int \frac{d^3p}{(2\pi)^3}. \tag{2.14}$$

These are the only formal changes to the Euclidean theory, compared to the situation at $T = 0$. The frequencies (2.13) are known as the *Matsubara frequencies*.

Any real-time correlator for which the time evolution in Eq. (2.5) is superfluous can be calculated equivalently in Euclidean or Lorentzian signature; examples include equal-time correlators. But to obtain a general correlator, analytic continuation must be used. There is a distinguished analytic continuation of the Euclidean amplitudes, in which all frequency arguments ω_i are taken from the discrete set of Matsubara frequencies to the full complex frequency plane, which is singled out by having only a branch cut singularity on the real (Lorentzian) axis in each ω_i and at most polynomial growth at large $|\omega_i|$ [23]. This coincides with the real-time retarded amplitudes [24, 25]. These are the real-time n-point amplitudes involving one Keldysh r- field and $(n-1)$ Keldysh a- fields; the terminology "retarded" is used because these vanish unless the r- field carries the largest time argument. More precisely, in this analytic continuation the branch cuts along the real frequency axis should be approached from above for each a-field. The ensuing analyticity of the amplitudes in the upper-half plane implies the "retarded" causality structure.

Consider for instance a two-point amplitude. At the Euclidean Matsubara frequencies this may be written as (throughout this section, for clarity, we make explicit only the frequency dependence):

$$\begin{aligned}
G^{\mathrm{E}}_{ij}(\omega^{\mathrm{E}}_n) &\equiv \frac{1}{Z}\int_0^\beta d\tau\, e^{i\omega^{\mathrm{E}}_n\tau}\mathrm{Tr}\,\left[e^{-\beta H}\mathcal{O}_i(\tau)\mathcal{O}_j(0)\right] \\
&= \frac{1}{Z}\sum_{m,n}\langle n|\mathcal{O}_i|m\rangle\langle m|\mathcal{O}_j|n\rangle\int_0^\beta d\tau\, e^{i\omega^{\mathrm{E}}_n\tau-\tau E_m-(\beta-\tau)E_n} \\
&= \frac{1}{Z}\sum_{m,n}\langle m|\mathcal{O}_i|n\rangle\langle n|\mathcal{O}_j|m\rangle\frac{e^{-\beta E_m}-e^{-\beta E_n}}{E_n-E_m+i\omega^{\mathrm{E}}_n},
\end{aligned} \tag{2.15}$$

where the sums run over complete sets of energy eigenstates. The "distinguished analytic continuation" of G^{E} is simply Eq. (2.15) with $i\omega^{\mathrm{E}}_n$ replaced with ω, where ω is real in Lorentzian signature. On the other hand, from its the definition (2.9), the retarded two-point amplitude evaluates to

$$G^{\mathrm{R}}_{ij}(\omega) = G^{ra}_{ij}(\omega) = i\frac{1}{Z}\sum_{m,n}\langle n|\mathcal{O}_i|m\rangle\langle m|\mathcal{O}_j|n\rangle\frac{e^{-\beta E_n}-e^{-\beta E_m}}{E_n-E_m+\omega+i\epsilon}. \tag{2.16}$$

Comparing, we find:

$$G^{\mathrm{R}}_{ij}(\omega) = -iG^{\mathrm{E}}_{ij}(i\omega^{\mathrm{E}}_n \Rightarrow \omega+i\epsilon). \tag{2.17}$$

This is the claimed nonperturbative identity between the retarded and Euclidean two-point amplitudes. Higher-point amplitudes are discussed in [24, 25].

Following [20] we now give the physical interpretation of retarded amplitudes, two-point and higher-point, in terms of (non)linear response theory. Consider adding a small perturbation $\delta_f H(t') = \sum_i f^i(t')\mathcal{O}_i(t')$ to the Hamiltonian of a system, taken initially to be in a thermal configuration at $t = -\infty$. This amounts to adding a perturbation $\delta_f L^1(t') = -\delta_f L^2(t') = -\delta_f H(t')$ to the Lagrangian along the contour $\mathcal{C}$, and thus amounts to the insertion of Keldysh a operators. The expectation value of the operator $\mathcal{O}_i(t)$ is equal to that of $\mathcal{O}^1_i(t)$ or of $\mathcal{O}^2_i(t)$, or of their averages, all being equal within unitary evolution[2] ,

$$\langle \mathcal{O}_i^1(t)\rangle_f = \langle \mathcal{O}_i^2(t)\rangle_f = \langle \mathcal{O}_i^r(t)\rangle_f. \tag{2.18}$$

Thus, expanding Eq. (2.6) in powers of f, we obtain the response to the perturbation:

$$\begin{aligned}\langle \mathcal{O}_i(t)\rangle_f &= \langle \mathcal{O}_i^r\rangle_\beta - i\int_{-\infty}^{t} dt' \sum_j G_{ij}^{ra}(t,t')f^j(t') \\ &\quad -\frac{1}{2}\int_{-\infty}^{t} dt'dt'' \sum_{jk} G_{ijk}^{raa}(t,t',t'')f^j(t')f^k(t'') \\ &\quad +\ldots,\end{aligned} \tag{2.19}$$

the first term being the unperturbed expectation value and the suppressed terms being proportional to f^3. The time integrations are restricted to $t', t'' < t$ since the integrands vanish outside of this region. Equation (2.19) contains the physical interpretation of the retarded amplitudes; in particular, retarded two-point amplitudes give the linear response to small perturbations.

2.3 Hard thermal loops

In a plasma, the naturally long-ranged gauge interactions get cut off at large distances by screening effects. Several physical quantities depend strongly on screening and would in fact receive (unphysical) infrared divergences were this not accounted for. These include, for instance, generic transport coefficients since without screening the transport scattering rates, e.g. scattering rates weighted by the square of the

[2] Note that for composite operators, $\mathcal{O}^r \equiv \frac{1}{2}(\mathcal{O}_1 + \mathcal{O}_2)$ is not in general a product of only r-fields.

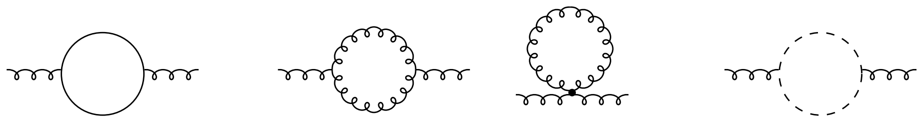

Figure 2–2: Self-energy diagrams, including fermions, gauge bosons and ghosts, which are resummed by the HTL theory.

deflection angle, would diverge logarithmically like $\int d^2\theta\theta^2/\theta^4$ at small θ. This is discussed for nonrelativistic plasmas in [26, 27], the relativistic case being qualitatively similar [15]. Thus it is crucial to properly describe screening.

A somewhat naive account of screening in the quark-gluon plasma could proceed by analogy with the simplest nonrelativistic plasmas, for which, in the Coulomb gauge ($\vec{\nabla}\cdot\vec{A} = 0$), screening takes the form of a constant mass term included in the electrostatic potential propagator [26, 27]:

$$G^{\mathrm{R}}_{00}\big|_{\text{non-relativistic}}(\omega, \vec{p}) = \frac{i}{\vec{p}^2 + m_{\mathrm{D}}^2}. \tag{2.20}$$

This interaction decays like $e^{-m_{\mathrm{D}}r}$ at large distances. Equation (2.20), however, is unsatisfactory in many respects for use in the quark-gluon plasma. First, since this plasma is relativistic, a static description only applies in a restricted region of phase-space where $\omega \ll |\vec{p}|$, in general one must account for the velocities of the constituents. Second, one would like a gauge-invariant formulation that does not rely on making the choice of the Coulomb gauge, which is more natural for non-relativistic systems.

The Hard Thermal Loop (HTL) resummation scheme developed by Braaten and Pisarski [28] fulfills both of these requirements (see also, Frenkel and Taylor's work [29]). Its name comes from the fact that it accounts for the effects of "hard" thermal particles, having momenta $p \sim T$, on "soft" modes with $p, \omega \sim g_{\rm s} T \ll T$. The soft scale $g_{\rm s} T \sim m_{\rm D}$ is where the screening effects become important. The HTL theory describes screening effects to the leading order at small $g_{\rm s}$ and it resums, into the gluon propagators, (approximations of) the one-loop self-energies drawn in Fig. 2–2. The screening effects are important whenever all external momenta of some subdiagram are of order $g_{\rm s} T$ or less, and for these cases one must also use HTL-resummed vertices, in addition to the resummed propagators; all HTL corrections become subdominant as soon as one component of a momentum leaves the soft scale, however, in which case they should not be included (the HTL description then becoming inaccurate).

The full HTL effective theory can be deduced from a manifestly gauge-invariant effective action [30, 31] (it is written down within the real-time formalism in [21]). Here we give only the corresponding propagators, known as *HTL-resummed propagators*, in the Coulomb gauge:

$$G^{\rm R}_{00}(\omega, \vec{p}) = \frac{i}{\vec{p}^2 + \Pi^{00}(\eta)}, \qquad G^{\rm R}_{ij}(\omega, \vec{p}) = \frac{-i\left(\delta^{ij} - \frac{p^i p^j}{\vec{p}^2}\right)}{\omega^2 - \vec{p}^2 - \Pi_T(\eta)}, \tag{2.21}$$

with $G^{\rm R}_{0i} = 0$ and where we have introduced $\eta = \omega/|\vec{p}|$. Screening comes about through the HTL self-energies:

$$\Pi^{00}(\eta) = m_{\rm D}^2 \left[1 - \frac{\eta}{2} \ln\left(\frac{\eta + 1 + i\epsilon}{\eta - 1 + i\epsilon}\right)\right], \tag{2.22a}$$

$$\Pi_T(\eta) = m_{\rm D}^2 \left[\frac{\eta^2}{2} + \frac{\eta(1-\eta^2)}{4} \ln\left(\frac{\eta + 1 + i\epsilon}{\eta - 1 + i\epsilon}\right)\right]. \tag{2.22b}$$

There exists also HTL self-energies for soft fermions, which we will not require.

Equations (2.21) and (2.22) provide a complete description of screening in the quark-gluon plasma at the leading order in g_s. The Debye mass is given as

$$m_\mathrm{D}^2 = \frac{g_\mathrm{s}^2 T^2}{3}\left[N_\mathrm{c} + N_\mathrm{f} T_\mathrm{f}\right]. \tag{2.23}$$

In QCD with N_c=3 and N_f quark flavors, $m_\mathrm{D}^2 = g_\mathrm{s}^2 T^2 (1 + \frac{1}{6} N_\mathrm{f})$. The poles of the HTL propagators (2.21) give the dispersion relations of quasiparticles, which at soft momenta have the interpretation of collective excitations of the plasma particles and soft gauge fields. In the longitudinal channel, the residue of the pole vanishes exponentially at $k \gg m_\mathrm{D}$.

The HTL effective propagators and vertices generate a loop expansion at the soft scale $g_\mathrm{s}T$ which proceeds in *single* powers of g_s [28]. The unusual power of g_s, compared to the familiar g_s^2, is due to the large Bose-Einstein population functions $n_\mathrm{B}(\omega) \sim 1/g_\mathrm{s}$ arising at the soft scale. In this sense, loops at the soft scale describe *classical* plasma physics effects [32, 16, 21].

2.4 Euclidean version of HTL theory

For computations in Euclidean signature, when no analytic continuation is required and only correlation functions at the Matsubara frequencies are demanded, HTL resummation can be simplified greatly. (When analytic continuation is needed, the fully-fledged HTL theory must be used.)

Fields carrying zero and non-zero Matsubara frequencies must be distinguished; HTL resummation is only needed for the former (and it would be, in any case, inaccurate for the latter). At the zero Matsubara frequency the HTL propagators

(2.21) simplify to

$$G_{44}^{\mathrm{E}}(\omega_n=0,\vec{p}) \to \frac{1}{\vec{p}^2+m_{\mathrm{D}}^2}, \quad G_{ij}^{\mathrm{E}}(\omega_n=0,\vec{p}) \to \frac{\delta^{ij}-\xi\frac{p^ip^j}{\vec{p}^2}}{\vec{p}^2} \tag{2.24}$$

where ξ is the ξ-gauge parameter of a three-dimensional gauge theory (which coincides with the four-dimensional ξ-parameter in the zero-frequency limit of the standard covariant gauges. The strict Coulomb gauge considered above corresponds to the value $\xi=1$ in Eq. (2.24).) Here A_4 is the gauge field component along the Euclidean temporal direction, e.g. the Wick rotation[3] of A_0. The interaction vertices do not require any resummation, contrary to the case in the real-time HTL theory, because the HTL vertices identically vanish at zero frequency [28].

A very efficient bookkeeping device to deal with the splitting between zero and nonzero Matsubara modes is provided by *dimensional reduction* [33, 34]. In this formalism, based on effective field theory ideas, the modes with nonzero Matsubara frequencies are first completely "integrated out" leaving a three-dimensional effective theory to describe the zero modes. This effective theory, called *electric QCD* or EQCD, is three-dimensional Yang-Mills theory with coupling g_{s}^2T coupled to a massive scalar field A_4, in the adjoint representation, whose mass is m_{D}^2. At the leading order its propagators are those shown in Eq. (2.24) and the scalar field has no self-interactions.

The three-dimensional loop expansion proceeds in powers of g_{s} (through the dimensionless ratio $g_{\mathrm{s}}^2T/m_{\mathrm{D}}$), just like the real-time HTL theory does at the soft

[3] In correlation functions depending explicitly on A_0, one should use $A_0 = iA_4$.

scale. Gradient and loop corrections from the hard scale, accounted for during the dimensional reduction process, generate higher-dimensional local operators in the EQCD Lagrangian plus $\mathcal{O}(g_s^2)$-suppressed corrections to the parameters present at leading order, but all of these effects in correlation functions are suppressed by at least $\mathcal{O}(g_s^2)$, or two loops, compared to leading-order results. These effects are beyond the accuracy which will be considered in this thesis and so they will not be described here [35].

2.5 Limitations of perturbation theory

Finite temperature perturbation theory has a fundamentally different structure than the zero-temperature case, because it involves the hierarchy of scales $g_s^2 T \ll m_D \ll T$; expansions in g_s necessarily contain both effects so "quantum" loop corrections are difficult to separate from corrections due to ratios of scales. More fundamentally, there is a limiting accuracy to which *ab initio* perturbative calculations can be pushed, due to nonperturbative dynamics driving the infrared scale $g_s^2 T$ [36] (as can be guessed from the Yang-Mills coupling $g_s^2 T$ of EQCD – the dimensionally-reduced theory "confines" at this scale). The order in g_s at which this physics becomes important depends on the particular observable of interest. For the thermodynamic pressure, perturbation theory is limited to $g_s^6 T^4 \log \frac{1}{g_s}$ accuracy [36] (though progress to include nonperturbative $g_s^6 T^4$ effects through lattice simulations of EQCD is under way [37]), but for other quantities this may come earlier.

Independently of this limitation, one may ask how well do g_s-expansions converge[4] . At zero temperature, perturbative expansions are typically expected to be reliable, once large logarithms are properly accounted for via renormalization group methods, provided α_s/π is small (though of course each application must be considered individually). At high temperatures, however, as established by a large body of work on the thermodynamic pressure [38, 39, 40], strict expansions in g_s are typically not reliable unless $\alpha_s \lesssim 0.1$.

Large (non)perturbative corrections to real-time observables currently mark a frontier in the analytic understanding of the quark-gluon plasma. Studying and dealing with these corrections will be a central theme to this thesis.

[4] Such expansions are always only asymptotic and do not converge like Taylor series. By "convergence" we refer to the rate at which the first few terms decrease at sufficiently small coupling.

CHAPTER 3
A technique for evaluating space-like and light-like correlators

The hard thermal loop effective theory discussed in section 2.3 simplifies dramatically when its Euclidean version, dimensional reduction, is applicable. Heuristically, the difference between Euclidean and Minkowskian physics is that between statics (or thermodynamics) and dynamics. Examples of Euclidean quantities are equal-time correlation functions, which admit representations as sums over Euclidean Matsubara frequencies [13]:

$$\begin{aligned} G_{ij}(t{=}0,\vec{x}) &\equiv \frac{1}{Z}\mathrm{Tr}\left[e^{-\beta H}\mathcal{O}_i(\vec{x})\mathcal{O}_j(0)\right] \\ &= T\sum_n \int \frac{d^3\vec{p}}{(2\pi)^3} e^{i\vec{p}\cdot\vec{x}} G^{\mathrm{E}}_{ij}(\omega_n,\vec{p})\,, \end{aligned} \tag{3.1}$$

where we use the notation $\omega_n = 2\pi i n T$ in this chapter.

The purpose of this essentially technical chapter is to generalize Eq. (3.1), and the formalism of dimensional reduction that applies to the computation of $G^{\mathrm{E}}(\omega_n,\vec{p})$, to any correlation function supported on a spacelike or lightlike hypersurface of the form $x^0 = \tilde{v}x^3$, where $|\tilde{v}| \leq 1$. Note that these do not depend on the operator ordering, since field operators at space-like separated points (anti)commute with each other; thus G_{ij} in Eq. (3.1) can be equivalently a Wightman function G^{12}_{ij} or G^{21}_{ij}, or a time-ordered propagator.

3.1 Field correlators on space-like hypersurfaces

We first treat the case $|\tilde{v}| < 1$, in which case the sought-after formula can be derived from the Lorentz invariance of the underlying theory. Specifically, consider a z-axis boost with velocity $\tilde{v}$, under which the spacelike hypersurface becomes equal-time and the thermal density matrix transforms to:

$$e^{-\beta H} \rightarrow e^{-\beta\tilde{\gamma}(H'+\tilde{v}P'^3)}, \tag{3.2}$$

where the primed quantities refer to quantities in the boosted frame and

$$\tilde{\gamma} = \frac{1}{\sqrt{1-\tilde{v}^2}}. \tag{3.3}$$

The identification of H' and P'^3 as the generators of time and space translation gives the "twisted" periodic identification $x'^\mu = x'^\mu + i\tilde{\gamma}(\beta, -\tilde{v}\beta, 0_\perp)$ for the geometry associated to Eq. (3.2), and the associated quantization condition on the Matsubara frequencies $p'^0 + \tilde{v}p'^3 = 2\pi i n T/\tilde{\gamma}$. The spatial momentum p'^3 must be kept real: it serves as a label for the physical states living on the $x'^0 = 0$ hypersurface. Thus only the frequency p'^0 is complex. This establishes the version of Eq. (3.1) applicable to equal-time two-point functions in the boosted frame:

$$G_{ij}(x'^0{=}0, \vec{x}') = \frac{T}{\tilde{\gamma}} \sum_n \int \frac{d^3\vec{p}}{(2\pi)^3} e^{i\vec{p}'\cdot\vec{x}'} G^{\mathrm{E}\prime}(p'^{\,0}_n, \vec{p}'), \tag{3.4}$$

with $p'^{\,0}_n = -\tilde{v}p'^3 + 2\pi i n\frac{T}{\tilde{\gamma}}$. The prefactor $T/\tilde{\gamma}$ comes from the spacing in energy.

It is convenient to boost this formula back to the plasma rest frame and to write it as a formula for general two-point functions at space-like separation, by setting

$\tilde{v} = \frac{x^0}{x^3}$:

$$G_{ij}(x^0, \vec{x}) = T \sum_n \int \frac{d^3\vec{p}}{(2\pi)^3} e^{ip_n^\mu x_\mu}\, G_{ij}^{\mathrm{E}}(p_n) \tag{3.5}$$

with

$$p_n^0 = 2\pi i n T, \quad p_n^3 = p^3 + 2\pi i n T \frac{x^0}{x^3}.$$

The reason why $G^{\mathrm{E}}(p)$ in Eq. (3.5) is the same as $G^{\mathrm{E}\,\prime}(p')$ in Eq. (3.4) is that the Euclidean function, at any four-momentum with a time-like imaginary part, is an intrinsically defined quantity. Namely, it is the Fourier transform of the physical real-time retarded function (see the discussion in section 2.2),

$$G^{\mathrm{E}}(p) = i \int d^4x e^{-ip^\mu x_\mu} G^{\mathrm{R}}(x), \tag{3.6}$$

the point being that $G^{\mathrm{R}}(x)$ is a physical quantity which can be evaluated in any frame and which transforms covariantly under Lorentz transformations, and that the Fourier transform converges and is unambiguous for said complex momenta.

Eq. (3.5) is the main result of this chapter. It differs from the standard Eq. (3.1) only due to the imaginary part to p_n^3, which ensures that the Fourier exponential is a pure phase so that the sum over n makes sense. It extends in a straightforward way to any higher-point correlator supported on ($\frac{x^0}{x^3} = \tilde{v}$)-type hypersurfaces: one gets a summation-integration $\sum_n \int_p$, with the p_n as in Eq. (3.5), for all external legs, subject to the usual restriction of momentum conservation (and of "n conservation"), as one would get for equal-time higher-point correlators.

In perturbation theory, the momenta running in loops must be the "twisted" ones like those entering Eq. (3.5), e.g. $\mathrm{Im}\, p^3 = \tilde{v}\mathrm{Im}\, p^0$, to reflect the boosted-frame origin of the formula. This ensures that the imaginary part of the momentum flowing in any propagator in a graph is timelike (and its real part is spacelike), which is the natural domain for Euclidean physics.

3.2 Light-like hypersurfaces

In the next chapter we will consider amplitudes relevant for ultrarelativistic particles moving with velocity $v = 1$, e.g. $x^3 = x^0$ (note that $\tilde{v} = 1/v$). Our derivation of Eq. (3.5) might seem compromised since an "infinite" boost with velocity $\tilde{v} = 1$ obviously doesn't exist. However, a more careful look at the argument reveals that the boost is not essential: after all it was undone at the end. All that is really important, is that we can imagine quantizing the system along hypersurfaces parallel to $\tilde{v}$, and express the thermal density matrix within these hypersurfaces. Since it is certainly possible to quantize a system along light fronts, the result (3.5) holds for $x^3 = x^0$.

In physical applications to amplitudes felt by a particle moving with velocity v, setting $x^3 = x^0$ in Eq. (3.5) corresponds to taking a $v \searrow 1$ limit whereas the physically relevant limit $v \nearrow 1$ lies beyond the reach of Eq. (3.5). Whether these two limits agree is nontrivial, and depends on the specific phenomena under consideration. Thus we will need to address this question before we apply Eq. (3.5) in the next chapter.

3.3 Dimensional reduction

Let us restrict our attention to correlation functions with soft external momenta, $p \sim g_{\rm s}T$. Naturally, the contributions to sums such as Eq. (3.5) will behave very differently for $n = 0$ and $n \neq 0$ and it is natural to begin by "integrating out" modes with $n \neq 0$, following the philosophy of dimensional reduction as in section 2.4.

First, we claim that loop diagrams for which all external momenta have $n = 0$ are equal to the standard ones, e.g. the $\tilde{v} = 0$ case. Both sets of diagrams each have $p^0 = 0$ and p_z real and thus they could only differ due to the "twisted" Matsubara momenta which circulate in the former; the claim is that this does not affect the result. The reason is that, as noted above, every momentum entering the former loops has a timelike imaginary part but a spacelike real part, and so p^2 has a positive-definite (spacelike) real part. This will remain so as the imaginary parts of the p^3 integration contours are deformed from $\mathrm{Im}\, p^3 = \tilde{v}\mathrm{Im}\, p^0$ to $\mathrm{Im}\, p^3 = 0$, ensuring that no propagator poles are crossed in this deformation, proving the claim.

This implies that correlation functions involving only $n = 0$ modes as external legs are described by precisely the EQCD three-dimensional effective theory of section 2.4. With the Wick rotation of the A_0 gauge field not performed, the degrees of freedom are actually (A_i, A_0) with the propagators

$$\tilde{G}_{00}(q) = \frac{-1}{q^2 + m_{\mathrm{D}}^2}, \qquad \tilde{G}_{ij}(q) = \frac{\delta_{ij}}{q^2} - \frac{\xi q_i q_j}{q^4}. \tag{3.7}$$

In addition to its interaction with the $n = 0$ modes, we must also include the direct coupling of the correlator of interest to the $n \neq 0$ modes. In the effective theory language, this amounts to a matching procedure between the original correlator and the one defined within EQCD. In the next chapter we will be calculating one-loop ($\mathcal{O}(g_{\mathrm{s}})$) effects and in this case a contribution from $n \neq 0$ modes is not expected since $\mathcal{O}(g_{\mathrm{s}})$ effects come from soft scale, not hard scale. Mathematically, and as proved in section 3.5 below, a contribution from the $n \neq 0$ modes would correspond, in a Minkowski-signature calculation, to a failure of the soft approximation $n_{\mathrm{B}}(p^0) \approx$

T/p^0. But such a failure would signal a contribution from the $p^0 \sim T$ region in Minkowski space, which would necessary be signaled by ultraviolet divergences in the soft approximation, since this approximation correctly describes the intermediate region $g_s T \ll p^0 \ll T$ and any contribution from the scale T should leave an imprint on this region.

The conclusion is that, provided no divergences from the $n = 0$ contribution alone (which computes exactly the soft approximation) are met, it is justified to ignore the direct coupling to the $n \neq 0$ modes in calculating $\mathcal{O}(g_s)$ effects and simply work within ordinary EQCD.

3.4 Application: elastic scattering rates for ultrarelativistic particles

An important role is played in the theory of bremsstrahlung in the quark-gluon plasma (to be reviewed in the next chapter) by the elastic scattering rate felt by an ultrarelativistic parton as a function of transverse momentum transfer $q_\perp$,

$$(2\pi)^2 \frac{d^2\Gamma_{\rm el}}{d^2 q_\perp} \equiv C_{\rm s} C(q_\perp) \tag{3.8}$$

where $C_{\rm s}$ is the (quadratic) Casimir of the hard parton under consideration. At the leading order in perturbation theory, for $q_\perp \ll E$ (with $E \gtrsim T$ being the energy of the hard parton), this is given by [41, 42]

$$C(q_\perp) = g_{\rm s}^2 \int_{-\infty}^{\infty} dz \int d^2 x_\perp e^{i q_\perp \cdot x_\perp} v^\mu v^\nu G^{rr}_{\mu\nu}(t = z, x_\perp) \tag{3.9}$$

where $v^\mu = (1, 0, 0, 1)$ is the parton's four-velocity and, for $q_\perp \sim m_{\rm D} \ll T$, $G^{rr}_{\mu\nu}$ is the HTL-resummed propagator (2.21). Physically, (3.9) accounts for the dominant s-channel scattering events against plasma particles. This interaction is proportional to $C_{\rm s}$, which has been factored out in (3.8). Equation (3.9) is of the form studied in the present chapter, supported on a null plane, and at $q_\perp \ll T$ it can thus be evaluated by means of Eqs. (3.5) and (3.7) with only the $n = 0$ term contributing:

$$C(q_\perp) = g_{\rm s}^2 T \left(\frac{1}{q_\perp^2} - \frac{1}{q_\perp^2 + m_{\rm D}^2} \right), \tag{3.10}$$

This remarkably compact expression was first obtained by Aurenche, Gelis and Zaraket [42], who studied Eq. (3.9) explicitly. While the present approach appears to be more direct, it will be instructive to discuss the connection.

3.5 Sum rules

Following Aurenche, Gelis and Zaraket, we consider computing Eq. (3.9) directly in four-dimensional Minkowski space [42]. This is readily reduced to a single integration over energy

$$C(q_\perp)/g_{\rm s}^2 = \int_{-\infty}^{\infty} \frac{dq^0}{2\pi} \, v^\mu v^\nu G^{rr}_{\mu\nu}(q^0 = q_z, q_\perp). \tag{3.11}$$

This integral was evaluated exactly in [42] by means of a sum rule, relying on the analyticity properties of the integrand in the complex q^0 plane. Following a similar approach we will be able to provide an independent proof of Eq. (3.5) that does not rely on the "boosted" path integral approach used above. We will then relate it to the calculation in [42].

3.5.1 Proof of Eq. (3.5) using sum rules

The relevant analyticity property is that of the (gauge-invariant) retarded correlator $v^\mu v^\nu G^{\rm R}_{\mu\nu}(q)$ [1] , which by causality is an analytic functions of the four-momentum q when a positive timelike or lightlike imaginary four-vector is added to it (see Eq. (3.6)).

In the classical approximation $n_{\rm B}(q^0) \approx T/q^0$, which is valid for small $q_\perp$, Eq. (3.11) becomes

$$T \int \frac{dq^0}{2\pi} v^\mu v^\nu \frac{G^{\rm R}_{\mu\nu}(q^0 = q_z, q_\perp) - G^{\rm A}_{\mu\nu}(q^0 = q_z, q_\perp)}{q^0}. \tag{3.12}$$

To evaluate this by contour integration we first displace the $q^0 = 0$ pole slightly off-axis, $1/q^0 \to 1/(q^0 - i\epsilon)$, which does not affect the result because the numerator vanishes at $q^0 = 0$. This allows the integrals of the $G^{\rm R}$ and $G^{\rm A}$ terms to be performed separately. Next, we note, using the standard HTL expressions (2.21), that $v^\mu v^\nu G^{\rm R,A}_{\mu\nu}$ vanishes at large $|q^0|$ (like $1/q_0^2$), making it possible to close the integration contours at infinity. Closing the contour for $G^{\rm R}$ ($G^{\rm A}$) in the upper (lower) half-surface, one obtains a unique residue $iTv^\mu v^\nu G^{\rm R}_{\mu\nu}(q^0 = q_z = 0, q_\perp)$ from the $G^{\rm R}$ term and nothing from the $G^{\rm A}$ term, due to their aforementioned analyticity properties, thus reproducing Eq. (3.10):

$$C(q_\perp)/g_{\rm s}^2 = T\left(\frac{1}{q_\perp^2} - \frac{1}{q_\perp^2 + m_{\rm D}^2}\right). \tag{3.13}$$

[1] This is gauge-invariant at the order we are considering, that is in the Abelian theory, when $v\cdot q = 0$, as is presently the case.

Had we not made the soft approximation to Eq. (3.12), we would have found additional poles in the above calculation, located at the poles of $n_{\rm B}(q^0)$ which are at the Matsubara frequencies $q^0 = q_z = 2\pi i n T$. It is easy to convince oneself that these terms precisely reproduce the $n \neq 0$ terms in Eq. (3.5). This way we see that Eq. (3.5) can be proved directly from the analyticity properties of the retarded Green's functions, without resorting to the "boosted path integral" argument.

One also sees from this derivation that making the classical approximation $n_{\rm B}(q^0) \approx T/q^0$ to real-time distribution functions is exactly the same as neglecting the $n \neq 0$ modes in an Euclidean formulation. In the same way we expect the same equivalence at the one-loop level.

3.5.2 Comparison with Aurenche, Gelis and Zaraket's sum rule

The above calculation is basically that of [42]. Nevertheless, it differs in some aspects that are worth clarifying. The authors of [42] study exactly the integral (3.12), but parametrized using the variable $x = q^0/q$ (so that $q^0(x) = q_z(x) = |q_\perp| x/\sqrt{1-x^2}$):

$$C(q_\perp)/g_{\rm s}^2 = |q_\perp| \int_{-1}^{1} \frac{dx}{2\pi(1-x^2)^{3/2}}\, v^\mu v^\nu G^{rr}_{\mu\nu}(x, q_\perp) \tag{3.14}$$

A key observation in [42] is that the HTL propagators, viewed as a function of x with $q_\perp$ fixed and $q^0 = q_z$, are analytic in the whole complex x-surface apart from a branch cut at real $x \in [-1, 1]$. Using methods of complex analysis they could then derive Eq. (3.13).

This analyticity property in x follows from the analyticity in $q^0{=}q_z$ that we have just used (e.g., from causality). To see this, we rewrite the change of variable above

Eq. (3.14) as

$$q^0(x) = q_z(x) = i|q_\perp|\frac{x}{\sqrt{x^2-1}}, \tag{3.15}$$

and choose to put the branch cut of the square root at real $x \in [-1,1]$. Thus $q^0 \to i|q_\perp|$ as $|x| \to \infty$ in any direction. With this choice of branch cut, $G^{\mathrm{R}}(q^0(x), q_z(x), q_\perp)$ goes into the standard retarded function as $\mathrm{Im}\, x \to 0^+$ and reproduces exactly the analytic structure of the function $G^{\mathrm{R}}(x, q_\perp)$ that is considered in [42]. Careful inspection of Eq. (3.15) then reveals that the imaginary part of $q^0{=}q_z$ is *positive* for all x. Thus analyticity in x away from the $[-1,1]$ branch cut (for $q^0 = q_z$ and fixed $q_\perp$) is a general consequence of causality.

The authors of [42] worked in the Coulomb gauge and found, at intermediate steps, contributions from a large circle at $|x| = \infty$ (proportional to $1/(q_\perp^2 + \frac{1}{3}m_{\mathrm{D}}^2)$). The point $x = \infty$ corresponds to $q^0{=}q_z = iq_\perp$ in our approach and no contribution can originate from there, so this raises an apparent puzzle. This puzzle is only apparent, however, since these contributions are found in [42] to cancel out in the end, between the transverse and longitudinal propagators. This happens because these terms are merely artefacts of decomposing Eq. (3.14) into transverse and longitudinal parts, which, taken separately, violate Lorentz-covariant causality (viz., both mediate instantaneous interactions). Since our approach assumes Lorentz-covariant causality from the start it cannot detect such unphysical contributions. Their appearance at intermediate steps can be easily avoided, either by working with gauge-invariant quantities, or by restricting to relativistically covariant gauges so that causality is respected at all intermediate steps.

3.6 Concluding remarks

In this technical chapter we have derived a Euclidean summation formula valid for general correlation functions on space-like hypersurfaces, and we have adapted the formalism of dimensional reduction to them. The technique rests on a "twist" of the standard Euclidean formalism by a Lorentz boost. We have illustrated its power by reproducing known results for the elastic collision rate as seen by an ultrarelativistic particle, and we have re-derived the general formula for two-point functions using a sum-rule that had previously appeared in the literature.

In the next chapter this technique will be applied to the same correlator, but at the next-to-leading order in the coupling $g_{\rm s}$.

CHAPTER 4
Jet quenching at next-to-leading order

4.1 Motivation and introduction

Jet quenching is the phenomenon of energy loss by highly energetic partons as they propagate through the medium produced in a heavy ion collision. After exiting the medium, these partons decay into collimated beams of hadrons, called jets, which are detected experimentally. Jet quenching is manifested as the suppression of observed jets having high energies, compared to expectations in the absence of a medium.

This suppression is quantified by comparing the spectra measured in Au+Au collisions to the result of N_{coll} independent binary p+p collisions, where N_{coll} is estimated from the geometry of the overlap region between the colliding nuclei and using the nuclear density profiles (see, for instance, chapter 5 of [6]). The ratio is called the nuclear suppression factor or R_{AA} (the "AA" is for a nucleus-nucleus collision). In the absence of initial state nuclear effects and final state interactions, one would have $R_{\mathrm{AA}} = 1$. Figure 4–1 displays the nuclear suppression factor as measured in Au+Au collisions at $\sqrt{s_{\mathrm{NN}}} = 200$ GeV; the value $R_{\mathrm{AA}} = 0.2 \div 0.4$ indicates the strong suppression of high-energy jets. The absence of such a suppression both in d+Au collisions at $\sqrt{s_{\mathrm{NN}}} = 200$ GeV and in peripheral collisions, in which a dense medium is not believed to be produced, gives strong evidence that this effect is not

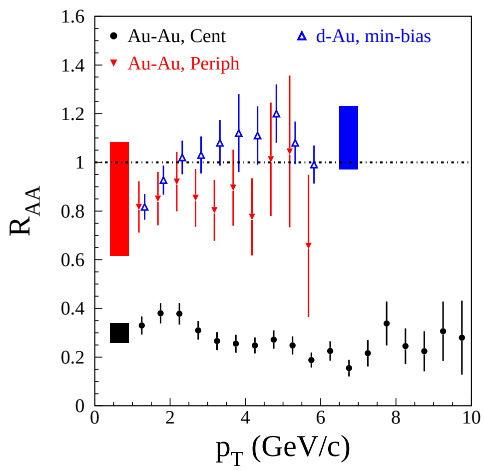

Figure 4–1: Nuclear modification factor R_{AA} for π^0 particles for central (0-10%) and peripheral (80-92%) Au+Au collisions and minimum-bias d+Au collisions. Taken from [6], Fig. 36 (PHENIX collaboration).

due to initial state nuclear effects. RHIC is the first heavy ion collider for which this effect has been measured.

Jet quenching is seen strikingly in azimuthal two-hadron correlations at high p_{T}. In p+p collisions or peripheral Au+Au collisions, a strong peak in the correlation is observed at an angle π, corresponding to the fact that hard jets are likely to be produced in back-to-back pairs. This peak dissolves for more central collisions, as shown in Fig. 4–2, an effect which is generally attributed to the energy degradation of the backward jet (which is pictured as having travelled a longer distance in the medium than the forward, or trigger, jet).

Jet quenching is thus an experimental fact. A long-standing proposal is to use it as a "tomographic"-like probe of the quark-gluon plasma [43, 44, 45, 46],

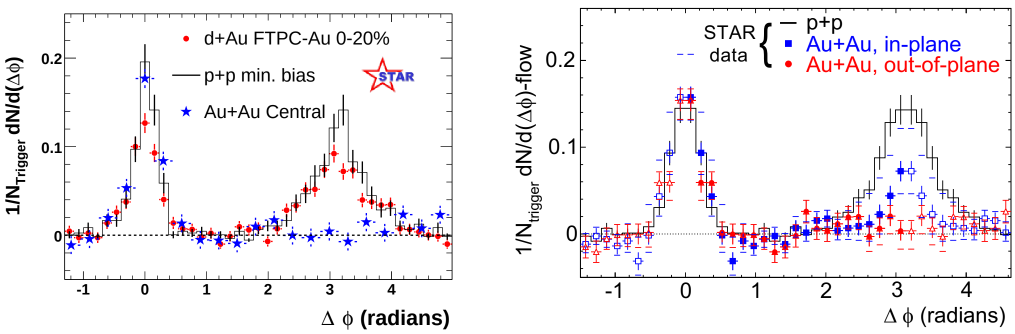

Figure 4–2: Di-hadron azimuthal correlations at high p_{T}. Left panel shows correlations for p+p, central d+Au and central Au+Au collisions (background-subtracted). Right panel shows the background-subtracted high p_{T} di-hadron correlation for different orientations of the trigger hadron relative to the Au+Au reaction plane. For more details, see Fig. 29 in [8] (STAR collaboration).

that is, to use it to constrain experimentally the evolving geometry of the quark-gluon plasma. This requires a good understanding, or modelling, both theoretical and experimental, of jet propagation in the quark-gluon plasma as a function of its properties (essentially, its geometry and local temperature).

The theoretical description of jet quenching (a good starting point is [47] and references therein) is based on the theory of jet evolution in thermalized media, whose uncertainties it is thus worthwhile to seek to reduce, or at least, quantify. This requires the calculation of higher-order effects, which we propose to do in this chapter in the regime of weak coupling.

As established by a large body of work on the thermodynamic pressure [38, 39, 40], mentioned in section 2.5, finite temperature perturbation theory meets with serious convergence difficulties. Unless the strong coupling α_{s} obeys $\alpha_{\mathrm{s}} \lesssim 0.1$, strict perturbation theory in powers of g_{s} does not seem to be reliable. Such a behavior appears to be generic: it is also observed for the next-to-leading order (NLO, or

$\mathcal{O}(g_s)$) corrections to thermal masses [48, 49, 50], as well as for the only transport property presently known at NLO, heavy quark momentum diffusion [51] (whose behavior seems to be even worse).

Following Braaten and Nieto [39], who studied the thermodynamic pressure, these large perturbative corrections can be attributed to purely classical (nonabelian) plasma effects. They have shown this by first making use of the scale separation $g_s T \ll 2\pi T$ to integrate out the scale $2\pi T$, leaving out a three-dimensional effective theory ("electric QCD", or EQCD) describing the scale $m_D \sim g_s T$ as well as more infrared scales. The claim then is that contributions from the scale $2\pi T$, as well as the parameters of the effective theory, enjoy well-behaved perturbative series; all large corrections are included in the effective theory. Furthermore, by treating this effective theory nonperturbatively using various resummation schemes [50, 52] or the lattice [53], reasonable convergence can be obtained down to $T \sim 3 - 5T_c$.

It is natural to expect large corrections from $g_s T$-scale plasma effects in other quantities as well. Unfortunately, for real time quantities such as are most transport coefficients and collision rates, a resummation program similar to that available in Euclidean space has yet to be fully developed and applied. This is because the real-time description of plasmas requires the Hard Thermal Loop (HTL) theory [28, 29, 30], discussed in section 2.3. In essence this theory is classical (nonabelian) plasma physics, or equivalently the Wong-Yang-Mills system, which is arguably more complicated than its Euclidean counterpart EQCD.

In this chapter we aim to point out progress which can be made for a specific class of "real-time" quantities: those which probe physics near the light cone. This includes the elastic collision kernel $C(q_\perp)$ that is relevant for the evolution of jets in transverse momentum space, whose crucial role in the theory of jet quenching will be reviewed below.

To explain the idea, we observe that the soft contribution to the elastic rate (that arising from soft collisions with $q_\perp \sim g_\mathrm{s}T$) is described by soft classical fields that are being probed passively by the high-energy jet passing through them. These soft classical fields are the Coulomb fields surrounding the plasma particles. We now observe that the components of these fields which move collinearly with the jet are not particularly important — the classic calculation of collision rates following Braaten and Thoma [54] (see Eq. (4.18) below) reveals that the target particles move with generic angles in the plasma frame, with even a suppression for the ones collinear to the jet (due to the reduced center-of-mass energy). In the absence of collinear components to the jet, the end result for the elastic rate cannot depend sensibly on the value of the jet velocity $v \approx 1$, and so must depend smoothly on it. The trick is then to set $v = 1+\epsilon$ — which, though unphysical, cannot affect the answer — thus making the hard particle's trajectory *space-like*. This makes Euclidean techniques directly applicable, thereby dramatically simplifying the calculation. In other words, at the classical level, the elastic collision rate seen by ultrarelativistic particles is more "thermodynamical" than actually dynamical.

In this chapter we will thus (analytically) compute the full $\mathcal{O}(g_\mathrm{s})$ corrections to the collision kernel $C(q_\perp)$ describing the evolution of the transverse momentum of a fast particle. The second moment of that kernel gives the phenomenologically interesting momentum broadening coefficient $\hat{q}$, which we also compute at NLO.

This chapter is organized as follows. In section 4.2 we summarize our results and explain their relevance to jet quenching; in particular we discuss the corrections to $\hat{q}$ and their relevance. Details of the calculation of $C(q_\perp)$ at NLO using the techniques of the previous chapter are given in section 4.3. Calculation of the (ultraviolet-regulated) second moment $\hat{q}$ is given in section 4.4. The relation between the collision rate $C(q_\perp)$ for the momentum broadening problem and for jet evolution — which turns out to be identical to the leading-order relation — is established in section 4.5, where we also discuss operator ordering issues that may be relevant in future higher-order calculations.

Alternative estimates of $\hat{q}$ and of jet evolution, based on gauge-string duality (see, for instance, [55, 56, 57, 58, 59, 60, 61]), will not be discussed here.

4.2 Summary of results

4.2.1 Collision kernel

The main result of the present chapter is the full next-to-leading order ($\mathcal{O}(g_\mathrm{s})$) (analytic) expression for the differential collision rate $C(q_\perp)$, defined as:

$$(2\pi)^2 \frac{d^2\Gamma_\mathrm{el}}{d^2q_\perp} \equiv C_\mathrm{s} C(q_\perp), \tag{4.1}$$

which describes the evolution of the transverse momentum of a hard particle (with $E \gtrsim T$). This is the same definition as Eq. (3.8).

The $\mathcal{O}(g_\mathrm{s})$ corrections to $C(q_\perp)$, given in Eq. (4.16), are due to $g_\mathrm{s}T$-scale physics and only arise for $q_\perp \sim g_\mathrm{s}T \ll T$; they are plotted in Fig. 4–3. Both the LO and NLO kernels $C(q_\perp)$ are proportional to the (quadratic) Casimir of the gauge group

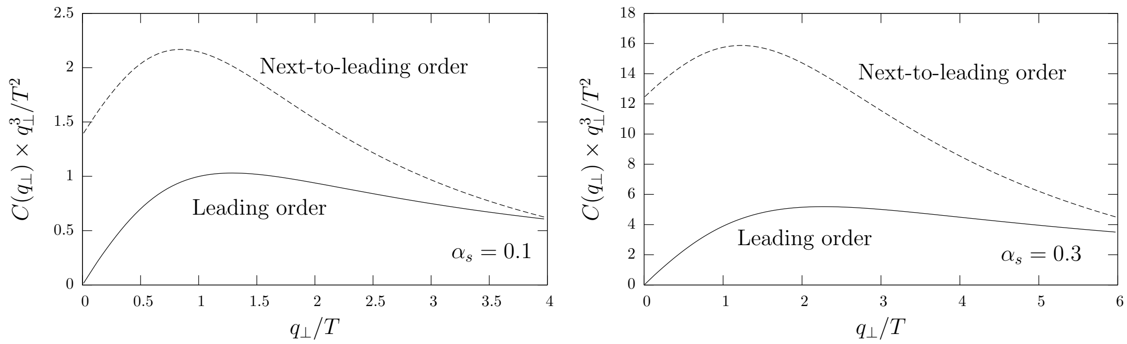

Figure 4–3: LO and NLO collision kernels $C(q_\perp) \equiv (2\pi)^2 d\Gamma/d^2q_\perp$ for a fast quark in $N_f = 3$ QCD, for $\alpha_s = 0.1$ and $\alpha_s = 0.3$ respectively. For gluons the curves are to be multiplied by 9/4.

representation of the jet. The NLO correction is proportional to C_A and vanishes in the Abelian theory.

The "leading order curves" in the plots extend to the hard region $q_\perp \gtrsim T$. There we have used the full (unscreened) Eq. (4.18) at hard momenta, multiplied by $q_\perp^2/(q_\perp^2+m_D^2)$ to make it merge smoothly with the analytic leading-order result (4.8) at low momenta, following the prescription given in [62]. The "next-to-leading order" curves use this expression, plus $C(q_\perp)^{(\mathrm{NLO})}$ as given by Eq. (4.16).

The NLO correction is already quite large for $\alpha_s = 0.1$, where it is nearly a factor of 2 around $q_\perp \approx T$. As discussed in section 4.1, this is consistent with the behavior observed for $\mathcal{O}(g_s)$ effects in other quantities. At $\alpha_s = 0.3$, a typical value used in comparisons with RHIC data (see, for instance, [63]), it is clear that the strength of the correction has grown out of control, meaning that (presently unknown) yet higher-order corrections will also be important. This is the most important finding of this calculation and more will be said about it below.

An interesting by-product of the present approach is that it extends naturally to higher orders, suggesting at least one natural way of resumming the large corrections. Namely, it makes perfect sense to evaluate the gauge-invariant Wilson loop, Eq. (4.6), nonperturbatively within *Euclidean* three-dimensional EQCD theory, as done perturbatively to $\mathcal{O}(g_s)$ in this chapter, for instance using the lattice. This would not include *all* $\mathcal{O}(g_s^2)$ corrections to $C(q_\perp)$ (contributions from the hard scale $2\pi T$ will be missed), but by analogy with the works on the pressure mentioned in the Introduction, these missing contributions can be expected to be numerically subdominant[1] . We leave this possibility to future work.

4.2.2 Application to jet quenching

The dominant energy loss mechanism for a high energy particles (at weak coupling) is bremsstrahlung (radiation of a nearly collinear gluon by a quark or a gluon, or of a collinear quark-antiquark pair by a gluon). These processes, while capable of changing energies by $\mathcal{O}(1)$ amounts, are triggered by considerably softer elastic collisions. Thus the elastic rates being presently discussed are directly relevant to jet quenching. Example of a relevant Feynman diagram is depicted in Fig. 4–4.

The theoretical description of these processes, at the leading order in the coupling, is well-established [44, 45, 64]. Specifically, the duration t_{form} or formation time of the radiation depends on the energy of the participants and it interpolates

[1] Their description could turn out be rather complicated, though; various contributing effects are described in section 6.4.1.

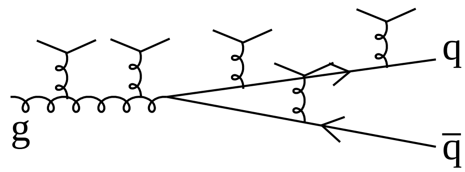

Figure 4–4: A typical Feynman diagram contributing to the production of a collinear quark-anti-quark pair from a gluon. Multiple elastic scatterings both trigger and occur during this process.

between the Bethe-Heitler (single scattering) regime $t_{\rm form} \sim E/q_\perp^2 \sim E/m_{\rm D}^2$ at energies $E \lesssim T$, and the Landau-Pomeranchuk-Migdal (LPM) [65] (multiple-scattering) regime at high energies $E \gg T$ with $t_{\rm form} \sim \sqrt{E/\hat{q}}$. The LPM regime is characterized by destructive interferences between different collisions playing a significant role.

In all of these regimes, interestingly, the description factors into a "hard" collinear splitting vertex (Dokshitzer-Gribov-Lipatov-Altarelli-Parisi, or DGLAP vertex [66]), times (the imaginary part of) a quantum mechanical amplitude (wavefunction in the transverse plane) which describes the in-medium evolution of the vertex. The latter accounts for the collisions which trigger, and occur during, the splitting process [44, 45, 64] (a discussion in a language closer to the present is available in [41], in the context of infinite length quark-gluon plasmas). The DGLAP vertices themselves only involve hard scale physics (in essence, they are Clebsch-Gordon coefficients between different helicity states) and thus cannot receive $\mathcal{O}(g_{\rm s})$ corrections; the NLO effects, associated with soft classical fields having $p \sim g_{\rm s}T$, only arise from the propagation amplitudes.

In section 4.5 we discuss these amplitudes at NLO and show that the relevant (three-body) collision kernel factors as a sum of the kernels $C(q_\perp)$, exactly like it does at LO [44, 45, 64, 41].

As a consequence, our results for $C(q_\perp)$ can be used to give a full NLO treatment of radiative jet energy loss: one must simply include the NLO shift (4.16) to the two-body kernel $C(q_\perp)$ which is an input in these calculations[2] .

4.2.3 Momentum broadening coefficient ($\hat{q}$)

When the effects of a large number of small collisions are added together, it is natural to replace them by an effective diffusive process. The diffusion coefficient relevant for transverse momentum broadening, $\hat{q}$, is the second moment of the collision kernel (4.1):

$$\hat{q} \equiv \int_0^{q_{\rm max}} \frac{d^2 q_\perp}{(2\pi)^2} q_\perp^2 C(q_\perp). \tag{4.2}$$

It is important to note that (4.2) only makes sense with a ultraviolet cutoff $|q_\perp| < q_{\rm max}$. This is due to the strong strong power-law tail $C(q_\perp) \sim g_{\rm s}^4 T^3/q_\perp^4$ at large $q_\perp$ ("Coulomb tail") and leads to a logarithmic dependence of $\hat{q}$ on $q_{\rm max}$. We emphasize that this is a *leading order* logarithm; below we shall comment on the value of the cutoff $q_{\rm max}$.

[2] For instance, one should simply correct "$C(q_\perp)$" in [67]. Note that $C(q_\perp)$ these is actually $C(q_\perp)/(g_{\rm s}^2 T)$ in our conventions.

Using our NLO kernel, Eq. (4.16), we have calculated the expansion of $\hat{q}$ up to terms of order g_s^2:

$$\begin{aligned}\frac{\hat{q}}{g_s^4 C_s T^3} &= \frac{C_A}{6\pi}\left[\log\left(\frac{T}{m_D}\right) + \frac{\zeta(3)}{\zeta(2)}\log\left(\frac{q_{\rm max}}{T}\right) + C_b\right] \\ &+ \frac{N_f T_f}{6\pi}\left[\log\left(\frac{T}{m_D}\right) + \frac{3}{2}\frac{\zeta(3)}{\zeta(2)}\log\left(\frac{q_{\rm max}}{T}\right) + C_f\right] \\ &+ \frac{C_A}{6\pi}\frac{m_D}{T}\xi^{(\rm NLO)} + \mathcal{O}(g_s^2)\,, \end{aligned} \tag{4.3}$$

with $\xi^{(\rm NLO)} = \frac{3}{16\pi}(3\pi^2 + 10 - 4\log 2) \simeq 2.1985$ a constant calculated in section 4.4, characterizing the strength of the NLO correction. Here $m_D^2 = g^2T^2(C_A + N_f T_f)/3$ is the leading-order Debye mass, with $C_A = 3$ and $N_f T_f = 1.5$ in QCD with three flavors of quarks. The leading-order constants $C_b \simeq -0.068854926766592$ and $C_f \simeq -0.072856349715786$ are given in [62], to which we refer the reader for further discussion of the leading order result.

The series (4.3) represents the g_s-expansion of $(1/(2\pi)$ times) the area under the curve in plots such as Fig. 4–3. For $\alpha_s = 0.1$ the area under the leading order curve in the figure (up to $q_{\rm max} = 4T$) yields $\hat{q}^{\rm LO} \approx 0.49\,T^3$ whereas the truncation (4.3) gives $\hat{q}^{\rm LO,truncated} \approx 0.40\,T^3$. The NLO shift seen from the figure is

$$\Delta\hat{q} \approx 0.43\,T^3, \tag{4.4}$$

which represents about a factor two correction (increase). On the other hand

$$\Delta\hat{q}^{\rm truncated} \approx 1.01\,T^3, \tag{4.5}$$

according to Eq. (4.3). Thus Eq. (4.3) suffers from sizeable truncation errors and integrals such as Eq. (4.4) should be preferred over the expansion (4.3). We would like to stress, however, that the NLO correction itself, Eq. (4.16), and Fig. 4–3, are not merely truncation errors from the lower-order contribution, but represent genuine NLO effects.

For $\alpha_{\rm s} = 0.3$ the area under the leading order curve in the figure (again with $q_{\rm max} = 4T$) yields $\hat{q}^{\rm LO} \approx 2.66\,T^3$ while the NLO correction is $\Delta\hat{q} \approx 5.8\,T^3$; the correction is, of course, beyond control.

It seems appropriate here to recall some subtleties associated with the phenomenological parameter $\hat{q}$, which do not arise when one instead works with the full collision kernel $C(q_\perp)$. First, the value of the cutoff $q_{\rm max}$ to be used in Eq. (4.3) is process-dependent: since the $q_\perp{>}q_{\rm max}$ tail of $C(q_\perp)$ describes collisions occurring on a finite rate[3] $\Gamma_{(q_\perp>q_{\rm max})} \sim g_{\rm s}^4 T^3/q_{\rm max}^2$, weighting them with $q_\perp^2$ in Eq. (4.19) ceases to make sense for $\Gamma^{-1}_{(q_\perp>q_{\rm max})} \gtrsim t_{\rm jet}$, with $t_{\rm jet}$ the jet's lifetime, to be replaced with a formation time $t_{\rm form}$ for bremsstrahlung pairs in the context of jet quenching calculations when this is shorter than the medium length. Therefore, parametrically, one should set $q_{\rm max} \sim \sqrt{g_{\rm s}^4 T^3 t_{\rm jet}}$. For bremsstrahlung in the deep LPM regime, $t_{\rm jet} \to t_{\rm form} \sim \sqrt{E/\hat{q}}$ so $q_{\rm max} \sim g(ET^3)^{1/4}$ [68], which is parametrically much lower than the often-used kinematic cutoff $q_{\rm max} \approx (ET)^{1/2}$.

Second, the presence of the ultraviolet tail implies that collisions having $q_\perp \sim q_{\rm max}$ (with $q_{\rm max}$ the physical cutoff as determined above), which are intrinsically non-diffusive, already contribute at next-to-leading logarithm to bremsstrahlung rates. Therefore, approximations based on diffusive physics (also known as the "harmonic

[3] I am indebted to G. D. Moore for discussion on this point.

oscillator" approximation [45]) are, at best, expansions in inverse logarithms of the energy. The quality of such expansions has been studied in [68], with the conclusion that formulas to *next-to-leading* logarithm can be trusted at least when $E_{\rm jet} \gtrsim 10T$ (E being the *smallest* energy of the participants). However it is appropriate to recall that the subleading term (e.g. the constant under the logarithm), included in [68], is not included at present in typical jet quenching calculations which employ $\hat{q}$ as an input parameter (see [47, 69, 70] and references therein for an overview of these approaches).

These limitations pertain to the infinite medium regime. For finite media the Coulomb tail should play a more important more due to the larger virtuality of the jet [64] (in particular, the small-length limit is dictated by the hard tail in the so-called $N = 1$ scattering approximation). Quite recently, the window, as a function of the length of the medium, over which the Coulomb tail can be neglected, has been estimated in the nice paper [71] (see, in particular Fig. (4) of that paper; see also, [72]); the estimates made there seem to cast doubt on the validity of the neglect of the Coulomb tail in finite length media.

In applying the present results to jet quenching it should thus be remembered that the NLO correction is large in the soft region but not in the Coulomb tail, both of which contribute to $\hat{q}$ but not both of which are necessarily always important. Whether the increase in the soft region can be accounted for by a simple rescaling of $\hat{q}$ in approaches which neglect the tail becomes nontrivial at this point.

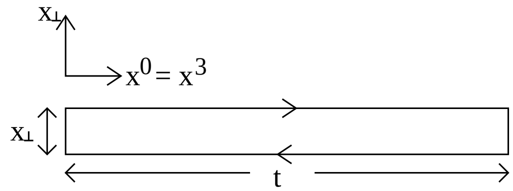

Figure 4–5: Wilson loop representation of the dipole amplitude.

4.3 Elastic collision rate at next-to-leading order

In this section we proceed to compute the differential collision rate $C(q_\perp)$, as felt by a high-energy particle. We express it as correlator supported on $x^3 = x^0$ trajectories, to which we will apply the Euclidean technique developed in the previous chapter. We only give details in the Feynman gauge $\xi = 0$; as a check on the calculation, however, we did check explicitly the ξ-independence of $C(q_\perp)$.

4.3.1 Operator definition of $C(q_\perp)$ and dimensional reduction

The evolution of the transverse momentum of a high-energy particle can be described by looking at its density matrix, as discussed in detail in [55]. For classical effects, however (and even more so because we are taking the velocity to be $v = 1+\epsilon$), we can neglect operator ordering issues in which case the evolution of a density matrix becomes equivalent to that of a dipole, that is, both are charge-anti-charge compounds. We will come back to operator ordering issues in section 4.5.2.

In the high energy limit a dipole ($E \gg m_{\rm D}$) propagates eikonally in the soft classical background, e.g. its impact parameter is constant over a coherence length of the background. Elastic collisions can thus be encoded in a (imaginary) potential acting on the dipole. Specifically, the collision kernel in momentum space is recovered as the Fourier transform of the potential extracted from the long-time limit of the dipole propagation amplitude W [44, 45, 73]:

$$\begin{aligned} W(t, x_\perp) &\sim e^{tC(x_\perp)+\mathcal{O}(1)},\ t \to \infty, \\ C(q_\perp) &\equiv \int d^2 x_\perp e^{iq_\perp \cdot x_\perp} C(x_\perp). \end{aligned} \tag{4.6}$$

$C(q_\perp)$ is short for $(2\pi)^2 d\Gamma/d^2q_\perp$, as in Eq. (4.1). The dipole amplitude $W(t, x_\perp)$ is given by the trace of a long, thin rectangular Wilson loop stretching along the light-cone coordinate x^+, with a small transverse extension $x_\perp$ (see Fig. 4–5).

We wish to apply the Euclidean formalism of the previous chapter to this observable. For this we must justify the passage from the $v \nearrow 1$, physical, ultrarelativistic limit to a $v \searrow 1$ limit, that is we must check regularity around $v = 1$. As explained above, this will be true provided the fields that contribute to the collision rate do not move collinearly to the jet, as is the the case for the Coulomb fields which surround the plasma particles. So we are led to ask, what other fields are there in a classical plasma? The only other fields are those of on-shell gluons. For a jet moving with $v > 1$ one will find a new, unphysical contribution to the collision rate which will be due to the (stimulated emission and absorption of) Čerenkov radiation of these gluons. However, it is easy to verify that this additional contribution vanishes, like $(v-1)$, as $v \searrow 1$. Therefore these fields are also regular as $v \to 1$. At higher orders in g_s (but still within the classical framework), the situation is only expected to become smoother, because of the smearing effect of interactions on kinematic constraints. Thus, within classical plasma physics, the limit $v \to 1$ is regular.

Note that it is important that $q_\perp$ be kept fixed while v is varied, because transferring a large transverse momentum $q_\perp \gg T$ to a plasma particle implies a large longitudinal momentum transfer $q^+ \sim q_\perp^2/T \gg q_\perp$ which would make the final product collinear to the jet. This makes the dependence on v sharper at large $q_\perp$ so the $q_\perp \to \infty$ and $v \to 1$ limits may not commute.

Starting at order g_s^2 in perturbation theory the classical approximation becomes inaccurate and quantum effects must be included. Then one finds a new class of fields which move collinearly with the jet, namely the components of its own wavefunction. Therefore smoothness in v is not guaranteed at this order[4] . Regularity of the rate (4.1) at order $\mathcal{O}(g_s)$ (and more generally within any classical description of the plasma) will be sufficient for our purposes.

The naive dimensional reduction of the Wilson loop (4.6) is a Wilson loop stretching along the z-axis of the three-dimensional EQCD theory, coupling to the linear combination $A_+ = (A_z + A_0)$ of the EQCD fields, reflecting its ultrarelativistic origin:

$$W(t, x_\perp) \simeq \langle \mathcal{P} \exp^{i \int_C (A_i dx^i + A_0 |dx|)} \rangle. \tag{4.7}$$

[4] In strongly coupled theories accessible to gauge-string duality, there is evidence suggesting that regularity does *not* hold. A calculation of $\hat{q}$ for a physical massive quark moving with $v < 1$ (in the sense of momentum broadening coefficient) by Teaney and Casalderrey-Solana [55], and by Gubser [56], found a divergence $\hat{q} \sim (1 - v^2)^{-1/4}\sqrt{\lambda}T^3$ as $v \nearrow 1$. This calculation is valid for energies $E < M^3/\lambda T^2$, beyond which the coherence time of the force acting on the quark becomes of order the time scale of its dynamics [56]; a time-independent description is then impossible. This suggests that $\hat{q}$ for $v < 1$ should depend on a cutoff time scale (as also happens at weak coupling due to the Coulomb tail in $C(q_\perp)$). On the other hand, the $v \searrow 1$ limit has been studied by Rajagopal, Liu and Wiedemann [57, 58], by embedding Euclidean worldsheets into AdS_5 space, and no divergences were met in this limit. These limits thus appear to be qualitatively quite distinct.

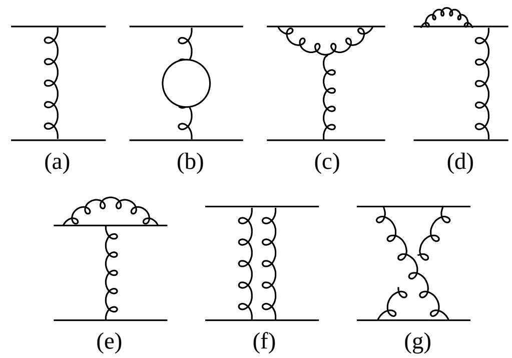

Figure 4–6: Tree- and one-loop diagrams contributing to $C(q_\perp)$.

The contour C is a long rectangle of length t stretching along the z-direction with transverse size $x_\perp$. This "naive" dimensional reduction corresponds to keeping only the direct coupling to the $n = 0$ modes. As explained in subsection 3.3, this will be justified provided we do not find ultraviolet divergences during the calculation.

At the lowest order in perturbation theory, only the single-gluon exchange diagram ((a) of Fig. 4–6) contributes,

$$\begin{aligned} C(q_\perp) &= g^2 T C_{\rm s} \int_{-\infty}^{\infty} dz \int d^2x_\perp e^{ip_\perp \cdot x_\perp} \tilde{G}_{++}(z, x_\perp) \\ &= g^2 T C_{\rm s} \left(\frac{1}{q_\perp^2} - \frac{1}{q_\perp^2 + m_{\rm D}^2} \right), \end{aligned} \tag{4.8}$$

where we have used Eq. (3.7), with $q_z = 0$ being a consequence of the z integration; this is the result of section 3.4. The Wilson loop (4.7) gives the correct generalization to the next-to-leading order.

4.3.2 Diagram (b)

We proceed with the next-to-leading order (one-loop) calculation of (4.6) with W as in (4.7). Self-energy insertions to single-gluon exchange, diagram (b), contribute an amount (we will often write "$q_\perp$" for a three-vector with $q_z = 0$, which should cause no confusion; "$\int_p$" is short for $\int \frac{d^3p}{(2\pi)^3}$):

$$\frac{C(q_\perp)_{(b)}}{g^2TC_{\rm s}} = \frac{\delta\Pi^{00}(q_\perp)}{(q_\perp^2{+}m_{\rm D}^2)^2} - \frac{\delta\Pi^{zz}(q_\perp)}{q_\perp^4}\,, \tag{4.9a}$$

$$\frac{\delta\Pi^{00}(q)}{g^2TC_{\rm A}} = \int_p \left[\frac{-(2q_\perp - p)^2}{p^2((q_\perp{-}p)^2 + m_{\rm D}^2)} + \frac{3}{p^2}\right], \tag{4.9b}$$

$$\begin{aligned}\frac{\delta\Pi^{zz}(q)}{g^2TC_{\rm A}} &= \int_p \left[\frac{-2p_z^2}{(p^2{+}m_{\rm D}^2)((q_\perp{-}p)^2{+}m_{\rm D}^2)} + \frac{1}{p^2{+}m_{\rm D}^2}\right] \\ &+ \int_p \left[\frac{-3p_z^2{-}2q_\perp^2{-}p^2}{p^2(q_\perp{-}p)^2} {+} \frac{2}{p^2} {+} \frac{p_z^2}{p^2(q_\perp{-}p)^2}\right].\end{aligned} \tag{4.9c}$$

Each bracket includes the contributions of one fish and one tadpole diagram, while the last one also includes the ghost loop.

The (linear) ultraviolet divergences in Eq. (4.9c) are to be canceled by matching counter-terms that can be unambiguously calculated within the framework of dimensional reduction [33, 34]. They merely represent the (described by hard thermal loop theory) coupling of the $n \neq 0$ gluons to the soft $n = 0$ ones, e.g. the gluon contribution to the A^0 mass squared $m_{\rm D}^2$. This fact, that the direct coupling to exchange gluons with $q^0 = q^3 \neq 0$ does not contribute to the divergences, is also equivalent to the convergence, with respect to q^3, of the real-time integral (4.18) (this justifies making the soft approximation on q^0). Thus the divergences in Eq. (4.9c) do not signal the presence of "new contributions" beyond the EQCD effective theory and can be safely regularized using dimensional regularization.

Employing dimensional regularization, the divergences simply go away[5] and the corresponding counter-terms are zero to $\mathcal{O}(g_\mathrm{s})$ [33, 34]. This way we obtain (all our arctangents run from 0 to $\pi/2$):

$$\frac{C(q_\perp)_{(b)}}{g_\mathrm{s}^4 T^2 C_\mathrm{s} C_\mathrm{A}} = \frac{-m_\mathrm{D} - 2\frac{q_\perp^2 - m_\mathrm{D}^2}{q_\perp}\tan^{-1}\left(\frac{q_\perp}{m_\mathrm{D}}\right)}{4\pi(q_\perp^2+m_\mathrm{D}^2)^2} + \frac{7}{32 q_\perp^3} + \frac{m_\mathrm{D} - \frac{q_\perp^2+4m_\mathrm{D}^2}{2q_\perp}\tan^{-1}\left(\frac{q_\perp}{2m_\mathrm{D}}\right)}{8\pi q_\perp^4}. \tag{4.10}$$

4.3.3 Diagram (c)

From diagram (c) plus its permutation we obtain:

$$\begin{aligned} \frac{C(q_\perp)_{(c)}}{g_\mathrm{s}^4 T^2 C_\mathrm{s} C_\mathrm{A}} &= \int_p \Bigg[\frac{2}{q_\perp^2(p^2+m_\mathrm{D}^2)((q_\perp-p)^2+m_\mathrm{D}^2)} \\ &\qquad - \frac{2}{(q_\perp^2+m_\mathrm{D}^2)(p^2+m_\mathrm{D}^2)(q_\perp-p)^2}\Bigg] \\ &= \frac{-\tan^{-1}\left(\frac{q_\perp}{m_\mathrm{D}}\right)}{2\pi q_\perp(q_\perp^2+m_\mathrm{D}^2)} + \frac{\tan^{-1}\left(\frac{q_\perp}{2m_\mathrm{D}}\right)}{2\pi q_\perp^3}. \end{aligned} \tag{4.11}$$

In the Feynman gauge there is no contribution involving only transverse gauge fields, because such a contribution would involve the (trivial) zzz three-gluon vertex. Eq. (4.11) is manifestly convergent.

4.3.4 Diagrams (d)-(g)

Taking the long-time limit of the dipole amplitude involves making a quasiparticle expansion, e.g. we set on-shell the external legs of scattering diagrams. This is

[5] The dimensionally-regulated integrals (4.9c) have poles in dimensions 2 and 4 but are finite and unambiguous in dimension 3.

why q_z was zero in the previous diagram. The relevant parameter for this expansion the ratio $\sim g_{\rm s}$ of the scattering width $\sim g_{\rm s}^2 T$ to their intrinsic frequency scale $m_{\rm D}$; this is the probability for scattering events to overlap. Thus in evaluating the external state corrections (d) we need only keep those effects which are not suppressed by the smallness of the width. A narrow resonance being described by just its position and the total area under it, this means that diagram (d), expanded to $\mathcal{O}(g_{\rm s})$, contains only mass-shell corrections and wave-function renormalization factors. The (here imaginary) "mass-shell" corrections have no effects: as they are identical in the initial and final legs the "energy" (z-momentum) transfer remains zero in any case. We can evaluate this wave-function renormalization contribution by taking an energy derivative of the (on-shell) eikonal self-energy, and diagram (e) is unambiguous. Adding them (including all diagrams with similar topology) yields:

$$\frac{C(q_\perp)_{(d)}}{g_{\rm s}^4 T^2 C_{\rm s}} = 2C_{\rm s}\,\tilde{G}_{++}(q_\perp)\int_p \tilde{G}_{++}(p)\frac{d}{dp_z}\frac{1}{p_z - i\epsilon}\,, \tag{4.12a}$$

$$\frac{C(q_\perp)_{(e)}}{g_{\rm s}^4 T^2 C_{\rm s}} = 2(C_{\rm s}-\frac{1}{2}C_{\rm A})\tilde{G}_{++}(q_\perp)\int_p \frac{\tilde{G}_{++}(p)}{(p_z - i\epsilon)^2}\,. \tag{4.12b}$$

The sum of (d) and (e) is proportional to $C_{\rm A}$ and identically vanishes in the abelian theory ($C_{\rm A} = 0$), as required by abelian exponentiation[6] . This confirms the righteousness of our evaluation of (d).

[6] Abelian Wilson loops, computed using Gaussian distribution for gauge fields (as is done by diagrams (d)-(g), for which only the two-point function of the gauge field enters), simply exponentiate: $\langle e^{\int A}\rangle = \exp(\frac{1}{2}\langle \int A \int A\rangle)$. As a consequence, the collision kernel as defined in (4.6) is tree-level exact in such theories: there is no interference between scattering events.

Part of diagram (f) is already included by the exponentiation of the leading-order "rung", diagram (a): this generates the approximation to (f) in which the intermediate eikonal propagators are put on-shell. To avoid double-counting this must be subtracted. We must first regulate the associated "pinching" ($q_z \to 0$) singularity, which we do by flowing a small external z-momentum ω into the Wilson loop. We then take the limit $\omega \to 0$ after the subtraction is done. Diagram (g) poses no difficulty.

$$
\begin{aligned}
\frac{C(q_\perp)_{(f)}}{g_s^4 T^2 C_s} &= C_s \int_p \tilde{G}_{++}(p)\tilde{G}_{++}(q-p) \times \lim_{\omega\to 0} \\
&\qquad \left[\frac{1}{(p_z+i\epsilon)(p_z+\omega-i\epsilon)} + \frac{2\pi i\delta(p_z)}{\omega - i\epsilon}\right], \qquad (4.13)\\
\frac{C(q_\perp)_{(g)}}{g_s^4 T^2 C_s} &= -(C_s - \frac{1}{2}C_A)\int_q \frac{\tilde{G}_{++}(p)\tilde{G}_{++}(q_\perp - p)}{(p_z - i\epsilon)^2}\,. \qquad (4.14)
\end{aligned}
$$

Eq. (4.13) has a well-defined $\omega \to 0$ limit, as follows from the identity $1/(p_z + i\epsilon - 1/(p_z - i\epsilon) = -2\pi i\delta(p_z)$. This limit takes a form identical to Eq. (4.14) and the sum is proportional to C_A, again as required by abelian exponentiation. Again, this confirms the correctness of our evaluation of (f).

In summary, diagrams (d)-(g) produce:

$$
\begin{aligned}
\frac{C(q_\perp)_{(d)-(g)}}{g_s^4 T^2 C_s C_A} &= \int_p \frac{\tilde{G}_{++}(p)\tilde{G}_{++}(q_\perp - p) - 2\tilde{G}_{++}(p)\tilde{G}_{++}(q_\perp)}{2(p_z - i\epsilon)^2} \\
&= \frac{m_D}{4\pi(q_\perp^2 + m_D^2)}\left[\frac{3}{q_\perp^2 + 4m_D^2} - \frac{2}{(q_\perp^2 + m_D^2)} - \frac{1}{q_\perp^2}\right]. \qquad (4.15)
\end{aligned}
$$

The function $\tilde{G}_{++}$ is $\tilde{G}_{00} + \tilde{G}_{zz}$ as given in Eq. (3.7). To evaluate the integral we found it convenient to first apply integration by parts to the $1/(p_z - i\epsilon)^2$ denominator, which removes the explicit p_z-dependence and reduces the integral to a set of standard isotropic Feynman integrals. This contribution is manifestly infrared- (and ultraviolet-) safe, upon enforcing $p \leftrightarrow (q_\perp - p)$ symmetry.

4.3.5 Final formulas

In summary, we have obtained all $\mathcal{O}(g_\mathrm{s})$ contributions to the collision kernel $C(q_\perp)$:

$$
\begin{aligned}
C(q_\perp)^{(\mathrm{LO})} &= \frac{g_\mathrm{s}^2 T C_\mathrm{s} m_\mathrm{D}^2}{q_\perp^2 (q_\perp^2 + m_\mathrm{D}^2)}\,, \\
\frac{C(q_\perp)^{(\mathrm{NLO})}}{g_\mathrm{s}^4 T^2 C_\mathrm{s} C_\mathrm{A}} &= \frac{7}{32 q_\perp^3} + \frac{-3m_\mathrm{D} - 2\frac{q_\perp^2 - m_\mathrm{D}^2}{q_\perp}\tan^{-1}\left(\frac{q_\perp}{m_\mathrm{D}}\right)}{4\pi (q_\perp^2 + m_\mathrm{D}^2)^2} \\
&\quad + \frac{m_\mathrm{D} - \frac{q_\perp^2 + 4m_\mathrm{D}^2}{2q_\perp}\tan^{-1}\left(\frac{q_\perp}{2m_\mathrm{D}}\right)}{8\pi q_\perp^4} \\
&\quad - \frac{\tan^{-1}\left(\frac{q_\perp}{m_\mathrm{D}}\right)}{2\pi q_\perp (q_\perp^2 + m_\mathrm{D}^2)} + \frac{\tan^{-1}\left(\frac{q_\perp}{2m_\mathrm{D}}\right)}{2\pi q_\perp^3} \\
&\quad + \frac{m_\mathrm{D}}{4\pi (q_\perp^2 + m_\mathrm{D}^2)}\left[\frac{3}{q_\perp^2 + 4m_\mathrm{D}^2} - \frac{1}{q_\perp^2}\right]. \qquad (4.16)
\end{aligned}
$$

These expressions are valid for $q_\perp \ll T$. The leading order kernel for $q_\perp \gtrsim T$ differs slightly from its soft approximation given here, see Eq. (4.18) below, but the NLO corrections are parametrically subdominant there.

The appearance of arctangents with two distinct arguments in (4.16) can be understood by looking in the complex $q_\perp^2$-plane: $\tan^{-1}(q_\perp/2m_\mathrm{D})$ has a branch cut starting at $q_\perp^2 = -4m_\mathrm{D}^2$ and represents the exchange of a pair of two quanta of mass m_D (longitudinal gluons), while the branch cut of $\tan^{-1}(q_\perp/m_\mathrm{D})$ starts at $q_\perp^2 = -m_\mathrm{D}^2$ and represents the exchange of one longitudinal and one transverse gluon. Both arctangents occur since both of these pairs of states can be exchanged. Exchange of two massless quanta also occurs, and generates $1/\sqrt{q_\perp^2}$-type discontinuities instead of arctangents.

4.4 Evaluation of $\hat{q}^{(\mathrm{NLO})}$

The effective theory approach we have used so far is valid for $q_\perp \ll T$. The momentum broadening coefficient $\hat{q}$ (second moment of $C(q_\perp)$) receives, however, contributions from all scales up to a process-dependent cut-off $q_{\max}$, on which it depends logarithmically. In this section, for definiteness, we assume $q_{\max} \gg T$.

To separate the soft and hard contributions to $\hat{q}$, we find convenient to introduce the auxiliary scale q^* obeying $m_{\mathrm{D}} \ll q^* \ll T$:

$$\hat{q} = \int_0^{q^*} \frac{d^2 q_\perp}{(2\pi)^2} q_\perp^2 C(q_\perp)^{\mathrm{soft}} + \int_{q^*}^{q_{\max}} \frac{d^2 q_\perp}{(2\pi)^2} q_\perp^2 C(q_\perp)^{\mathrm{hard}} \,. \tag{4.17}$$

The soft kernel $C(q_\perp)^{\mathrm{soft}}$ is given by Eq. (4.16). The hard kernel $C(q_\perp)^{\mathrm{hard}}$ describes tree-level $2 \to 2$ scattering processes against plasma constituents, with self-energy corrections omitted on the exchange gluon (since they represent only $\sim g^2$ corrections when $q_\perp \sim T$). The large particle energy $E \gg T$ guarantees that the Mandelstam invariants $s \sim ET$ and $-t = q_\perp^2$ obey $|t| \ll s$, so that the relevant scattering matrix elements assume the universal (eikonal) form $\propto s^2/t^2$. The kinematics force $q^0 = q_z$ for the momentum transfer q. In fact, these processes are precisely described by the central cut of (the four-dimensional version of) diagram (b) of Fig. 4–6. Performing the q_z integration in the expression for the collision rate (as done in [54]; more details can be found in [62]), one obtains:

$$C(q_\perp)^{\rm hard} = \frac{g_{\rm s}^4 C_{\rm s}}{q_\perp^4} \int \frac{d^3p}{(2\pi)^3} \frac{p - p_z}{p} \left[2C_{\rm A} n_B(p)(1+n_B(p')) \right.$$
$$\left. + 4N_f T_f n_F(p)(1 - n_F(p')) \right], \tag{4.18}$$

with p, p' the initial and final momentum of the target particle; $p' = p + q_z$, $q_z = q^0 = \frac{q_\perp^2 + 2q_\perp \cdot p}{2(p-p_z)}$. In the regime $q_\perp \ll T$, $p' \approx p$ and Eq. (4.18) reduces (as it must) to the large $q_\perp$ limit of Eq. (4.8), $C(q_\perp) \approx g^2 m_{\rm D}^2 C_{\rm s} T / q_\perp^4$.

Integrating Eq. (4.18) over q to obtain the hard contribution to Eq. (4.17), and expanding it in powers of q^*/T, yields:

$$\begin{aligned} \frac{\hat{q}^{\rm hard}}{g_{\rm s}^4 C_{\rm s} T^3} &= \frac{C_{\rm A}}{6\pi} \left[\log\left(\frac{T}{q^*}\right) + \frac{\zeta(3)}{\zeta(2)} \log\left(\frac{q_{\rm max}}{T}\right) + C_b \right] \\ &+ \frac{N_f T_f}{6\pi} \left[\log\left(\frac{T}{q^*}\right) + \frac{3}{2}\frac{\zeta(3)}{\zeta(2)} \log\left(\frac{q_{\rm max}}{T}\right) + C_f \right] \\ &+ \frac{C_{\rm A}}{6\pi} \frac{3}{16} \frac{q^*}{T} + \ldots \end{aligned} \tag{4.19}$$

with the omitted terms suppressed by $(q^*/T)^2$ or more. We have verified by numerical integration the first five significant digits of the numerical constants C_g, C_f, as quoted below Eq. (4.3) from the results of [62]. The $\sim q^*/T$ term arises from soft bosons with $p, p' \ll T$ and can be obtained in the soft approximation $n_B(p), n_B(p') \to T/p, T/p'$; it is also given in [62].

The soft contribution to Eq. (4.17), e.g. the second moment of Eq. (4.16), admits the expansion:

$$
\begin{aligned}
\frac{\hat{q}^{\rm soft}}{C_{\rm s}} &= \frac{g_{\rm s}^4 T^2 C_{\rm A} m_{\rm D}}{2\pi}\left[-\frac{q^*}{16 m_{\rm D}} + \frac{3\pi^2 + 10 - 4\log 2}{16\pi}\right] \\
&+ \frac{m_{\rm D}^2 g^2 T}{2\pi}\log\left(\frac{q^*}{m_{\rm D}}\right) + \ldots
\end{aligned} \tag{4.20}
$$

with the omitted terms being suppressed by powers of $m_{\rm D}/q^*$. The q^* dependence of Eqs. (4.19) and (4.20) cancels out in their sum, as it must do, producing the claimed formula, Eq. (4.3). This cancellation is a nontrivial check on the calculation.

The reader might inquire as to whether we have consistently included all $\mathcal{O}(g_{\rm s})$ contributions to $\hat{q}$. Taking $q^* \sim g^{1/2}T$, for instance, the omitted terms $\sim (q^*/T)^2$ in Eq. (4.19) might naively appear to be $\mathcal{O}(g_{\rm s})$, suggesting contributions from other, omitted terms. Estimates of this kind can be misleading, however, because q^* is not a physical scale in this problem. The matching region $m_{\rm D} \ll q^* \ll T$ can be described equivalently using the low-energy description (EQCD) or the full theory, ensuring that q^* always disappears from final expressions. This is seen explicitly for the leading truncation errors $\sim q^*/T$ in Eqs.(4.19) and (4.20): instead of producing $\mathcal{O}(g_{\rm s}^{1/2})$ corrections, as one would naively expect setting $q^* \sim g^{1/2}T$, they cancel against each other and the leading correction is $\mathcal{O}(g_{\rm s})$ not $\mathcal{O}(g_{\rm s}^{1/2})$. Since similar cancellations are bound to occur at all orders, this simply means that the scale q^* should not enter power-counting estimates. Because higher loop diagrams are $\sim g^2$ when $q_\perp \sim T$ and because we have included all $\mathcal{O}(g_{\rm s})$ effects when $q_\perp \sim m_{\rm D}$, we thus conclude that we have included all $\mathcal{O}(g_{\rm s})$ contributions.

Finally, we note that, in the spirit of [74], we could have used dimensional regularization to separate the q integration, instead of the sharp cutoff q^*. In this scheme, the hard q^*/T term in Eq. (4.19) disappears: there is no suitable dimensionful parameter to replace q^*. The $\mathcal{O}(g_\mathrm{s})$ corrections then come solely from the (unambiguous) dimensionally-regulated soft integral (4.16).

4.5 Momentum broadening versus bremsstrahlung

We now extend the calculation, which so far had been concerned with the momentum broadening of a single particle, to obtain the collision kernel which is relevant for bremsstrahlung and pair production processes. The difference is that, except for QED processes, the relevant object to evolve in the plasma is not a "dipole" but involves three charged states. For instance, to describe the gluon bremsstrahlung process $\psi \to g\psi$, one must evolve an operator which annihilates a quark and creates a quark-gluon pair (see [44, 45, 41]), which, however, use somewhat different notations):

$$\mathcal{O}_{\psi\to\psi g} = |\psi, g\rangle\langle\psi|\,. \tag{4.21}$$

The three color charges in Eq. (4.21) are paired together to form a color-singlet state, as dictated by the (DGLAP) gluon emission vertex which generates this operator.

Only one transverse momentum suffices to describe the internal state of the object (4.21), as a consequence both of momentum conservation and of rotational symmetry: by suitably choosing the z-axis it is always possible to "gauge" to zero one of the transverse momenta (see the discussion preceding eq. (6.6) in [41][7]). In the following, for concreteness, we shall gauge to zero the transverse momentum of particle 1 and $q_\perp$ will refer to the transverse momentum of particle 2.

At the leading order, the relevant collision kernel is expressible as a sum over two-body contributions [44, 45, 64, 41]:

$$\frac{d\Gamma_3(q_\perp)}{d^2q_\perp/(2\pi)^2} = \frac{C_2+C_3-C_1}{2}C(q_\perp)+\frac{C_1+C_3-C_2}{2}C(\frac{E_1}{E_2}q_\perp) + \frac{C_1+C_2-C_3}{2}C(\frac{E_1}{E_3}q_\perp)\,. \quad (4.22)$$

with C_i and E_i respectively the Casimir and longitudinal momenta of the participating particles, and $C(q_\perp)$ is the (Casimir-stripped) single-particle rate as defined earlier. In the special limit in which one of the E_i becomes much smaller than the other ones, the motion of this particle dominates and the kernel Eq. (4.22) reduces to the one for single-particle diffusion, $C(q_\perp)$, for $i = 2, 3$, and $C(\frac{E_1}{E_2}q_\perp)$ when $i = 1$.

As we presently show, it turns out that formula (4.22) also holds at NLO, provided the NLO result for $C(q_\perp)$, Eq. (4.16), is used within it.

4.5.1 "Three-pole" propagation at next-to-leading order

To keep the discussion simple we will assume that particle 3 is a gluon (or any color adjoint state), which is sufficient to cover all splitting processes in QCD (and

[7] For high-energy jets (when at least *one* of the energy of the participant is large, $E_{\max} \gg T$), these rotations can be taken to have energy-suppressed angles $\sim q_\perp/E$, and thus to have negligible effects on the longitudinal momenta. Even when $E_{\max} \sim T$, the angles are at most $\sim g$ and the changes in longitudinal momenta are $\sim g^2$, beyond the accuracy considered in this chapter.

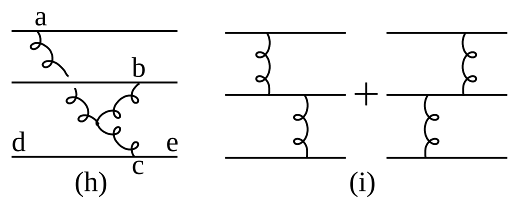

Figure 4–7: Additional diagrams for the evolution of a triplet of charges.

$\mathcal{N} = 4$ super Yang-Mills). This implies that particles 1 and 2 are antiparticles to each other. We denote by $|s\rangle$ the relevant singlet state in the tensor product of the three charges; explicitly, $|s\rangle$ is given by the representation matrices $(t_1)^a_{ij}$.

The dipole diagrams (a)-(g) treated previously must now be summed over the three possible pairs of particles, and we must recompute their group theory factors. Diagrams (a)-(b) involve, in the case the interaction is between particles 1 and 2,

$$\begin{aligned} -\langle s|t_1^a \otimes t_2^a|s\rangle &= \langle s|\frac{t_1^a t_1^a + t_2^a t_2^a - (t_1{+}t_2)^a(t_1{+}t_2)^a}{2}|s\rangle \\ &= \frac{C_1{+}C_2{-}C_3}{2}, \end{aligned} \tag{4.23}$$

which reproduces the structure of Eq. (4.22), upon summing over pairs and using rotational invariance to gauge to zero particle 1's $\perp$-momentum. Diagrams (c)-(g) fit within the same structure, as follows from the fact that they organize themselves into commutators. For instance,

$$\begin{aligned} (c) \propto if^{abc}\langle s|t_1^a t_1^b \otimes t_2^c|s\rangle &= -\frac{C_\mathrm{A}}{2}\langle s|t_1^a \otimes t_2^a|s\rangle, \\ (f)+(g) \propto \langle s|[t_1^a, t_1^b]\otimes\frac{[t_2^a, t_2^b]}{2}|s\rangle &= -\frac{C_\mathrm{A}}{2}\langle s|t_1^a \otimes t_2^a|s\rangle. \end{aligned} \tag{4.24}$$

Here we have used the identities $[t^a, t^b] = if^{abc}t^c$ and $f^{abc}f^{abc'} = C_\mathrm{A}\delta^{cc'}$. Thus, Eq. (4.22) will be proved at NLO provided other contributions vanish.

The other contributions are the added diagrams (Fig. 4–7), which couple the three particles together nontrivially. In diagram (h) (see Fig. 4–7), the Yang-Mills 3-vertex generates a factor f^{abc} and the coupling to the gluon line is given by $(t_3)^c_{de} \propto f^{cde}$, whence:

$$(h) = \langle s|t_1^a t_2^b t_3^c|s\rangle f^{abc} \propto \mathrm{Tr}_{\,1}\left(t^a t^d t^b t^e\right) f^{abc} f^{dec} = 0\,, \tag{4.25}$$

with the trace taken in the representation of the particle 1. We could prove this identity by making extensive use of the antisymmetry of the f^{abc}. Diagrams (i) are similar to diagram (g) treated in subsection 4.3.4, and the main point is that there is a sign between the two diagrams, due to the reversed middle propagator, thus yielding zero:

$$(i) \propto \langle s|t_1^a \otimes [t_2^a, t_2^b] \otimes t_3^b|s\rangle = 0\,. \tag{4.26}$$

Thus the new diagrams (h)-(i) vanish and the factorization formula (4.22) remains valid at NLO. We view this as somewhat surprising and this could be an artefact of the relatively low order in perturbation theory to which we are working.

4.5.2 Operator ordering

We now briefly discuss operator ordering issues, for the Wilson lines in Eq. (4.6) and their three-particle generalization, Eq. (4.21). Although this is not directly relevant to the purely classical effects which are the main object of this chapter, since nonperturbative definitions of $\hat{q}$ have been used in the literature [55, 57] a discussion of them could be of interest.

To help clarify the physical significance of these issues, let us first consider, in QED, the processes of photon bremsstrahlung from a charge, and of pair production from a photon. These processes differ in that the former takes place within the electromagnetic field generated by the initial charge, while the latter takes place in an essentially undisturbed medium (the induced field being suppressed by the small size of the produced dipole). The elastic collision rates relevant to these two processes could thus be different, due to the different backgrounds, and should be defined differently. In the eikonal regime it is the role of the Wilson lines trailing behind the charges to account for these effects, which requires that they be properly ordered.

The proper ordering can be readily guessed using the language of the Schwinger-Keldysh "doubled fields" (see section 2.1), in which amplitudes and their complex conjugate are described by type-1 and type-2 fields, respectively. For photon bremsstrahlung, evolving the relevant $|\psi\gamma\rangle\langle\psi|$ matrix element clearly requires one type-1 ψ (and γ) and one type-2 $\overline{\psi}$ field, whereas for pair production, evolving $|\psi\overline{\psi}\rangle\langle\gamma|$ requires both charged fields to be type-1 (and γ to be type-2). In the latter case the Wilson lines approximately cancel against each other (for a small dipole), whereas in the former case they fail to cancel due to operator ordering issues (they live on different branches of the Keldysh contour): instead they source an electromagnetic field. This way the expected physics is reproduced.

The story for QCD must be similar: for instance, evolving a $|\psi, g\rangle\langle\psi|$ operator, relevant for gluon bremsstrahlung, should require type-1 ψ and g fields, and a type-2 $\overline{\psi}$ field, with the obvious replacements to be made for other processes. Thus the strong coupling calculations of the momentum broadening coefficient in [55] and [56], strictly speaking, gives a $\hat{q}$ applicable to *photon* bremsstrahlung from a quark, whereas the "jet quenching parameter" defined in [57], being defined from a space-like limit of correlators, is by hypothesis independent of operator ordering. It would be very interesting to quantify the importance of operator ordering at strong coupling, where it would presumably be sensitive to the amount of broadening which is due to the induced radiation.

4.6 Concluding remarks

We have evaluated the perturbative corrections to the rate of elastic collisions at small $q_\perp \sim g_{\rm s}T$, as seen by a ultrarelativistic projectile moving in a thermalized quark-gluon plasma. The correction was found to be more than a factor two (increase in the rate) at $\alpha_{\rm s} = 0.3$, signaling poor convergence of the perturbative expansion. Even at $\alpha = 0.1$, the correction is sizable and the reliability of the perturbative series is not clear.

Since in heavy ion collisions $g_{\rm s}T = \mathcal{O}(T)$, we conclude that existing perturbative estimates of $C(q_\perp)$ are unreliable for $q_\perp \lesssim T \div 3T$. The shape of the collision rate at these momenta should thus *not* be considered as a theoretical known in studies of jet quenching.

The large corrections we have found are solely attributable to *classical* plasma physics at the electric scale (effects contained within the EQCD effective theory). As such they are unrelated to quantum effects which only begin at order $g_{\rm s}^2$, and which we have argued are expected to become important, at these momenta, only at a much lower temperatures (larger couplings). Also, the magnetic scale $g_{\rm s}^2T$, although correctly described by EQCD, is not probed by the present calculation; it will enter $\hat{q}$

starting at relative order g_s^2. It would be very interesting to estimate the importance of this nonperturbative scale through three-dimensional simulations of EQCD.

The two-body factorization form (4.22) for the full collision operator $\mathcal{C}$ entering the theory of bremsstrahlung does not receive $\mathcal{O}(g_s)$ corrections. Since no evidence suggests important corrections to this form, it seems justified to assume it in future phenomenological studies and focus on modifications of the single-particle elastic rates $C(q_\perp)$ (also known as dipole amplitude) which is the building block for it.

It is *not possible* for us to comment on whether an increase in $C(q_\perp)$ (and $\hat{q}$) is at present favored by the data and by the data analyses, or not; some groups (in particular, [75]) tend to need a larger $\hat{q}$ than estimated from perturbation theory, while this conclusion not shared by all studies [63]. Steps towards comparing the different treatments were made in [47]; they differ by the approximations that are being made in computing the radiation rate starting from $C(q_\perp)$ (or, in certain cases, starting from only $\hat{q}$. Intrinsic limitations of this quantity have been discussed in section 4.2.3). When this discrepancy (in the theory!) is resolved it will be possible to draw firmer conclusions about the strength of $C(q_\perp)$ from the experiments.

The overall magnitude of jet quenching is a very inclusive measurement and more informative measurements involve some amount of geometry. Similarly, in all approaches, changes in the overall "strength" of $C(q) \propto \alpha_s^2$ can be largely undone by rescaling α_s, and more robust signature of NLO effects should be sought after instead in relation with the shape of $C(q_\perp)$.

Due to interference effects between plasma collisions and the original hard scattering events where a jet takes birth [44, 45, 64] (a very clear recent presentation is in

[76]), at early times the effect of soft collisions is suppressed and only hard collisions are important (the so-called Coulomb tail). This was briefly discussed in section 4.2.3. Therefore, an increase of C in the soft region combined with a decrease in the hard region (so as to retain the same overall R_{AA}), should reduce the energy loss felt along shorter trajectories. Thus, we speculate that NLO corrections will tend to *reduce* surface bias in jet emission. This would be helpful in connection with the so called fragility problem [77, 78]. We look forward to seeing this effect in numerical simulations using realistic hydrodynamic models for the plasma evolution.

CHAPTER 5
Heavy quark momentum diffusion

5.1 Introduction

Heavy quarks are potentially good probes of the properties of the quark-gluon plasma, with “heavy” referring to the charm and bottom quarks. Due to their large masses these are produced only at the very beginning of nuclear collisions, the threshold energy $2m_c \approx 2.5$ GeV for production of a charm quark pair not being available afterwards. Correspondingly, just like hard jets, heavy quarks probe the entire history of the plasma. However, due to their masses different microscopic mechanisms are responsible for the degradation of their spectra; thus independent information can in principle be gained. The identification of the dominant mechanism and its modelling is a subject of ongoing debate; for a recent review see [79].

One of the very interesting discoveries of the RHIC program at Brookhaven National Laboratory has been that heavy quarks (particularly the charm quarks) appear to thermalize just about as effectively as the light quarks. This has been inferred from measuring the electron p_T-spectra produced by the decays of the heavy quarks, showing indications of the same type of hydrodynamic flow as experienced by the lighter quarks [80].

On the theoretical side, the historical starting point for a QCD-based understanding of the behavior of heavy quarks in a thermal environment was the determination of their energy loss rate to the leading order in the QCD coupling constant,

α_s [81]. The energy loss is directly related to a number of other concepts, such as the diffusion and the thermalization rates of the heavy quarks [82, 83]. In particular, assuming that the effective value of α_s is relatively small leads to the thermalization rate $\Gamma \sim \alpha_s^2 T^2/M$, where T is the temperature and M is the heavy quark mass [83]. The comparable thermalization rate for a light quark or gluon is $\Gamma \sim \alpha_s^2 T$, or at very high energies $\Gamma \sim \alpha_s^2 T\sqrt{T/E}$ [84]. Hence heavy quarks with $M \gg T$ are expected to thermalize slowly, particularly at weak coupling.

As already mentioned, the empirical facts appear however to be in conflict with a slow thermalization rate [80]. This has lead to a lot of new theoretical ideas, with the hope of bringing the theoretical determination of Γ beyond the leading order in α_s. In particular, possibilities for a lattice determination were explored [85]; computations in a strongly coupled theory with some similarities with QCD were carried out [86, 87]; phenomenological model treatments of bound states were considered [88]; and the first weak-coupling corrections to the leading order result were determined [89]. The studies [86]–[89] showed that there could indeed be substantial corrections (of a positive sign) to the leading order result; at the same time, the study [85] showed that a direct lattice determination of the heavy quark related observables would be extremely hard, because the physics resides in a "transport peak" of a certain spectral function, of width $\Delta\omega \sim \Gamma \sim \alpha_s^2 T^2/M \ll T$, which regime is practically impossible to explore with Euclidean techniques.

The purpose of this chapter is to reconsider the prospects for a lattice determination, making use of heavy quark effective theory [90] in order to systematically consider the behavior of the heavy quarks in the limit $M \gg T$. Essentially, this allows us to restrict the attention to the "numerator" of the thermalization rate, $\sim \alpha_\mathrm{s}^2 T^2$, which remains finite in the heavy quark limit. In fact, our main goal will be to derive an observable measurable on the lattice which has its structure at "large" frequencies, $\omega \sim \alpha_\mathrm{s}^{1/2} T \gg \Gamma$, and can be addressed much more easily than Γ itself.

We note that, in many respects, our study parallels that in ref. [87]. The main differences are that we use the imaginary-time formalism rather than the real-time one, in order to make contact with the Euclidean spacetime accessible to lattice techniques; and that we try to keep explicit track of $\mathcal{O}(\alpha_\mathrm{s})$ quantum corrections and renormalization issues.

The plan of this chapter is the following. In section 5.2 we derive, by going through several intermediate steps, the observable alluded to above, consisting of color-electric fields along a Polyakov loop. In section 5.3 we analyze the corresponding spectral function perturbatively, demonstrating a relatively flat behavior at small $\omega \lesssim \alpha_\mathrm{s}^{1/2} T$. In section 5.4 we suggest a lattice discretization for the object derived in section 5.2, while section 5.5 offers some conclusions and an outlook.

5.2 Reduction of the current-current correlator

In order to proceed with our derivation, we focus on one of the heavy quarks of physical QCD; either the charm or the bottom quark. We assume for the moment the use of dimensional regularization in order to regulate the theory (though we do not indicate this explicitly). Then there is only one large scale in the system, namely the (renormalized) heavy quark mass, M, and the task is to account for its effects analytically in the basic observable to be defined presently (Eq. (5.1)). In section 5.4 we return to the complications emerging in lattice regularization.

5.2.1 Definitions

The diffusive motion of heavy quarks within a thermalized medium can be characterized by four different quantities, all of which are related to each other (at least in the weak-coupling limit). We start by defining the "diffusion coefficient", D, proceeding then to the "relaxation rate" or "drag coefficient", η_D, and the "momentum diffusion coefficient", κ. The fourth quantity, the energy loss $\mathrm{d}E/\mathrm{d}x$, is historically the first one addressed within QCD [81]; yet it is not obvious how it could be related to the others on the non-perturbative level, so we omit it from the discussion below.

Among the three quantities, the one that can most directly be defined within quantum field theory is the diffusion coefficient D. Consider the spectral function related to the current-current correlator,

$$\rho_V^{\mu\nu}(\omega) \equiv \int_{-\infty}^{\infty} \mathrm{d}t\, e^{i\omega t} \int \mathrm{d}^3\vec{x} \left\langle \frac{1}{2} [\hat{\mathcal{J}}^\mu(t,\vec{x}), \hat{\mathcal{J}}^\nu(0,\vec{0})] \right\rangle , \tag{5.1}$$

where $\hat{\mathcal{J}}^\mu \equiv \hat{\bar{\psi}}\,\gamma^\mu\,\hat{\psi}$; $\hat{\psi}$ is the heavy quark field operator in the Heisenberg picture; $\langle \ldots \rangle \equiv \mathcal{Z}^{-1}\mathrm{Tr}\,[(\ldots)e^{-\beta\hat{H}}]$ is the thermal expectation value; and $\beta \equiv 1/T$ is the inverse temperature. Diffusive motion leads to a pole in the spectral function at $\omega = -iD\vec{k}^2$, where $\vec{k}$ is the momentum (already set to zero in Eq. (5.1)). Solving for the pole position and making use of various symmetries leads to the Kubo relation (see, e.g., chapter 6 of ref. [13])

$$D = \frac{1}{3\chi^{00}} \lim_{\omega\to 0} \sum_{i=1}^{3} \frac{\rho_V^{ii}(\omega)}{\omega} . \tag{5.2}$$

Here χ^{00} corresponds to a "susceptibility" related to the conserved charge $\int \mathrm{d}^3\vec{x}\,\hat{\mathcal{J}}^0$,

$$\chi^{00} \equiv \beta \int \mathrm{d}^3\vec{x} \left\langle \hat{\mathcal{J}}^0(t,\vec{x})\,\hat{\mathcal{J}}^0(t,\vec{0}) \right\rangle . \tag{5.3}$$

For a dilute system of heavy quarks, $T\chi^{00}$ defines their "number density"[1] . Note that the conserved vector current $\hat{\mathcal{J}}^\mu$ does not require renormalization, so that the definitions in Eqs. (5.2) and (5.3) are guaranteed to be ultraviolet finite at any order.

To define the other quantities, we need to assume that the spectral function around zero frequency possesses a narrow transport peak. Due to a heavy quark's large inertia, this is certainly true for M sufficiently large, which we assume to be the case from now on. In this limit, the spectral function will on general grounds take the form of a Lorentzian[2] ,

$$\sum_i \frac{\rho_V^{ii}(\omega)}{\omega} \overset{\omega \lesssim \omega_{\rm UV}}{=} 3\chi^{00} D \frac{\eta_D^2}{\eta_D^2 + \omega^2} , \tag{5.4}$$

where $\omega_{\rm UV}$ is a frequency scale at which the Lorentzian is overtaken by other types of physical processes.

The other two transport coefficients are then defined from the properties of the transport peak. We define the "drag coefficient" η_D to be the width of the Lorentzian, and the (a priori mass-dependent) "momentum diffusion coefficient" $\kappa^{(M)}$ to be $M_{\rm kin}^2$

[1] In the non-relativistic limit and at zero chemical potential, $T\chi^{00} = 4N_{\rm c}(MT/2\pi)^{3/2}\exp(-\beta M)$; however, our basic arguments hold also at a non-zero chemical potential for the heavy quarks, whereby the exponential suppression could be removed from $T\chi^{00}$.

[2] Two concrete examples for how such a dependence on ω can arise are reviewed in appendix A.

times the coefficient of the power-law falloff of its tails,

$$\kappa^{(M)} \equiv \frac{M_{\rm kin}^2 \omega^2}{3T\chi^{00}} \sum_i \frac{2T\rho_V^{ii}(\omega)}{\omega} \bigg|^{\eta_D \ll |\omega| \lesssim \omega_{\rm UV}} \; . \tag{5.5}$$

Here $M_{\rm kin}$ refers to the heavy quark's kinetic mass, to be defined presently (cf. Eq. (5.7)). Later on we will define a transport coefficient κ from the $M \to \infty$ limit of $\kappa^{(M)}$.

The physical motivation for the definition in Eq. (5.5) is as follows. In the dilute limit the current $\hat{\mathcal{J}}^\mu$ couples individually to the heavy quarks; the spectral function $\rho_V^{\mu\nu}(\omega)$ is thus a product of their number density $T\chi^{00}$ times a contribution from one heavy quark. For a single quark, $\int {\rm d}^3\vec{x}\, \hat{\mathcal{J}}^i \equiv \hat{v}^i$ represents a non-perturbative measurement of its velocity. Recalling Newton's law, $M_{\rm kin}{\rm d}\hat{\mathcal{J}}^i/{\rm d}t$ is the force acting on the heavy quark; thus $\kappa^{(M)}$ is a correlator of that force with itself at different times, transformed into frequency space. The factor $2T/\omega$ relates the spectral function to a time-symmetric correlator, for which this classically motivated argumentation applies. Thus Eq. (5.5) generalizes, in a non-perturbative way, the force-force correlator definition of κ given in ref. [87]. The condition on ω instructs us to integrate this force over a time scale, long compared with the medium's correlation time (set by $t \sim \omega_{\rm UV}^{-1}$), but short compared with the dynamics of the heavy quark (set by $t \sim \eta_D^{-1}$).

The coefficients D, η_D and $\kappa^{(M)}$ thus defined are related by fluctuation-dissipation relations, which follow from the fact that the area under the transport peak defines the (coarse-grained) equal-time mean-squared velocity of a heavy quark,

$$\langle \mathbf{v}^2 \rangle \equiv \frac{1}{T\chi^{00}} \int_{-\infty}^{\infty} \frac{{\rm d}\omega}{2\pi} \sum_i \frac{2T\rho_V^{ii}(\omega)}{\omega} G_{\rm UV}(\omega) \; . \tag{5.6}$$

Here we have introduced a cutoff function $G_{\rm UV}(\omega)$ designed to isolate the transport peak from other types of physics, for instance $G_{\rm UV}(\omega) = \theta(\omega_{\rm UV} - |\omega|)$. In the time domain we are thus averaging over a time scale $t_{\rm UV} \gtrsim \omega_{\rm UV}^{-1}$. Such a time averaging is mandatory to make $\langle \mathbf{v}^2 \rangle$ finite and well-defined, since an instantaneous measurement of the heavy quark's velocity would induce it to radiate (or absorb) large amounts of energy, thereby changing its state. We emphasize that, were there no sharp zero-frequency peak in the spectral function, there would be no unambiguous notion of a heavy quark's (coarse-grained) mean squared velocity.

Motivated by the standard non-relativistic thermodynamic result, we can now define a kinetic mass via

$$\langle \mathbf{v}^2 \rangle \equiv 3 \frac{T}{M_{\rm kin}} \, . \tag{5.7}$$

Eqs. (5.4)–(5.6) then yield the fluctuation-dissipation, or Einstein, relations:

$$D = \frac{2T^2}{\kappa^{(M)}} \, , \qquad \eta_D = \frac{\kappa^{(M)}}{2 M_{\rm kin} T} \, , \tag{5.8}$$

both of which involve $\mathcal{O}(\eta_D/\omega_{\rm UV})$ relative uncertainties. Note that $\eta_D \sim 1/M_{\rm kin}$ in the large mass limit, assuming that $\kappa^{(M)}$ contains no (power-like) dependence on $M_{\rm kin}$, justifying the narrow peak assumption.

Thermodynamic considerations relate the kinetic mass defined in Eq. (5.7) to the standard notion. Namely, thanks to the slow dynamics of a heavy quark, one can (approximately) define a free energy $F(\vec{v})$ as a function of its velocity (time-averaged over a period $\sim t_{\rm UV}$); expanding it as $F(\vec{v}) = M_{\rm rest} + M_{\rm kin}\vec{v}^2/2 + \mathcal{O}(\vec{v}^4)$ at small $\vec{v}$ and taking a thermodynamic average should reproduce Eq. (5.7).

The only approximations we have made so far concern the assumption of a narrow transport peak. Parametrically, in weakly coupled QCD [83], $\rho_V^{ii}(\omega)/(\chi^{00}\omega)$ has a peak value $D \sim 1/g^4T$, where $g^2 \equiv 4\pi\alpha_{\rm s}$; a width $\eta_D \sim g^4T^2/M$; and a perturbative ultraviolet contribution which will start to depart from the $1/\omega^2$ Lorentzian tail at the scale $\omega_{\rm UV} \sim gT$ (see section 5.3). Thus errors are of order $\eta_D/gT \sim g^3T/M$. In strongly coupled multicolor ($N_{\rm c} \to \infty$) $\mathcal{N} = 4$ Super-Yang-Mills theory [86], with a 't Hooft coupling $\lambda = g^2N_{\rm c}$, the width of the transport peak is $\eta_D \sim \sqrt{\lambda}T^2/M$, and the continuum takes over at $\omega_{\rm UV} \sim T$; thus ambiguities are suppressed by $\sqrt{\lambda}T/M$.

Expecting the force-force correlator $\kappa^{(M)}$ to actually be mass-independent at large $M_{\rm kin}$, as will be verified *a posteriori*, we are finally led to take the $M_{\rm kin} \to \infty$ limit of Eq. (5.5), inside of which it is essential to retain ω small but non-zero:

$$\kappa \equiv \frac{\beta}{3}\sum_{i=1}^{3}\lim_{\omega\to 0}\omega^2\left[\lim_{M\to\infty}\frac{M_{\rm kin}^2}{\chi^{00}}\int_{-\infty}^{\infty}{\rm d}t\, e^{i\omega t}\int{\rm d}^3\vec{x}\,\left\langle\frac{1}{2}\left\{\hat{\mathcal{J}}^i(t,\vec{x}),\hat{\mathcal{J}}^i(0,\vec{0})\right\}\right\rangle\right]\,. \tag{5.9}$$

The factor $2T/\omega$ has been accounted for by replacing the spectral function by a time-symmetric correlator. Eq. (5.9) will be the starting point for the further steps to be taken.

5.2.2 Heavy quark limit

Starting from the definition in Eq. (5.9), our next goal is to carry out the limit $M \to \infty$. As a first step we note that, making use of time translational invariance and carrying out partial integrations, the definition in Eq. (5.9) can be rephrased as

$$\kappa = \frac{\beta}{3}\sum_{i=1}^{3}\lim_{\omega\to 0}\left[\lim_{M\to\infty}\frac{M_{\rm kin}^2}{\chi^{00}}\int_{-\infty}^{\infty}{\rm d}t\, e^{i\omega(t-t')}\int{\rm d}^3\vec{x}\left\langle\frac{1}{2}\left\{\frac{{\rm d}\hat{\mathcal{J}}^i(t,\vec{x})}{{\rm d}t},\frac{{\rm d}\hat{\mathcal{J}}^i(t',\vec{0})}{{\rm d}t'}\right\}\right\rangle\right]\,. \tag{5.10}$$

In order to evaluate the time derivatives here, let us rewrite the QCD Lagrangian, $\mathcal{L}_{\rm QCD} = \bar\psi(i\gamma^\mu D_\mu - M)\psi + \mathcal{L}_{\rm light}$, after a Foldy-Wouthuysen transformation [91]: expanding in $1/M$ and dropping total derivatives, this yields

$$
\begin{aligned}
\mathcal{L}_{\rm QCD} &= \theta^\dagger \left(iD_0 - M + \frac{c_2\,\vec{D}^2 + c_B\,\sigma\cdot g\vec{B}}{2M} \right)\theta \\
&+ \phi^\dagger \left(iD_0 + M - \frac{c_2\,\vec{D}^2 + c_B\,\sigma\cdot g\vec{B}}{2M} \right)\phi \\
&+ \frac{i\,c_E}{2M}\left(\theta^\dagger\sigma\cdot g\vec{E}\,\phi - \phi^\dagger\sigma\cdot g\vec{E}\,\theta \right) + \mathcal{O}\left(\frac{1}{M^2}\right) + \mathcal{L}_{\rm light}\,,
\end{aligned}
\tag{5.11}
$$

where $D_i = \partial_i - igA_i$, $gB_i \equiv \frac{i}{2}\epsilon_{ijk}[D_j, D_k]$, $gE_i \equiv i[D_0, D_i]$, and θ, ϕ are two-component spinors. The mass M is the pole mass[3] ,

$$
M = m(\bar\mu)\left\{ 1 + \frac{3g^2C_F}{(4\pi)^2}\left[\ln\frac{\bar\mu^2}{m^2(\bar\mu)} + \frac{4}{3} \right] + \mathcal{O}(g^4) \right\}, \tag{5.12}
$$

where $m(\bar\mu)$ is the $\overline{\rm MS}$ mass. In regularization schemes respecting Lorentz invariance, the coefficient c_2 must equal unity (because the combination needed for solving for the pole mass is $\sim p_0^2 - \vec{p}^2 - M^2$), and we assume this to be the case in the following. The matching coefficients c_B, c_E equal unity at leading order but have quantum corrections; these are not needed in the present study. Note that the linearly appearing "rest mass" M is normally shifted away (or rather replaced with 0^+); however, we

---

[3] This is true in schemes producing no additive mass renormalization, such as dimensional regularization. There is no multiplicative renormalization to M in Eq. (5.11) either, because M could be shifted to zero by the field redefinitions $\theta \to e^{-iMt}\theta$, $\phi \to e^{iMt}\phi$ and would then remain zero quantum mechanically.

prefer to keep it explicit for the moment, because the shifts needed are non-trivial at a non-zero temperature, where the Euclidean time extent is finite.

Setting $c_2 = 1$ in Eq. (5.11), we can read off the conserved Noether current and the Hamiltonian in the heavy quark-mass limit:

$$\hat{\mathcal{J}}^0 = \hat{\theta}^\dagger\hat{\theta} + \hat{\phi}^\dagger\hat{\phi} \, , \tag{5.13}$$

$$\hat{\mathcal{J}}^j = \frac{i}{2M}\Big[\hat{\theta}^\dagger(\overleftarrow{D}^j - \overrightarrow{D}^j)\hat{\theta} - \hat{\phi}^\dagger(\overleftarrow{D}^j - \overrightarrow{D}^j)\hat{\phi}\Big] + \mathcal{O}\Big(\frac{1}{M^2}\Big) \, , \tag{5.14}$$

$$\hat{H} = \int \mathrm{d}^3\vec{x} \,\Big[\hat{\theta}^\dagger(-gA_0 + M)\hat{\theta} - \hat{\phi}^\dagger(gA_0 + M)\hat{\phi}\Big] + \mathcal{O}\Big(\frac{1}{M}\Big) \, . \tag{5.15}$$

Here we treat the fermionic fields as operators but the gauge fields as c-numbers, anticipating a path integral treatment of the gauge fields. The time derivatives needed for Eq. (5.10) can subsequently be taken according to the canonical equations of motion,

$$\frac{\mathrm{d}\hat{\mathcal{J}}^i}{\mathrm{d}t} = i\big[\hat{H}, \hat{\mathcal{J}}^i\big] + \frac{\partial \hat{\mathcal{J}}^i}{\partial t} \, , \tag{5.16}$$

where the partial derivative operates on the background gauge fields. The commutator is readily evaluated with the help of equal-time anticommutators, and we also note that since Eq. (5.10) includes a spatial integral over the currents, partial integrations are allowed. Adding together the two parts in Eq. (5.16) then yields

$$\frac{\mathrm{d}\hat{\mathcal{J}}^i}{\mathrm{d}t} = \frac{1}{M}\Big\{\hat{\phi}^\dagger gE^i\hat{\phi} - \hat{\theta}^\dagger gE^i\hat{\theta}\Big\} + \mathcal{O}\Big(\frac{1}{M^2}\Big) \, . \tag{5.17}$$

This can now be inserted into Eq. (5.10), whereby the explicit factors of M duly cancel, since $M_{\mathrm{kin}} = M$ up to $\mathcal{O}(T/M)$ thermal corrections which vanish in the heavy quark-mass limit:

$$\kappa = \frac{\beta}{3}\sum_{i=1}^{3}\lim_{M\to\infty}\frac{1}{\chi^{00}}\int \mathrm{d}t\,\mathrm{d}^3\vec{x} \times \left\langle \frac{1}{2}\left\{ \left[\hat{\phi}^\dagger g E^i \hat{\phi} - \hat{\theta}^\dagger g E^i \hat{\theta}\right](t,\vec{x})\,, \left[\hat{\phi}^\dagger g E^i \hat{\phi} - \hat{\theta}^\dagger g E^i \hat{\theta}\right](0,\vec{0}) \right\} \right\rangle . \quad (5.18)$$

At this point the heavy quarks have become purely static; the ordering of the limits no longer matters, so we have set $\omega \to 0$ inside the Fourier transform.

Given that our derivation made no use of weak-coupling approximations, we believe that Eq. (5.18) is free from (even finite) renormalization to all orders in perturbation theory, in the assumed regularization schemes with no additive mass renormalization and c_2 equal to unity. This shows, in particular, that κ is M-independent.

5.2.3 Euclidean correlator

Eq. (5.18) is a two-point function of gauge-invariant local operators; it therefore satisfies the standard KMS conditions which allow us to relate it to a Euclidean correlation function. In particular, let us define the Euclidean correlator

$$G_E(\tau) \equiv -\frac{\beta}{3}\sum_{i=1}^{3}\lim_{M\to\infty}\frac{1}{\chi^{00}}\int \mathrm{d}^3\vec{x}\left\langle \left[\phi^\dagger g E_i \phi - \theta^\dagger g E_i \theta\right](\tau,\vec{x})\,\left[\phi^\dagger g E_i \phi - \theta^\dagger g E_i \theta\right](0,\vec{0})\right\rangle . \quad (5.19)$$

Hats have been left out because regular Euclidean path integral techniques apply for this object, and the minus sign accounts for the fact that a Euclidean electric field differs by a factor i from the Minkowskian one. The corresponding spectral function can be determined by inverting (for recent practical recipes see, e.g., refs. [92][4]) the relation

$$G_E(\tau) = \int_0^\infty \frac{\mathrm{d}\omega}{\pi}\rho(\omega)\frac{\cosh\left(\frac{\beta}{2}-\tau\right)\omega}{\sinh\frac{\beta\omega}{2}} \; , \tag{5.20}$$

or analytically from

$$\begin{aligned} \tilde{G}_E(\omega_n) &\equiv \int_0^\beta \mathrm{d}\tau\, e^{i\omega_n\tau} G_E(\tau) \; , & (5.21) \\ \rho(\omega) &= \mathrm{Im}\, \tilde{G}_E(\omega_n \to -i[\omega + i0^+]) \; . & (5.22) \end{aligned}$$

The momentum diffusion coefficient then follows from

$$\kappa = \lim_{\omega\to 0}\frac{2T}{\omega}\rho(\omega) \; . \tag{5.23}$$

Note also that by making use of Eq. (5.13), the susceptibility χ^{00} defined in Eq. (5.3) can in the Euclidean theory be written as

$$\chi^{00} = \int_0^\beta \mathrm{d}\tau \int \mathrm{d}^3\vec{x} \Big\langle \Big[\phi^\dagger\phi + \theta^\dagger\theta\Big](\tau,\vec{x}) \; \Big[\phi^\dagger\phi + \theta^\dagger\theta\Big](0,\vec{0}) \Big\rangle \; . \tag{5.24}$$

In order to work out the contractions in Eqs. (5.19), (5.24), we need the heavy quark propagators within the Euclidean theory

$$\mathcal{L}_E = \theta^\dagger(D_\tau + M)\theta + \phi^\dagger(D_\tau - M)\phi + \mathcal{O}\Big(\frac{1}{M}\Big) \; . \tag{5.25}$$

[4] The inversion leads to well-known systematic uncertainties, and we have nothing concrete to add on how to treat those. However, as will be demonstrated below, our spectral function is smoother at small ω than the ones in refs. [92], which should somewhat ameliorate the problems in reconstructing the spectral function.

Making use of the equations of motion satisfied by the propagators, together with the proper boundary conditions, it can be shown that in the $M \to \infty$ limit and for $\tau > 0$,

$$\begin{aligned}
\Big\langle \theta_\alpha(\tau,\vec{x})\,\theta^*_\beta(0,\vec{y}) \Big\rangle &= \delta^{(3)}(\vec{x-y})U_{\alpha\beta}(\tau,0)e^{-\tau M} \;, && (5.26)\\
\Big\langle \theta_\alpha(0,\vec{x})\,\theta^*_\beta(\tau,\vec{y}) \Big\rangle &= -\delta^{(3)}(\vec{x-y})U_{\alpha\beta}(\beta,\tau)e^{(\tau-\beta)M} \;, && (5.27)\\
\Big\langle \phi_\alpha(\tau,\vec{x})\,\phi^*_\beta(0,\vec{y}) \Big\rangle &= \delta^{(3)}(\vec{x-y})U^\dagger_{\alpha\beta}(\beta,\tau)e^{(\tau-\beta)M} \;, && (5.28)\\
\Big\langle \phi_\alpha(0,\vec{x})\,\phi^*_\beta(\tau,\vec{y}) \Big\rangle &= -\delta^{(3)}(\vec{x-y})U^\dagger_{\alpha\beta}(\tau,0)e^{-\tau M} \;, && (5.29)
\end{aligned}$$

where U is now a straight fundamental Wilson line in the Euclidean time direction. With these propagators, we obtain

$$\begin{aligned}
&\int \mathrm{d}^3\vec{x} \Big\langle \Big[\phi^\dagger gE_i\phi - \theta^\dagger gE_i\theta\Big](\tau,\vec{x})\; \Big[\phi^\dagger gE_i\phi - \theta^\dagger gE_i\theta\Big](0,\vec{0}) \Big\rangle \\
&\quad = \; 4\delta^{(3)}(\vec{0})e^{-\beta M}\Big\langle \mathrm{Re}\,\mathrm{Tr}\,[U(\beta,\tau)\,gE_i(\tau,\vec{0})\,U(\tau,0)\,gE_i(0,\vec{0})] \Big\rangle \;. \qquad (5.30)
\end{aligned}$$

Similarly, the susceptibility χ^{00} can be written as

$$\begin{aligned}
\chi^{00} &= 4\delta^{(3)}(\vec{0})e^{-\beta M}\int_0^\beta \mathrm{d}\tau \,\Big\langle \mathrm{Re}\,\mathrm{Tr}\,[U(\beta,\tau)U(\tau,0)] \Big\rangle \\
&= 4\delta^{(3)}(\vec{0})e^{-\beta M}\beta\Big\langle \mathrm{Re}\,\mathrm{Tr}\,[U(\beta,0)] \Big\rangle \;. \qquad (5.31)
\end{aligned}$$

In total, then,

$$G_E(\tau) = -\frac{1}{3}\sum_{i=1}^{3} \frac{\Big\langle \mathrm{Re}\,\mathrm{Tr}\,\Big[U(\beta,\tau)\,gE_i(\tau,\vec{0})\,U(\tau,0)\,gE_i(0,\vec{0})\Big] \Big\rangle}{\Big\langle \mathrm{Re}\,\mathrm{Tr}\,[U(\beta,0)] \Big\rangle} \;, \qquad (5.32)$$

and κ can be obtained from the corresponding spectral function through Eq. (5.23). Note that the correlation function $G_E(\tau)$ is *positive* (in a gauge with vanishing A_0, one can think of it as $-\partial_\tau \partial_\sigma F(\tau-\sigma)|_{\sigma=0}$, where F is the correlation function of A_i). Eq. (5.32) is our main result. A related formula in Minkowski signature was given in ref. [87].

It is appropriate to remark that the meaning of Eq. (5.32) is unclear in the confinement phase of pure SU(N_c) gauge theory, where the expectation value of the Polyakov loop vanishes. In this situation, however, there would be a flux tube which drags the heavy quark in a way that is quite unlike diffusion, so it need not be surprising if the result for a diffusion coefficient were ill-defined.

5.3 Perturbation theory

The derivation of our main result, Eq. (5.32), made no use of the weak-coupling expansion, and is meant to be applicable everywhere in the deconfined phase, particularly at the phenomenologically interesting temperatures of a few hundred MeV. Nevertheless, to gain some understanding on the general shape of the corresponding spectral function, we now go to very high temperatures, where the weak-coupling expansion is applicable. Our goal is to demonstrate explicitly that even in this regime, where spectral functions in general have more peaks and cusps than in a strongly-coupled regime, ours is relatively smooth.

The leading-order (free theory) behaviors of the correlation function in Eq. (5.32) and of the spectral function in Eq. (5.22) are easily found:

$$G_E(\tau) = g^2 C_F \, \pi^2 T^4 \left[\frac{\cos^2(\pi\tau T)}{\sin^4(\pi\tau T)} + \frac{1}{3\sin^2(\pi\tau T)} \right] + \mathcal{O}(g^4) \; , \tag{5.33}$$

$$\rho(\omega) = \frac{g^2 C_F}{6\pi} \omega^3 + \mathcal{O}(g^4) \; , \tag{5.34}$$

where $C_F \equiv (N_c^2 - 1)/(2N_c)$. This shows that at the free level the spectral function has no zero-frequency peak, in contrast to the spectral functions relevant for transport coefficients and vector current correlators (which have δ-function peaks at this order). Given that $\rho(\omega)$ in Eq. (5.34) vanishes faster than $\propto \omega$, the diffusion constant κ of Eq. (5.23) is zero; we must work harder to find the leading non-trivial behavior at small frequency.

At next-to-leading order, $\mathcal{O}(g^4)$, the intercept κ becomes non-vanishing [83]:

$$\kappa = \frac{g^2 C_F T}{6\pi} m_\mathrm{D}^2 \left(\ln \frac{2T}{m_\mathrm{D}} + \frac{1}{2} - \gamma_\mathrm{E} + \frac{\zeta'(2)}{\zeta(2)} + \frac{N_\mathrm{f} \ln 2}{2N_\mathrm{c} + N_\mathrm{f}} \right) \Big(1 + \mathcal{O}(g) \Big) \,, \qquad (5.35)$$

where $m_\mathrm{D}^2 = g^2 T^2 (N_\mathrm{c}/3 + N_\mathrm{f}/6)$. As indicated, corrections to this expression start already at $\mathcal{O}(g)$, and have in fact recently been determined [89].

In order to learn how "easy" it is to extract the intercept κ in practice, let us calculate more carefully the small-ω behavior of the spectral function in Eq. (5.22). We restrict, in the following, to frequencies at most of the order of the plasmon (or Debye) scale, $\omega \lesssim gT$. Defining $\kappa(\omega)$ to be the product on the right-hand side of Eq. (5.23), the difference $[\kappa(\omega) - \kappa]$ gets contributions only from soft momenta $k \sim m_\mathrm{D}$, and can be calculated at tree-level using Hard Thermal Loop propagators. Moreover, the Wilson lines in Eq. (5.32) can be set to unity. Inserting the gluon propagator

$$\langle A_\mu^a(x) A_\nu^b(y) \rangle = \delta^{ab} \sum\!\!\!\!\!\!\!\int_K e^{iK\cdot(x-y)} \left[\frac{P_{\mu\nu}^T(K)}{K^2 + \Pi_T(K)} + \frac{P_{\mu\nu}^E(K)}{K^2 + \Pi_E(K)} + \xi \frac{K_\mu K_\nu}{(K^2)^2} \right] \,, \quad (5.36)$$

where ξ is the gauge parameter, and carrying out the Fourier transform in Eq. (5.21), we get

$$\tilde{G}_E(\omega_n) = -\frac{g^2 C_F}{3} \int \frac{\mathrm{d}^3\vec{k}}{(2\pi)^3} \left[\frac{2\omega_n^2}{\omega_n^2 + k^2 + \Pi_T(\omega_n, \vec{k})} + \frac{\omega_n^2 + k^2}{\omega_n^2 + k^2 + \Pi_E(\omega_n, \vec{k})} \right] , \quad (5.37)$$

where $k \equiv |\vec{k}|$. After the analytic continuation in Eq. (5.22), $\omega_n \to -i[\omega + i0^+]$, the self-energies become (see, e.g.. ref. [13])

$$\Pi_T(-i(\omega + i0^+), \vec{k}) = \frac{m_\mathrm{D}^2}{2} \left\{ \frac{\omega^2}{k^2} + \frac{\omega}{2k} \left[1 - \frac{\omega^2}{k^2} \right] \ln \frac{\omega + i0^+ + k}{\omega + i0^+ - k} \right\} , \quad (5.38)$$

$$\Pi_E(-i(\omega + i0^+), \vec{k}) = m_\mathrm{D}^2 \left[1 - \frac{\omega^2}{k^2} \right] \left[1 - \frac{\omega}{2k} \ln \frac{\omega + i0^+ + k}{\omega + i0^+ - k} \right] . \quad (5.39)$$

This leads to Landau cut contributions at $k > \omega$, and plasmon pole contributions at $k < \omega$. Concretely,

$$\begin{aligned} \kappa(\omega) - \kappa \;=\; & \frac{2g^2 C_F T}{3} \times \frac{4\pi}{(2\pi)^3} \times \pi m_\mathrm{D}^2 \times \Bigg\{ \\ & \int_{\hat\omega}^{\infty} \mathrm{d}\hat{k}\, \hat{k}^2 \frac{2\hat\omega \times \frac{\hat\omega}{4\hat{k}} \left(1 - \frac{\hat\omega^2}{\hat{k}^2}\right)}{\left(\hat{k}^2 - \hat\omega^2 + \frac{1}{2}\left[\frac{\hat\omega^2}{\hat{k}^2} + \frac{\hat\omega}{2\hat{k}}\left(1 - \frac{\hat\omega^2}{\hat{k}^2}\right) \ln\frac{\hat{k}+\hat\omega}{\hat{k}-\hat\omega}\right]\right)^2 + \left(\frac{\hat\omega\pi}{4\hat{k}}\right)^2 \left(1 - \frac{\hat\omega^2}{\hat{k}^2}\right)^2} \\ & + \int_0^\infty \mathrm{d}\hat{k}\, \hat{k}^4 \left[\frac{\theta(\hat{k} - \hat\omega) \times \frac{1}{\hat\omega} \times \frac{\hat\omega}{2\hat{k}}}{\left(\hat{k}^2 + 1 - \frac{\hat\omega}{2\hat{k}} \ln\frac{\hat{k}+\hat\omega}{\hat{k}-\hat\omega}\right)^2 + \left(\frac{\hat\omega\pi}{2\hat{k}}\right)^2} - \frac{\frac{1}{2\hat{k}}}{(\hat{k}^2+1)^2} \right] \\ & + 2\hat\omega\, \frac{\hat{k}_T^3(\hat\omega^2 - \hat{k}_T^2)}{|3(\hat{k}_T^2 - \hat\omega^2)^2 - \hat\omega^2|} \Bigg|_{\hat{k}_T^2 - \hat\omega^2 + \frac{1}{2}[\frac{\hat\omega^2}{\hat{k}_T^2} + \frac{\hat\omega}{2\hat{k}_T}(1 - \frac{\hat\omega^2}{\hat{k}_T^2}) \ln\frac{\hat\omega + \hat{k}_T}{\hat\omega - \hat{k}_T}] = 0} \\ & + \frac{1}{\hat\omega}\, \frac{\hat{k}_E^3(\hat\omega^2 - \hat{k}_E^2)}{|3(\hat{k}_E^2 - \hat\omega^2) + 1|} \Bigg|_{\hat{k}_E^2 + 1 - \frac{\hat\omega}{2\hat{k}_E} \ln\frac{\hat\omega + \hat{k}_E}{\hat\omega - \hat{k}_E} = 0} \qquad \Bigg\} , \end{aligned} \quad (5.40)$$

where $\hat\omega \equiv \omega / m_\mathrm{D}$ and $\hat{k} \equiv k / m_\mathrm{D}$. The four terms correspond to the transverse cut, electric cut, transverse pole, and electric pole, respectively.

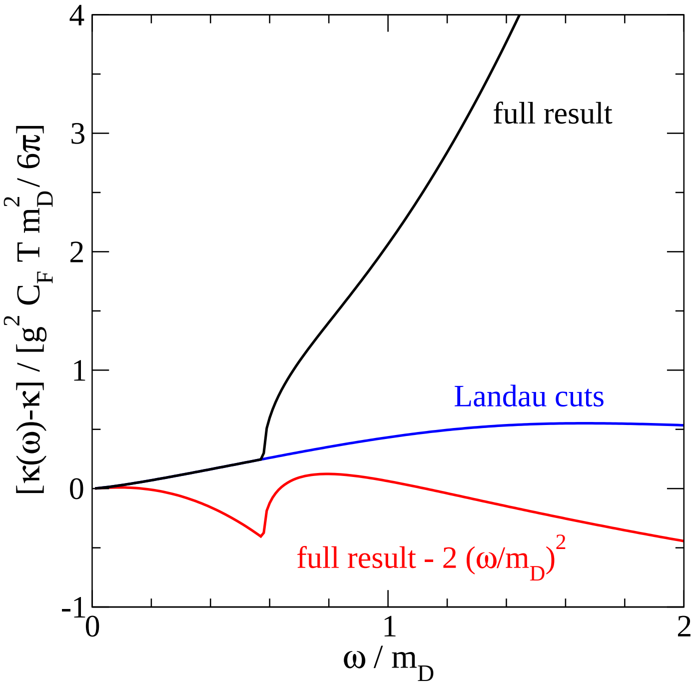

Figure 5–1: A numerical evaluation of Eq. (5.40), in units of $g^2 C_F T m_{\rm D}^2/6\pi$. The cusp is a feature of the weak-coupling expansion, as discussed in the text.

The outcome of a numerical evaluation of Eq. (5.40) is plotted in Fig. 5–1, in units of the coefficient $g^2 C_F T m_{\rm D}^2/6\pi$ multiplying the logarithm in Eq. (5.35). For $\hat\omega < 1/\sqrt{3}$, the result comes exclusively from the Landau cuts; for $\hat\omega > 1/\sqrt{3}$, plasmon poles contribute as well. For $\omega \gg m_{\rm D}$, the result is dominated by the transverse pole, and extrapolates towards $\kappa(\hat\omega \gg 1) \to g^2 C_F T m_{\rm D}^2/6\pi \times 2\hat\omega^2$, the free theory result.

The pattern in Fig. 5–1 illustrates an important point: even at weak coupling there is no transport peak around the origin; rather $\rho(\omega)/\omega$ displays a relatively flat behavior at $\omega \lesssim m_{\rm D}/\sqrt{3}$, with a significant rise only above the Debye scale. The only singularity is associated with the onset of the plasmon contributions; however this should be smoothed out in the full dynamics. The amount of smoothening can be estimated from the (zero-momentum) plasmon damping rate calculated in ref. [93], $\Gamma_{\rm pl} = 6.64 g^2 N_{\rm c} T/24\pi$. Already for $\alpha_{\rm s} = 0.05$ this gives (for $N_{\rm c} = 3, N_{\rm f} = 0...4$) a width $\Gamma_{\rm pl}/m_{\rm D} \gtrsim 0.2$ comparable to that of the cusp; therefore we expect the true behavior to be completely regular. A more detailed study of the shape, including the effects of interactions in the small-ω regime and ultraviolet features in the large-ω regime, is deferred to a future publication [94]. We also remark that the corresponding spectral functions computed for $\mathcal{N} = 4$ Super-Yang-Mills theory at infinite 't Hooft coupling show an analogous behavior, with the smooth infrared part ending in that case at $\omega \sim T$ [87, 95].

5.4 Correlator in lattice regularization

Let us finally move to lattice regularization. In principle correlators of the type in Eq. (5.32) can be measured with standard techniques on the lattice, in fact even at low temperatures where the signal is very small [96]. There is the problem, however, that the lattice electric fields require in general multiplicative renormalization factors (see, e.g., ref. [97]); these depend on the details of the discretization chosen, and it is also not clear how they could be determined on the non-perturbative level[5] .

It appears, however, that the problem can at least be ameliorated if we choose a discretization of the electric fields inspired by lattice heavy quark effective theory (see, e.g., ref. [99]). The spatial components of the current (Eq. (5.14)) could be

[5] For recent progress with lattice magnetic fields, see ref. [98].

thought of as

$$\hat{\mathcal{J}}^j = \frac{i}{2aM}\Big[\hat{\theta}^\dagger(x+\hat{j})U_j^\dagger(x)\hat{\theta}(x) - \hat{\theta}^\dagger(x)U_j(x)\hat{\theta}(x+\hat{j}) - (\hat{\theta} \longrightarrow \hat{\phi})\Big]\,, \tag{5.41}$$

where a is the lattice spacing; $\hat{j}$ is a unit vector in the j-direction; and U_j is a spatial link matrix. Discretizing also the time derivatives in Eq. (5.10) and carrying out the contractions, we end up with a representation of Eq. (5.32) which can best be represented graphically:

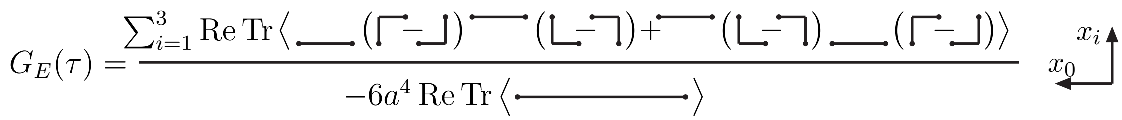

(5.42)

Here the direct lines within parentheses are link matrices; reading from the right, the long horizontal Wilson lines in the numerator have lengths $\tau - a$ and $\beta - \tau - a$, if the sources are placed around $x_0 = a/2$ and $x_0 = \tau + a/2$, respectively; and the denominator stands for the trace of the Polyakov loop. It appears that Eq. (5.42) should be less ultraviolet sensitive than the usual discretizations of the electric fields [96, 97].

Continuing with the framework of the lattice heavy quark effective theory, the renormalization of Eq. (5.42) can also be discussed in concrete terms, and be related to two separate issues. First of all, the linearly appearing mass parameter M in Eq. (5.11) is no longer the pole mass but requires additive renormalization; second, the coefficient c_2 can differ from unity due to the absence of (Euclidean) Lorentz invariance. It appears that both of these issues could be addressed perturbatively and, in fact, even non-perturbatively [99]. Since the explicit results depend on the particular lattice discretization chosen we do not, however, go into details here.

5.5 Concluding remarks

The main purpose of this chapter has been to give a non-perturbative definition to the heavy quark momentum diffusion coefficient, κ, allowing in principle for its lattice measurement. The basic definition is given in terms of a certain limit of the vector current correlation function, Eq. (5.9). Making use of heavy quark effective theory, we have furthermore shown that the definition can be reduced to a much simpler purely gluonic correlator, given in Eq. (5.32), with κ then following from Eq. (5.23).

An important consequence of these relations is that they show that κ does not contain any logarithms of the heavy quark mass M. Our formulae could in principle also serve as the starting point for a first computation of a finite-temperature real-time quantity to relative accuracy α_s, revealing in particular how the renormalization scale should be fixed.

Moving to the non-perturbative level, we have also suggested a particular discretization of Eq. (5.32), given in Eq. (5.42), which could be free of significant renormalization factors. It remains to be tested in practice, however, how noisy the correlator is, and how fast the continuum limit can be approached. In addition, current practical recipes [92] related to the inversion of Eq. (5.20) suffer from uncontrolled systematic uncertainties which our method does not remove completely, although we hope that from the practical point of view they are less serious than in many other cases.

Assuming that a non-perturbative value can be obtained for κ, we can finally proceed to consider the thermalization rate of heavy quarks. A concrete and theoretically satisfactory meaning for a thermalization rate is provided by the heavy quark relaxation rate, or drag coefficient, denoted by η_D and defined around Eq. (5.5) (the relation to thermalization follows from Eq. (7.1)). Employing the fluctuation–dissipation relation in Eq. (5.8), η_D can be estimated as $\eta_D \simeq \kappa/2MT$, where M is the heavy quark pole mass and T is the temperature. Although this relation does have ambiguities related to the definition of the quark mass (a pole mass has inherent non-perturbative ambiguities at the level of several hundreds of MeV [100]; a treatment free of this problem can only be given in terms of non-perturbatively renormalized heavy quark effective theory [99]), such ambiguities should be subdominant compared with the large corrections related to infrared sensitive thermal physics, at least for the bottom quarks. These large thermal corrections are properly captured by our definition of κ, so η_D should lie in the right ballpark as well. We are therefore very much looking forward to the first numerical estimates of κ.

CHAPTER 6
Supersymmetry in high-energy processes at finite temperature

6.1 Preamble

While there is a clear need for nonperturbative methods at soft momenta, at hard scales perturbation theory can reasonably be expected to work provided some suitable way to "factor" soft and hard scale physics applies.

For instance in chapter 4 we have factored the medium-dependence of jet quenching into the collision kernel $C(q_\perp)$, which was physically well-motivated in the high-energy limit, including $\mathcal{O}(g_\mathrm{s})$ corrections. Chapter 5 was based on a Langevin model of heavy-quark dynamics that depends only on the transport coefficient κ and on T, which was well-motivated in the limit of large quark mass and nonrelativistic velocities. Yet it would be valuable to account for a variety of typically "hard" corrections, for instance the running of the coupling including a precise fixing of its scale. Also, one would like for instance to include DGLAP evolution of the constituents of the medium, whenever scatterings with large $q_\perp$ occur. For heavy quarks, one would like to connect the Langevin regime with the relativistic regime where it breaks down.

Clearly, doing perturbative computations is a good way to address such perturbative effects, and to identify how to best parameterize their dependence on difficult-to-calculate soft physics. Such calculations are evidently rather difficult (no single real-time quantity has yet been calculated including $\mathcal{O}(g_\mathrm{s}^2)$ effects), whence a need for simplified models in which these calculations can be eased.

Supersymmetry could provide such a simplifying organizing principle. The aim of this chapter will be to explore this possibility.

At zero temperature, supersymmetric theories enjoy a great degree of simplicity over non-supersymmetric ones, due to the enhanced symmetry. Various calculations can be performed to all orders in perturbation theory, or even exactly (nonperturbatively); to wit (and to name only a few), the variety of non-renormalization theorems [101, 102]; the exact determination of the space of vacua of the theory and a rigorous proof of a certain form of confinement [103]. In fact, it has been argued that the "simplest" non-free quantum field theory in four dimensions is exactly the most supersymmetric one, $\mathcal{N} = 4$ super Yang-Mills [104]. Tree-level scattering amplitudes in gauge theories enjoy remarkable simplicity including powerful recursion relations (some are reviewed in [105], where a general generating functional in the $\mathcal{N} = 4$ case is given). Contrary to other theories, however, multi-loop amplitudes in $\mathcal{N} = 4$ certainly also enjoy remarkable structure [106]. Clearly it would be of great interest if at least some of these developments could be "recycled" at nonzero temperature.

Of course, in the advent that supersymmetry is confirmed as a symmetry of nature, the study of thermal supersymmetric theories will acquire a strong impetus from the phenomenology of the early Universe. The viewpoint taken here is that a good motivation may also occur provided mathematical simplification happens in these theories.

Introductions to supersymmetry can be found in [107, 108]; a good technical reference is [102].

6.2 Introduction

Supersymmetry is usually considered as being broken at nonzero temperature (see e.g., [109]). A simple reason is the different statistics and population functions assumed by Bose and Fermi fields, making it hard to see how a Bose-Fermi symmetry could be preserved. In Euclidean space, Bose-Fermi symmetry is explicitly broken by boundary conditions along the periodic time direction (which has period $1/T$), which are respectively periodic for bosonic fields and anti-periodic for fermionic fields. More simply, the expectation value of the energy density is not zero. Nevertheless, one can still ask whether the supersymmetry of the underlying equations of motion leaves any trace in physical observables.

One example along these lines was described in [110]: due to the existence of a conserved supercurrent, the effective hydrodynamics theory which describes the long-wavelength modes of the plasma must contain fermionic degrees of freedom. In this chapter we will consider the opposite end of the energy spectrum, high-energy observables.

In the strict high-energy limit one expects the plasma to decouple, and supersymmetry to be recovered, provided it is present in the vacuum theory. More interestingly, one may look to the leading thermal corrections received by high-energy observables. We see no obvious reason why these should preserve supersymmetry. Nevertheless, the aim of this chapter is to report the intriguing fact that, for a wide class of high-energy observables, the leading corrections indeed do.

This work was motivated by the well-known observation of supersymmetry preservation for asymptotic thermal masses in weakly coupled plasmas. We will find that it also applies to other quantities, in fact to all high-energy correlators we could study. More precisely, parameterizing supersymmetry violations by the relative power of the energy E^{-n} by which they are suppressed, in all cases we find $n > 2$ with strict inequality. Since the leading thermal corrections have $n \leq 2$ in all cases, this is a nontrivial statement.

We will discuss in turn the relevant effective theories for the various observables we have considered. These include: the effective particle masses at weak coupling, in section 6.3, where previously unknown next-to-leading order results will also be reported; the imaginary part of self-energies at weak coupling (including collinear bremsstrahlung processes and $2 \to 2$ collisions), in section 6.4; the self-energies of neutral particles in strongly interacting plasmas having a gravity dual, in section 6.5; and finally the operator product expansion for deeply virtual correlators, in section 6.6.

By use of the phrase "effective theory" we mean to emphasize that the details of the plasma are always probed only through a restricted set of low-energy operators, whose expectation values provide the parameters of medium-independent high-energy effective theories. In the spirit of factorization, we thus understand supersymmetry preservation as an intrinsic property of these effective theories: the thermal or equilibrium nature of the underlying medium plays no important role.

6.3 Thermal masses at weak coupling

At the leading order in perturbation theory, thermal dispersion relations (of massless particles) are known to approach the form $E^2 = p^2 + m_\infty^2$ for any energy $E \gg g_s T$ [111], with $g_s = \sqrt{4\pi\alpha_s}$ a coupling strength. In applications to supersymmetric theories, it has been repeatedly observed that the asymptotic masses $m_\infty \sim g_\mathrm{s} T$ are the same among particles within a supersymmetry multiplet [1]. Compiling results from the literature [112], or by direct evaluation of one-loop diagrams such as those shown in Fig. 6–1, they can be summarized by the formulae:

$$\begin{aligned} m^2_{\infty,g} = m^2_{\infty,\lambda} &= g_\mathrm{s}^2 C_A \left(Z_g + Z_f^\lambda\right) \\ &+ g_\mathrm{s}^2 N_\mathrm{matter} T_M \left(Z_f^\psi + Z_\phi\right), \end{aligned} \tag{6.1a}$$

$$\begin{aligned} m^2_{\infty,\psi} = m^2_{\infty,\phi} &= g_\mathrm{s}^2 C_M \left(Z_g + Z_f^\lambda + Z_f^\psi + Z_\phi\right) \\ &+ y^2 \left(Z_f^\psi + Z_\phi\right), \end{aligned} \tag{6.1b}$$

where the Z_i are tree-level condensates that we give shortly; g, λ, ϕ and ψ stand for gluon, gluino, scalar and fermionic matter fields respectively, N_matter is the number of chiral superfields and $C_{A,M}$, $T_{A,M}$ and $d_{A,M}$ are the quadratic Casimirs, Dynkin indices and dimensions of the adjoint and matter representations, respectively. For simplicity, the Yukawa contribution in Eqs. (6.1) is normalized to correspond to a term $\sim \frac{y}{\sqrt{2}} \phi\, \psi\psi + \mathrm{c.c.}$ in the Lagrangian of a single-field Wess-Zumino model. We expect supersymmetry to be preserved for more general (e.g., nonrenormalizable) superpotentials, though we have not checked this explicitly.

Nonzero expectation values for the D or F auxiliary fields, not considered in Eqs. (6.1), could break the supersymmetry by lifting bosonic masses. As this is not a

[1] During private conversations this observation has been described to the author as "well known". A recent occurrence is in [113].

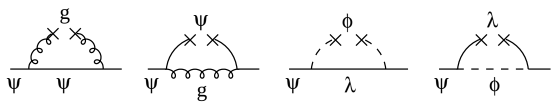

Figure 6–1: One-loop fermion self-energy of a fermion ψ due to the gauge interaction, at large energy E. At leading order the asymptotic thermal mass is the sum of four condensates, which are extracted by letting each of the propagator become soft in turn (e.g., with all components $\sim T$ in Minkowski spacetime) and expanding the rest of the diagram in powers of T/E.

specifically thermal source of supersymmetry breaking [2] , this will not be considered here.

The (non-local) dimension-two condensates in Eqs. (6.1), each normalized to give the contribution from two degrees of freedom, admit the following gauge-invariant (non-renormalized) definitions and tree-level thermal expectation values:

$$Z_g \equiv \frac{1}{d_A}\langle v_\sigma F^{\sigma\mu}\frac{-1}{(v\cdot D)^2}v_{\sigma'}F^{\sigma'}{}_{\mu}\rangle \;=\; 2\int_q \frac{n_B(q)}{q} = \frac{T^2}{6}\,, \tag{6.2a}$$

$$Z_S \equiv \frac{2}{d_M}\langle\phi^*\phi\rangle \;=\; 2\int_q \frac{n_B(q)}{q} = \frac{T^2}{6}\,, \tag{6.2b}$$

$$Z_f^\psi \equiv \frac{1}{2d_M}\langle\bar\psi\frac{\not v}{v\cdot D}\psi\rangle \;=\; 2\int_q \frac{n_F(q)}{q} = \frac{T^2}{12}\,. \tag{6.2c}$$

Here $v^\mu = (1, \mathbf{v})$ is the four-velocity of the hard particle, $\int_q = \int d^3q/(2\pi)^3$ and $n_{B,F}$ are the standard Bose-Einstein and Fermi-Dirac distribution functions. All condensates are time-ordered products, as is appropriate due to the high energy of the

[2] Turning on a temperature will not necessarily generate a nonzero expectation values for these fields. For instance, at the leading order in perturbation theory, $F \sim \phi^\dagger\phi^\dagger$ vanishes (it involves two antiholomorphic fields), and so does $D^a \sim \phi^\dagger t^a\phi$ for t^a traceless.

probe [3] . Useful examples include the thermal masses in $\mathcal{N} = 4$ SYM, which are all equal to $m_\infty^2 = g_s^2 N_c T^2$, and the gluon and gluino masses in pure glue SQCD, $m^2_{\infty,g(\lambda)} = \frac{1}{4} g_s^2 N_c T^2$.

The structures in Eqs. (6.2) are identical to those entering the Hard Thermal Loop (HTL) effective action [29, 30]. These are in fact the unique dimension-two gauge-invariant operators that can be built out of a light-like four-vector v^μ.

Although our derivation of Eqs. (6.1) was only carried out at the leading order in the coupling, we claim that it correctly describes next-to-leading order (NLO) corrections, which are $\mathcal{O}(g_s)$. The point is that, $\mathcal{O}(g_s)$ corrections arise only from $g_s T$ scale HTL physics [28] but not from the hard scale $\sim E$ (from which only $\sim g_s^2$ quantum corrections arise). But Eqs. (6.1) are precisely designed to separate high-energy physics from low-energy physics, in the spirit of a (real-time) operator product expansion, so at $\mathcal{O}(g_s)$ only the matrix elements in Eqs. (6.2) can receive corrections and not the coefficients, which contain only hard scale physics. In particular, the $\mathcal{O}(g_s)$ corrections also preserve supersymmetry. The evaluation of the condensates (6.2) at $\mathcal{O}(g_s)$, which requires HTL resummation, has not previously appeared in the literature and is performed in the Appendix 7. For completeness we record the

[3] At high energies, the retarded self-energies from which the thermal mass shifts are defined coincides with time-ordered self-energies. Furthermore, at high energies, time-ordered and anti-time-ordered propagation amplitudes decouple (see, for instance, the discussion in [114]).

results here (with $Z_f^{\rm NLO} = Z_f^{\rm LO} + \mathcal{O}(g_{\rm s}^2 T^2)$):

$$Z_g^{\rm NLO} = \frac{T^2}{6} - \frac{T m_{\infty,g}}{\pi\sqrt{2}} + \mathcal{O}(g_{\rm s}^2 T^2)\,, \tag{6.3a}$$

$$Z_S^{\rm NLO} = \frac{T^2}{6} - \frac{T m_{\infty,S}}{2\pi} + \mathcal{O}(g_{\rm s}^2 T^2)\,. \tag{6.3b}$$

Since the energy scale from which the corrections originate is $g_{\rm s}T$, the NLO mass shifts obtained by substituting Eqs. (6.3) into Eqs. (6.1) should be valid, up to $\mathcal{O}(g_{\rm s}^2)$ effects, for any energy $E \gg g_{\rm s}T$.

Next-to-leading order (momentum-averaged) thermal masses were also obtained in [50] by means of an indirect thermodynamic argument, by relating them to the well-known $\sim g_{\rm s}^3 T^3$ corrections to the QCD entropy. The final results are in agreement with Eqs. (6.3) [4] .

We have no idea about how one should make sense of Eqs. (6.1) and Eqs. (6.2) beyond NLO order when genuine quantum corrections and renormalization effects will appear (starting from order $g_{\rm s}^2$); at present the factored form (6.1) should be

[4] Although we obtain identical NLO mass shifts, it is worth noting that we disagree with their interpretation given in [50] and in [115]. Strictly speaking, the results of [50] only give momentum-averaged mass shifts, which they argue could be momentum-dependent. What we have shown is that the NLO mass shifts are momentum-independent for $E \gg g_{\rm s}T$, and this is supported by the fact that the constant values we find agree with the mean values obtained in [50]. After the present appeared as a preprint, the work of [115] was brought to our attention, in which a non-constant asymptotic behavior is found numerically at NLO. We do not understand at present the origin of the discrepancy between our analytic work and the work of [115].

viewed only as a convenient means to summarize the physics relevant at leading-order (and NLO, we have argued). In particular, we have no idea as to whether supersymmetry will survive at higher orders in perturbation theory, should it be possible at all to define asymptotic masses.

The supersymmetry of the thermal masses can be interpreted as a statement about the couplings of soft particles (of all spins) to hard propagators: these turn out to be the same among hard superpartners.

6.4 Imaginary parts of self-energies at weak coupling

The imaginary parts of self-energies at weak coupling, or scattering rates, are due to $2 \to 2$ scattering against plasma particles as well as to induced collinear radiative processes (bremsstrahlung or pair production). For charged particles in gauge theories, the dominant contribution to $\mathrm{Im}\,\Pi$ is $\sim g_s^2 T E$ due to small angle elastic Coulomb scattering, though the dominant inelastic contribution $\sim g_s^4 T^{3/2} E^{1/2}$ (barring logarithms) is due to radiative which we will discuss first. These processes also dominate the self-energies of neutral particles in gauge theories, provided these particles are allowed to pair-produce charged ones. In non-gauge theories, self-energies begin at $\sim g_s^4 T^2 E^0$ due to ordinary $2 \to 2$ scattering, which we will discuss in subsection 6.4.2.

6.4.1 Collinear radiation

At the risk of oversimplifying matters, the key aspects of collinear radiative processes may be briefly summarized as follows. These processes are only relevant in gauge theories, where they are initiated by the very frequent small-angle (Coulomb) scatterings suffered by either the parent or the daughter particles. At high-energies

$E \gg g_{\rm s}T$, their long long formation times (associated with the collinearity) allows multiple soft scatterings to occur during them and these must be summed coherently. This causes a parametrically significant destructive interference, the so-called LPM effect [65], that is responsible for the non-analytic power $\Pi \propto E^{1/2}$ (neglecting logarithms). For relativistic plasmas, a complete leading-order treatment was given in [116, 41] (see also [44, 45], in which different approximations are made). Somewhat schematically, the result may be written in the form ($-2{\rm Im}\,\Pi = 2E\Gamma$):

$$-2{\rm Im}\,\Pi_a(E) = \sum_{bc} \int_0^1 dz P_{a\to bc}(z) F_{a\to bc}(E,z)\,, \tag{6.4}$$

where $P_{a\to bc}$ are ordinary DGLAP kernels [66], governing collinear physics, the sum is over final states (bc) and $z = E_b/E_a$ is the longitudinal momentum fraction. We have omitted final state Bose-enhancement or Pauli-blocking factors, which are not needed unless z or $(1-z)$ are very small, $\sim T/E$. The functions $F(E,z)$ depend in a complicated way on E and z, and are to be obtained by solving an effective inhomogeneous Schrödinger equation for the wavefunction of the pair in the transverse plane [116]. This equation depends on the details of the plasma through a collision kernel $d\Gamma/d^2q_\perp$, which is a function of the transverse momentum transfer.

Its only property that we need, however, is that it involves only eikonal physics: it cares not about the spins of the particles. For our purposes, $F(E,z)$ in Eq. (6.4) is thus just some universal function that is the same for all final states among a given supersymmetry multiplet. In the leading logarithmic approximation [116], $F(E,z) \sim g_{\rm s}^4 N_c^2 T^{\frac{3}{2}} E^{\frac{1}{2}} z^{-\frac{1}{2}} (1-z)^{-\frac{1}{2}} (\log(\frac{ET}{g_{\rm s}^2 T^2 z(1-z)}))^{1/2}$.

Process	DGLAP kernel $P(z)$	Sum
$\gamma \to \psi^\dagger\psi$	$e^2\left[z^2+(1-z)^2\right]$	e^2
$\gamma \to \phi^\dagger\phi$	$e^2\left[2z(1-z)\right]$	
$\tilde{\gamma} \to \phi^\dagger\psi$	$e^2\left[2z\right]$	e^2
$g \to gg$	$2g_\mathrm{s}^2 C_A\left[\frac{(1-z)}{z}+\frac{z}{1-z}+z(1-z)\right]$	$g_\mathrm{s}^2 C_A\left[\frac{2}{z}+\frac{2}{1-z}-3\right]$
$g \to \lambda^\dagger\lambda$	$g_\mathrm{s}^2 C_A\left[z^2+(1-z)^2\right]$	
$\lambda \to g\lambda$	$g_\mathrm{s}^2 C_A\left[\frac{4z}{1-z}+2(1-z)\right]$	$g_\mathrm{s}^2 C_A\left[\frac{2}{z}+\frac{2}{1-z}-3\right]$
$\phi \to \psi^\dagger\psi^\dagger$	$y^2\left[1\right]$	y^2
$\psi \to \phi^\dagger\psi^\dagger$	$y^2\left[2z\right]$	y^2

Table 6–1: DGLAP splitting kernels for various branching processes. Supersymmetry is restored when complete supermultiplets of final states are summed over.

The only ingredients in Eq. (6.4) which could break supersymmetry are thus the DGLAP splitting kernels $P_{a\to bc}(z)$. Such kernels are listed in table 6–1, for various supermultiplets of initial and final states. As shown in the table, when complete supermultiplets of final states are summed over (thereby enforcing the symmetry under $z \to (1-z)$), supersymmetry with respect to the initial particle is restored. Not shown in the table (it is related to the first three entries by a crossing symmetry [117]), but which also preserves supersymmetry, is the process of bremsstrahlung of a gauge multiplet off a matter particle. Thus, all in-medium splitting rates preserve supersymmetry.

Observations of supersymmetry in DGLAP kernels were made long ago in [117], and subsequently given an explanation in [118]. Here we are simply reporting on their implications in a medium.

The $\mathcal{O}(g_\mathrm{s})$ corrections received by Eq. (6.4) have been discussed in chapter 4. Since these corrections involve only eikonalized hard particles, they manifestly preserve the supersymmetry.

The $\mathcal{O}(g_s^2)$ corrections to Eq. (6.4) are expected to possess a much more interesting and richer structure. For instance, they will most certainly require dealing with the scale dependence of the partonic constituents of the plasma, which could ultimately lead to "saturation" effects [119] at very high energies, upon summation of large logarithms $\alpha_s \log(E/T)$ and $\alpha_s \log(q_\perp^2/T^2)$ with $q_\perp^2 \sim E^{1/2}T^{3/2}$. The scale evolution of the constituents of the probe, which has to be treated in the presence of the LPM effect, should also enter at this order. Other interesting (though manifestly supersymmetry-preserving) effects may include sensitivity to nonperturbative $g_s^2 T$-scale magnetic physics, which we believe contributes to $\hat{q}$ at $\mathcal{O}(g_s^2)$. We leave to future work a detailed analysis of these effects, and of the question of whether they preserve supersymmetry.

As for effects subleading in T/E at leading order in g_s, we expect supersymmetry-breaking effects in Π not to be larger than $\sim T^{5/2}E^{-1/2}$ (relative to the $\sim E^2$ natural size); these could arise from various $\sim T/E$ or $\sim q_\perp^2/E^2 \sim (T/E)^{3/2}$ corrections to ingredients entering $F(E,z)$, such as the eikonal vertices.

6.4.2 $2 \to 2$ scattering at weak coupling

Ordinary $2 \to 2$ collisions dominate self-energies in non-gauge models, which we will now discuss; their total rate will also be found to preserve supersymmetry. We first recall the general formula for the total collision rate:

$$
\begin{aligned}
-2\mathrm{Im}\,\Pi(p_1) \quad = \quad & \int \frac{d^3p_2 d^3p_3 d^3p_4}{(2\pi)^5 2E_2 2E_3 2E_4}\,\delta^4(p_1+p_2-p_3-p_4) \\
& \times \sum_{s_2 s_3 s_4} |\mathcal{M}_{1s_2\to s_3 s_4}|^2 \\
& \times\; n_b(E_2)(1 \pm n_c(E_3))(1 \pm n_d(E_4)). \qquad (6.5)
\end{aligned}
$$

Process	$\lvert\mathcal{M}\rvert^2/4y^2$	Processes	$\lvert\overline{\mathcal{M}}\rvert^2/4y^2$
$\psi\psi \to \psi\psi$	1	$\psi\psi \to X$, $\phi\psi \to X$	1
$\phi\phi \to \phi\phi$	1	$\psi\overline{\psi} \to X$, $\phi\overline{\psi} \to X$	$\left[2 + \frac{u}{t} + \frac{t}{u}\right]$
$\phi\psi \to \phi\psi$	$-u/s$	$\psi\phi \to X$, $\phi\phi \to X$	1
		$\psi\overline{\phi} \to X$, $\phi\overline{\phi} \to X$	$\left[2 + \frac{u}{t} + \frac{t}{u}\right]$

Table 6–2: Left panel: scattering amplitudes $|\mathcal{M}|^2$ in Wess-Zumino model, with amplitudes related by crossing symmetry not shown. Right panel: amplitudes summed over final states, for which supersymmetry is restored as a function of particle 1 with particle 2 held fixed.

Here the particle labels are as defined as in Fig. 6–2, the s_i label the corresponding particle species and n_i are the corresponding distribution functions.

Let us first assume, for a moment, that the distribution functions can be omitted in the final state ("Bose-enhancement" and "Pauli-blocking") factors $(1 \pm n_i)$, which is justified for generic final state energies $E_3 \sim E_4 \sim \sqrt{E_1 E_2} \sim \sqrt{ET}$. The integrand then depends only on the sum $\sum_{s_3 s_4} |\mathcal{M}|^2_{1 s_2 \to s_3 s_4}$. Such matrix elements summed over final states turn out to obey supersymmetry identities, with respect to the particle 1, for fixed identities of particle 2. This is exemplified in table 6–2 for single-field Wess-Zumino model with cubic superpotential and a general proof will be given shortly. Therefore, contributions to Eq. (6.5) from the region $E_3, E_4 \gg T$ preserve supersymmetry.

It is easy to convince oneself that for bounded amplitudes $|\mathcal{M}|^2$, the regions $E_3 \sim T$ or $E_4 \sim T$ suffer from $\sim T/E$ phase-space suppressions, justifying the neglect of the final state distributions in Eq. (6.5). However, $s/t \sim ET/T^2$ singularities in squared matrix elements when $t \lesssim T^2$ can overcome this suppression and a separate discussion is required for the singular terms [5] ($u \to 0$ singularities can be treated similarly). To establish the supersymmetry of these contributions, for which the distribution function $n(E_4)$ must be kept, we need another ingredient: the universality of the $1/t$ singularities. Indeed, the coefficient of $1/t$ at $t \to 0$, which is due to soft fermion exchange, is left unchanged when the hard particle 1 is replaced by its superpartner (e.g. if particles 1 and 3 are exchanged in Fig. 6–2 (a)). This shows that the complete $\sim T^2 E^0$ self-energies in the Wess-Zumino model preserve supersymmetry, up to $\sim T^3 E^{-1}$ corrections.

This universality of soft couplings is reminiscent of that which played a role for thermal masses in section 6.3, and can in fact be analyzed using the same tools. Indeed, the region $E_4 \sim T$, $t \sim T^2$ in Fig. 6–2 is characterized by soft fields coupled to a hard line and is thus governed by the gradient expansion of Fig. 6–1. This means that the $\sim T^2 E^0$ contribution to Eq. (6.5) from soft fermion exchange is equivalently captured by an imaginary part of the dimension-two fermion condensates in Eqs. (6.2), at one-loop in thermal perturbation theory [6] .

We now prove, as claimed, that the supersymmetry of scattering amplitudes summed over final states holds in any supersymmetric theory as a property of its

[5] The total integral of such $\sim 1/t$ singularities is logarithmically divergent at $t \to 0$. This is cured by resumming hard thermal loop self-energies [28] to the soft exchanged fermion propagator. This does not interfere with the present argument.

[6] Conversely, for scalar exchange, the locality of the scalar condensate $\phi^* \phi$ in Eqs. (6.2) (which implies that it is purely real) is related to the absence of $1/t$ singularities coming from scalar exchange.

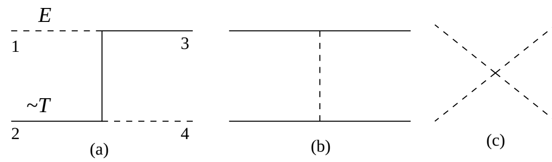

Figure 6–2: 2 → 2 scattering processes in Wess-Zumino model; solid lines are fermions and dashed lines are scalars.

vacuum S-matrix. Introducing the notation $P_{i_1\ldots i_n}$ for projection operators which perform the sum over complete supermultiplets of scattering states with n particles (at fixed momenta), this follows from considering the following trace (over scattering states):

$$\mathrm{Tr}\left[S^\dagger P_{34} S\left(|2\rangle\langle 2| \otimes \left[Q, |1\rangle\langle\tilde{1}|\right]\right)\right], \tag{6.6}$$

with S the S-matrix and $\tilde{1}$ denotes the superpartner of particle 1. For any supersymmetry generator Q which does not annihilate particle 1, the commutator $[Q, |1\rangle\langle\tilde{1}|] \propto (|1\rangle\langle 1| - |\tilde{1}\rangle\langle\tilde{1}|)$ so Eq. (6.6) computes the difference:

$$\sum_{s_3,s_4}\left(\left|M_{12\to s_3 s_4}\right|^2 - \left|M_{\tilde{1}2\to s_3 s_4}\right|^2\right). \tag{6.7}$$

For a massless particle 2 it is always possible to choose Q so as to annihilate particle 2; such a Q commutes with $|2\rangle\langle 2|$, with the S-matrix as well as with the projectors $P_{i_1\ldots i_n}$ (by construction), showing that Eq. (6.6) (and thus Eq. (6.7)) vanishes, being the trace of a commutator. Thus the contributions to Eq. (6.5) from $E_3, E_4 \gg T$ preserve supersymmetry in any theory.

Combining the results of the preceding sections, we have reached a simple conclusion: the full thermal self-energies of gauge-neutral particles preserve supersymmetry, at leading order in the coupling, up to corrections suppressed by a at least $T^{5/2}E^{-1/2}$.

Although it seems conceivable that the analysis of this subsection could be generalized to charged particles (for which it is made more complicated by the stronger singularities $\mathcal{M} \sim 1/t$ associated with gluon exchange [7] and by various sources of infrared divergences which make these self-energies less cleanly defined), here we will refrain from doing so: we are content with a robust result for gauge-invariant self-energies.

6.5 Self-energies at strong coupling

Maldacena's conjectured gauge/gravity correspondence [121] renders possible, among other things, the calculation of correlators of currents in certain strongly coupled large N_c gauge theories. In theories which have a continuous R-symmetry, such as the SU(4) of $\mathcal{N} = 4$ super Yang-Mills, "photons" and "photinos" can be introduced by weakly gauging a U(1) subgroup of the R-symmetry, whose self-energies are then given by two two-point functions of currents and of their superpartners.

In the case of the on-shell photon self-energy in $\mathcal{N} = 4$ SYM, it was argued by means of a WKB approximation [122] (in appendix) that at high energy the

[7] In the effective theory language of Fig. 6–1 these are related to certain pure-imaginary operators that are not constrained by the equality of the thermal masses. An example is the (gauge-invariant) dimension-1 eikonal amplitude $iv{\cdot}A\delta(-iv{\cdot}D)v{\cdot}A$, whose expectation value reproduces the universal (logarithmically infrared divergent) damping rate of charged particles [120]. It did not appear in our discussion of thermal masses because it is purely imaginary. At dimension-2 I also find operators like $iv{\cdot}A\delta(-iv{\cdot}D)D$ (representing e.g., an interference term between t-channel gluon exchange and D-term scalar self-interaction in $\phi\phi \to \phi\phi$ scattering) as well as its superpartner involving λ. I do not know whether these operators actually get generated and the circumstances under which they are nonzero.

calculation localizes itself near the boundary of the AdS space. Here we generalize this phenomenon to other backgrounds, which leads to a (simplistic) effective theory for high-energy photon/photino propagation in these theories, of which we can state two of its properties. First, it only probes the underlying low-energy medium through the expectation value of the energy-momentum tensor (actually, only through one component $\propto p_\mu p_\nu T^{\mu\nu}$), which determines the leading corrections to the metric at large radii. Second, it preserves supersymmetry: the absorption rates and dispersion relations of a photon and of a photino are identical.

We will be considering five-dimensional metrics of the general form

$$ds^2 = R^2 \frac{g(z)dz^2 + h_{\mu\nu}(z)dx^\mu dx^\nu}{z^2}\,, \tag{6.8}$$

for which, near the boundary $z = 0$, the metric approaches that of AdS_5 with radius R (for which $g(z) = 1$ and $h_{\mu\nu}(z) = \eta_{\mu\nu}$). The metric (6.8) should be sufficiently general to cover any system invariant under space-time translation that admits a gravity dual. For the AdS_5 black hole, relevant for $\mathcal{N} = 4$ SYM at finite temperature T, $-h_{00} = 1 - (\pi T z)^4$, $h_{ij} = \delta_{ij}$, $h_{i0} = 0$ and $g(z) = (-h_{00})^{-1}$. At certain steps below, rotational invariance will be assumed; these steps will be highlighted.

6.5.1 Bulk equations

The bulk dual of the spin-1 current which couples to the photon is a five-dimensional gauge field, whose field strength tensor obeys Maxwell's equations:

$$0 = \frac{z}{G(z)}\partial_z\left(\frac{h^{\nu\sigma}G(z)}{zg(z)}F_{z\sigma}\right) + h^{\nu\sigma}h^{\mu\rho}\partial_\mu F_{\rho\sigma}\,, \tag{6.9}$$

$$\partial_\alpha F_{\mu\nu} = \partial_\mu F_{\alpha\nu} - \partial_\nu F_{\alpha\mu}\,, \tag{6.10}$$

with $G(z) = \sqrt{g(z)\det(-h(z))}$. Here μ, ν, σ, ρ are space-time indices and α may cover all five coordinates. We will restrict our attention to space-time momentum eigenstates $\partial_\mu = ip_\mu$. A closed equation for the transverse electric field $F_{0\perp}$, for $\nu =\perp$ a component perpendicular to p_μ, may be obtained by acting on the first equation with a partial time derivative ∂_0, and using the second equation. Specifically, one uses relations such as $\partial_0 F_{z\perp} = \partial_z F_{0\perp}$, which follow from dropping perpendicular derivatives $\partial_\perp$ in the latter. To fully exploit such simplifications, rotational invariance must be assumed, so that upstairs derivative $h^{\perp\sigma}\partial_\sigma$ also vanish. This yields the closed equation:

$$\frac{zh_{\perp\perp}}{G(z)}\partial_z\left(\frac{h^{\perp\perp}G(z)}{zg(z)}\partial_z F_{0\perp}\right) = h^{\mu\nu}p_\mu p_\nu F_{0\perp}, \tag{6.11}$$

in which no summation over $\perp$-indices is implied.

The bulk dual of the spin-$\frac{1}{2}$ operator coupling to the photino is a five-dimensional Dirac fermion with bulk mass $m = \frac{1}{2}$ [123] (in units with $R = 1$). It possesses as many components as two four-dimensional Weyl spinors but it is dual to only one such spinor, the symmetry between the two Weyl components being broken by the sign of m. The bulk Dirac equation reads:

$$[\not{D} + m]\,\psi = 0 \equiv \left[\gamma^a e_a^\alpha\left(\partial_\alpha + \frac{1}{4}\omega_\alpha{}^{ab}\gamma_a\gamma_b\right) + m\right]\psi\,, \tag{6.12}$$

with $\alpha, a = 0\ldots4$ and e_a^α the orthogonal basis. Under the assumption of rotational invariance, the term involving the spin connection ω is proportional γ_z and can be removed by a z-dependent field rescaling. We choose the rescaling $\psi = z^2(\det(-h))^{-1/4}e^{-m\int^z dz\,\sqrt{g(z)}/z}\tilde{\psi}$, which leads to the following equations for the Weyl components of $\psi_{L,R}$ of $\tilde{\psi}$:

$$\partial_z \psi_L = \sqrt{g(z)}\, \not{p}_R \psi_R, \tag{6.13a}$$

$$\left[\frac{1}{\sqrt{g(z)}}\partial_z - \frac{2m}{z}\right] \psi_R = \not{p}_L \psi_L. \tag{6.13b}$$

Here $\not{p}_{L,R}$ are the Weyl operators associated with the four-dimensional metric $h_{\mu\nu}(z)$. With $m = +\frac{1}{2}$ the component relevant near the $z = 0$ boundary is ψ_L and we are calculating the self-energy of a left-handed photino. The Eqs.(6.13) square to a closed equation for ψ_L,

$$\not{p}_R \left[\frac{1}{\sqrt{g(z)}}\partial_z - \frac{2m}{z}\right] \frac{1}{\not{p}_R \sqrt{g(z)}}\partial_z \psi_L = h^{\mu\nu} p_\mu p_\nu \psi_L \,. \tag{6.14}$$

6.5.2 WKB solution and supersymmetry

We are now in position to discuss the WKB approximation. By a change of variable $y \equiv y(z)$, Maxwell's equation (6.11) may be cast in a Schrödinger form with potential proportional to the squared energy p_0^2, provided

$$\frac{dy}{dz} = 2zh_{\perp\perp}\sqrt{\frac{g(z)}{\det(-h(z))}}\,. \tag{6.15}$$

For black holes (like the AdS$_5$ black hole metric given above) the function $g(z)$ has a pole at a finite value of z (the location of the horizon), while the function $\det(-h)$ vanishes there. In this limit y is mapped logarithmically to infinity. The rescaled potential remains finite there, though, and depends only on the energy $E = p^0$.

The qualitative features of the Schrödinger potential entering the equation $[\partial_y^2 - V(y)]F_{0\perp} = 0$ are sketched in Fig. 6–3. The shape of the potential depends on the

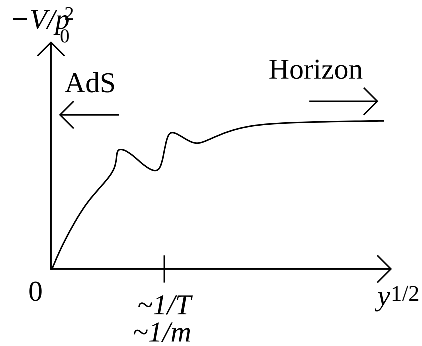

Figure 6–3: Schematic features of the Schrödinger potential $V(y)/p_0^2$, when $p^2 = 0$. It approaches the universal linear behavior (6.16) near the boundary and tends to a constant at the horizon $y \to \infty$, with a transition regime that may depend on the details of the theory and on possible intrinsic mass scales m.

geometry but not on the energy, which only determines its overall normalization. At large y the potential becomes constant, while for $y \to 0$ the leading term becomes, for on-shell and off-shell momenta respectively,

$$V(y) \to \begin{cases} \dfrac{1}{4y} p^2, & p^2 \neq 0, \\ \dfrac{y}{4} p_\mu p_\nu \dfrac{d\, h^{\mu\nu}(z)}{d(z^4)} = -y \dfrac{\pi^2 T^{\mu\nu} p_\mu p_\nu}{2N_c^2}, & p^2 = 0. \end{cases} \tag{6.16}$$

Here we have used that the leading corrections to the metric near the boundary are proportional to z^4 and are related to the expectation value of the stress-energy tensor $T_{\mu\nu}$; its trace part, if nonzero, does not contribute when $p^2 = 0$. The normalization in Eq. (6.16) is appropriate to the $\mathcal{N} = 4$ SYM theory.

At the horizon $y \to \infty$ the solutions are oscillatory and in-falling boundary conditions $F_{0\perp} \propto e^{i\omega}$ must be imposed for calculating retarded correlators [124], with $\omega = p^0 \pi T/2$ the natural frequency near the horizon. To obtain correlators of currents, as described shortly, this solution must be evolved to the AdS_5 boundary $z = 0$.

For sufficiently large energies compared to all intrinsic scales in the metric a WKB approximation can be used. This is applicable for y down to $y \sim 1/p^2$ (respectively $y \sim (T^4E^2)^{-1/3}$) for $p^2 \neq 0$ (respectively $p^2 = 0$), at which it breaks down due to the redshift factors [8] . These scales are the intrinsic scales of the Schrödinger equations with approximate potentials (6.16). The problem is thus reduced to exactly solving those approximate equations, with large y behavior matching the WKB form $\propto V^{-1/4} e^{i\int^y dy\sqrt{V}}$.

The analysis is similar for the Dirac equation (6.14), with the change of variable (6.15) replaced with $\frac{dy}{dz} = 2z\sqrt{g(z)}\,\not{p}_R(z)/\not{p}_R(z{=}0)$. For the on-shell component ψ_L^- of a left-handed photino in a rotationally-invariant background, the operator $\not{p}_R$ is nonsingular with eigenvalue $E(\sqrt{|h^{00}|} + \sqrt{h^{33}})$. Here h^{33} is the metric component along the longitudinal direction. Like for Eq. (6.15), near the boundary $y \sim z^2$ and the horizon is mapped logarithmically to $y = \infty$, and the same WKB approximation applies. More significantly, one readily sees comparing Eq. (6.14) with Eq. (6.11) that the approximate potentials near the boundary will be *identical* to the photon case (6.16).

Correlation functions are obtained by prescribing the limiting values of the fields $F_{0\perp}$ and ψ_L near the boundary and evaluating boundary terms $\propto \partial_y F_{0\perp}$ (see e.g.

[8] The transition between the two regimes $p^2 \neq 0$ and $p^2 = 0$ occurs smoothly around $|p_s^2| \sim E^{2/3}T^{4/3}$, at which value of p^2 the two estimates for y cross each other, which is exactly the "saturation scale" $p_s \sim T/x_s$ discussed in [125] (viewed as a function of E, with $x_s \equiv p_s^2/2ET$).

[122]), or proportional to $\overline{\psi}\psi \sim \psi_R/z \sim \frac{1}{\not p_R}\partial_y\psi_L$ [123]. In equations,

$$\Pi_\gamma = \frac{-N_c^2T^2}{8\pi^2}\lim_{y\to 0}\frac{\partial_y F_{0\perp}(y)}{F_{0\perp}(y)}, \quad \Pi_{\tilde{\gamma}} = \frac{-N_c^2T^2}{8\pi^2}\lim_{y\to 0}\frac{\partial_y \psi_L^-(y)}{\psi_L^-(y)}. \tag{6.17}$$

Here $\Pi_{\tilde{\gamma}} \equiv \overline{u}\Sigma u$ is the photino self-energy sandwiched between on-shell polarization spinors u, whose real part yields the thermal mass squared. The normalization of Eq. (6.17) has been obtained by matching to the well-known supersymmetry-preserving vacuum result, $\Pi_\gamma = \Pi_{\tilde{\gamma}} = -N_c^2p^2/32\pi^2\log(p^2/\mu^2)$, $p^2 = \mathbf{p}^2 - p_0^2$. On the light-cone, Schrödinger's equation with the approximate potential (6.16) is solved in terms of Bessel (Hankel) functions $F_{0\perp}(y) \sim \psi_L^- \sim y^{\frac{1}{2}}H_{\frac{1}{3}}(\frac{2}{3}\tilde{\omega}y^{\frac{3}{2}})$ with $\tilde{\omega}^2 = \pi^2T_{\mu\nu}p^\mu p^\nu/2N_c^2$, yielding with Eq. (6.17) the result:

$$\Pi_\gamma(p) = \Pi_{\tilde{\gamma}}(p) = \frac{N_c^2\Gamma\left(\frac{2}{3}\right)}{16\pi^2\Gamma\left(\frac{1}{3}\right)}\left(3^{\frac{1}{3}} - i3^{\frac{5}{6}}\right)\tilde{\omega}^{\frac{2}{3}} \tag{6.18}$$

at large $p^0 = p$. The imaginary part of this result reproduces that given in [122] (see also [125]) in $\mathcal{N} = 4$ SYM (employing that $\tilde{\omega} = p^0T^2\pi^2/2$ then). Corrections in T/E to this result may be found by expanding the potential (6.16) to higher orders near the boundary; for the AdS$_5$ black hole this expansion proceeds in powers of $y^2 \sim \tilde{\omega}^{-4/3}$, so the first subleading corrections to Π are $\sim \tilde{\omega}^{-2/3}$.

We find it remarkable that photon self-energies at strong coupling and high energies depend on only *one* property of the plasma: its stress-energy tensor. On the gravity side this may be understood as due to the universal, spin-independent gravitational attraction towards the black hole at large distances. An heuristic field-theoretic picture of strongly coupled plasmas, based on the idea of parton saturation, has been proposed recently [125] in which such a universality also comes out naturally.

6.6 Deeply virtual correlators

Deeply virtual correlators, which for instance can be related to sum rules for spectral functions (e.g., dilepton production rates) or to their asymptotics, may be analyzed by means of the operator product expansion (OPE) [126]. The OPE is a systematic means of separating short-distance and long-distance physics, allowing the thermal corrections to deeply virtual (short-distance) correlators with $E \gg T$ to be expressed in terms of the expectation value of local operators. Thermal corrections are thus suppressed by powers $\sim E^{-\Delta}$ with the Δ's determined by the scaling dimensions of local operators [9] .

The difference between a correlator of operators and of their superpartners is a supersymmetry variation (in agreement with the fact that it vanishes in supersymmetry-preserving vacua). For instance, for correlators of transverse currents $\epsilon_\mu J^\mu$ and of their superpartners λ_α, one schematically has:

$$\epsilon_1{\cdot}J(p)\,\epsilon_2{\cdot}J - \frac{1}{2}\lambda^\dagger(p)\,\not{\epsilon}_1\,\not{p}\,\not{\epsilon}_2\lambda \propto \epsilon_1^{\alpha\dot{\alpha}}\,Q_\alpha\Big(\lambda^\dagger_{\dot{\alpha}}(p)\epsilon_2{\cdot}J\Big)\,, \tag{6.19}$$

with $p_\mu\epsilon^\mu_{1,2} = 0$, $\alpha, \dot{\alpha}$ spinor indices, and Q_α a supersymmetry transformation. As an operator equation, the OPE must commute with the supersymmetries, so from the OPE of the right-hand side of Eq. (6.19) one concludes that the operators on its left-hand side must be *supersymmetry variations*. This has a simple consequence:

[9] It may be worth noting that the OPE is most rigorously formulated in Euclidean signature, even though we are considering applying it in Minkowski signature, where it does not enjoy the same rigorous status (see e.g., [127]).

supersymmetry violations of order E^{-2} or stronger, in the deeply virtual region, can only be seen if there exists *local* gauge-invariant fermionic operators of dimension $\frac{3}{2}$ or less.

In a wide class of theories there is an accidental symmetry: such operators do not exist. These theories certainly include all weakly coupled gauge theories containing no U(1) vector multiplets and no gauge-singlet chiral superfields. In these theories, the only gauge-invariant dimension-2 bosonic operators (such as $\mathrm{Tr}\,\phi\phi$ or $\mathrm{Tr}\,\phi^*\phi$) do not correspond to any supersymmetry variations, and thus cannot cause supersymmetry violations. The lowest-dimensional fermionic operators are dimension-$\frac{5}{2}$ supercurrents, from which we conclude that thermal supersymmetry breaking can only be seen through dimension-3 operators, $\sim E^{-3}$.

When neutral chiral superfields or U(1) vector multiplets are present, nonzero expectation values for $D \sim \phi^*\phi$ or $F \sim \phi^*\phi^*$ auxiliary fields (which enter the supersymmetry transformations of gauginos and fermionic matter fields, respectively) could produce supersymmetry violations at dimension 2. A similar possibility was observed for thermal masses in section 6.3 but, as we discussed there, we do not view it as being specifically related to thermal effects. Thus, we conclude that in weakly coupled theories, there generically cannot be supersymmetry breaking (in deeply virtual correlators) due to thermal effects below dimension-3.

It is not possible to analyze general theories at finite values of the coupling constants, because finite anomalous dimensions can alter the power counting. Nevertheless, for certain strongly coupled theories accessible to the AdS/CFT correspondence, it is easy to be more quantitative. For instance, it is known [128] that in $\mathcal{N} = 4$ SYM at large 't Hooft coupling $\lambda \gg 1$, only protected (chiral) operators have finite dimensions $\Delta \ll \lambda^{1/4}$ and that the lowest-dimensional fermionic operator has dimension $2+\frac{1}{2} = \frac{5}{2}$ (it is the supersymmetry variation of a dimension-2 primary field). Similarly, the $\mathcal{N} = 1$ theory dual to IIB string theory on $\mathrm{AdS}_5 \times \mathrm{T}^{11}$ [129] is known to contain no fermionic operator of dimension less than 2 [130]. Thus, in these theories, supersymmetry violations (in the deeply virtual regime) can only be seen at $\sim E^{-3}$ or $\sim E^{-\frac{5}{2}}$ levels, respectively. A discussion of more general strongly coupled theories will not be attempted here.

6.7 Concluding remarks

In this chapter we have shown that supersymmetry is a generic property of the effective theories which describe high-energy correlators in supersymmetric theories, even in the presence of an underlying medium. The correlators studied include self-energies at high energies on the light-cone as well as far away from it (large virtuality).

For all correlators (except for the more tractable deeply virtual correlators treated in section 6.6) our analysis has been limited to the leading nontrivial order (and sometimes NLO) at both weak and strong coupling. Without an understanding of the structure of higher order corrections, which is presently lacking, it seems hard however to decide whether our findings highlight general structural properties of supersymmetric theories, or whether they are artefacts of these extreme limits. Nevertheless we find the presented evidence quite suggestive, especially since it includes both weakly and strongly coupled regimes.

We have found that thermal supersymmetry violations in all correlators are suppressed by a power of the energy E^{-n} relative to the vacuum correlators, with n *strictly greater than* 2. (Violations with $n = 2$ were observed in sections 6.3 and 6.6 due to nonvanishing D-term or F-term expectation values, but we do not regard these effects as being of a specifically thermal origin.) We find pleasing that such a simple and uniform bound holds: this makes one wonder whether it could be a consequence of some general principle which would be valid independently of a perturbation theory, though at present we have no concrete proposal to make along these lines.

Finally, our results strongly suggest that hard processes in supersymmetric theories will be considerably simpler to describe, beyond the leading order in the coupling, than in non-supersymmetric ones since supersymmetry is essentially preserved at the hard scale. We hope that the study of hard processes in these theories will lead in the future to fruitful insights into factorization at finite temperature in general.

CHAPTER 7
Conclusion and outlook

We summarize briefly what we have done in this thesis, highlighting possibilities for extensions in the near future.

In chapter 2 we have reviewed the general formalism of finite temperature field theory.

In chapter 3 we have presented a novel technique for calculating a class of spacelike and lightlike observables using Euclidean field theory, which applies to any correlator localized on a spacelike or timelike hyperplane. The technique is new and general, and in a special case it was used to shed light on a previously known sum rule.

In chapter 4 we have used it to evaluate for the first time the effects on jet quenching of interferences occurring between in-medium scatterings. Namely, we have shown that in the high-energy (eikonal) limit, such interferences can be accounted for by a modification of the scattering rate. We have calculated this rate to the next-to-leading order in the coupling g_{s}, and shown that it suffers, at soft momentum transfers of order the temperature ($g_{\mathrm{s}}T$ to be more precise), from severe uncertainties at any realistic value of the coupling, and even much smaller ones.

There are several possibilities for short-term and middle-term improvements of the theory of jet quenching. As discussed in that chapter, there presently exists in the literature discrepancies regarding the estimated values of microscopic parameters, due to different theoretical modelling of the experimental data. This is a well-recognized outstanding issue, whose resolution will open the way to an unbiased discussion of the properties of the quark-gluon plasma.

Our results indicate that the rates for soft collisions should not be considered as being known when jet quenching data is fit. Therefore, it would be valuable to quantify, using simulations of jet quenching including realistic hydrodynamical modelling of the fireball, possible signatures on jet quenching observables of specifically soft collisions, which would allow for the experimental extraction of their rate. One such signature was proposed at the end of that chapter.

Finally, we have suggested that numerical lattice simulations within a simplified, three-dimensional, Euclidean effective theory could correctly pick up the largest corrections to the soft collision kernel. This would, for the first time for a transport coefficient, nonperturbatively resum a set of corrections that are known to be large, thereby greatly improving the quality of comparison between theory and experiments.

In chapter 5 we have discussed the Langevin model of heavy-quark energy loss from the viewpoint of the underlying microscopic theory QCD. We have substantiated the heuristic notion of the Langevin momentum diffusion coefficient as a "force-force correlator" by defining the appropriate QCD correlator, for the first time taking into account quantum-mechanical renormalization effects. More concretely, we have related it to the zero-frequency slope of a spectral function whose corresponding Euclidean correlator we have defined. This Euclidean correlator could in principle be measured through non-perturbative simulations of four-dimensional Euclidean lattice gauge theory. We have argued that the spectral function should be remarkably featureless at low frequencies (no sharp peaks), making the prospects for its reconstruction from Euclidean lattice data particularly good.

If this reconstruction can be carried out, which may ultimately rest on the statistics that can be achieved for this correlator, the result would be a robust parameter-free description of heavy-quark energy loss at low velocities. Combined with an improved understanding of the relativistic regime coming from jet quenching studies, this would significantly narrow the present uncertainties in describing heavy-quark energy loss.

In chapter 6, motivated by the need to perform perturbative calculations at the hard scale and by the simplifications of hard scale scattering amplitudes which occur in supersymmetric theories, in particular in $\mathcal{N} = 4$ super Yang-Mills theory, we have studied hard processes in finite-temperature supersymmetric theories. We have shown, through explicit leading-order computations at weak and strong coupling, that supersymmetry is preserved at high energies roughly as much as it could possibly be: all supersymmetry violations due to finite temperature effects can be factored into low-energy data. This makes the prospects for higher-order computations at the hard scale particularly good in these theories, and one would further hope that a factorization scheme capable of preserving hard scale supersymmetry at higher orders, whose existence it is natural to conjecture at this stage, could find applications in other theories as well.

In conclusion, relativistic many-body systems constitute an exciting and relatively young field of study, with potentially many important discoveries awaiting in the future. This is especially so in view of the ongoing experimental program at RHIC and of the coming one at the LHC. RHIC has entered an era of precision measurements, during which hard probes of the quark-gluon plasma will be called upon to play an increasingly important role. We hope to have conveyed in this thesis a good sense of some of the possible developments.

Appendix A: Examples of dynamics leading to a transport peak

In this appendix, we review briefly two arguments through which the Lorentzian form of the transport peak in Eq. (5.4) can be established explicitly.

Consider first non-relativistic quantum mechanics. Let us define $\hat{v}_i = \hat{p}_i/M_{\rm kin}$, where $\hat{p}_i$ is the momentum operator of the heavy quarks (i.e. the generator of translations in their Hilbert space). Suppose that we have, through some external source field, managed to prepare a non-equilibrium state where there is a heavy quark with a non-zero velocity. In thermal equilibrium, the average velocity must vanish, so we may expect the system to behave as

$$\frac{\mathrm{d}}{\mathrm{d}t}\langle \hat{v}_i(t)\rangle_{\text{non-eq}} = -\eta_D \, \langle \hat{v}_i(t)\rangle_{\text{non-eq}} + \mathcal{O}\Big(\langle \hat{v}_i(t)\rangle^2_{\text{non-eq}}\Big) \; . \tag{7.1}$$

Once t is so large that $\langle \hat{v}_i(t)\rangle_{\text{non-eq}} \sim [\langle \hat{v}_i^2\rangle_{\text{eq}}]^{1/2}$, Brownian motion sets in, and the system effectively equilibrates. In equilibrium we may define the correlator

$$\Delta_{ii}(t) \equiv \left\langle \frac{1}{2}\{\hat{v}_i(t), \hat{v}_i(0)\} \right\rangle_{\text{eq}} \; . \tag{7.2}$$

This is an even function of t and must vanish for $t \to \infty$; in fact, at least on certain time scales, it can be argued that it vanishes with the *same* exponent as the non-equilibrium correlator in Eq. (7.1) (see, e.g., §118 of ref. [131]):

$$\Delta_{ii}(t) \stackrel{|t|\gg\beta}{\simeq} \bar{\Delta}_{ii}\, e^{-\eta_D |t|} \; , \tag{7.3}$$

where $\bar{\Delta}_{ii}$ is a constant. Taking a Fourier transform yields

$$\tilde{\Delta}_{ii}(\omega) \equiv \int_{-\infty}^{\infty} \mathrm{d}t\, e^{i\omega t}\, \Delta_{ii}(t) \overset{|\omega| \ll T}{\simeq} \bar{\Delta}_{ii} \frac{2\eta_D}{\omega^2 + \eta_D^2} \;, \tag{7.4}$$

and making use of the general relation $\tilde{\Delta}_{ii}(\omega) = [1 + 2n_{\mathrm{B}}(\omega)]\, \rho_{ii}(\omega)$ (see, e.g., ref. [13]), where $n_{\mathrm{B}}(\omega) \equiv 1/[\exp(\beta\omega) - 1]$ and $\rho_{ii}(\omega)$ is the spectral function, we arrive at

$$\frac{\rho_{ii}(\omega)}{\omega} \overset{|\omega| \ll T}{\approx} \frac{1}{2T} \tilde{\Delta}_{ii}(\omega) \overset{|\omega| \ll T}{\simeq} \bar{\Delta}_{ii} \frac{\beta\eta_D}{\omega^2 + \eta_D^2} \;. \tag{7.5}$$

This indeed agrees with the functional form of Eq. (5.4).

Another example is given by classical Langevin dynamics (see also ref. [85]). Essentially, we replace $\langle \hat{p}_i(t) \rangle_{\text{non-eq}} \to p_i(t)$, and assume the dynamics to be contained in

$$\dot{p}_i(t) \;=\; -\eta_D\, p_i(t) + \xi_i(t) \;, \tag{7.6}$$

$$\langle\!\langle \xi_i(t) \xi_j(t') \rangle\!\rangle \;=\; \kappa_{\mathrm{cl}}\, \delta_{ij} \delta(t - t') \;, \qquad \langle\!\langle \xi_i(t) \rangle\!\rangle = 0 \;, \tag{7.7}$$

with ξ a Gaussian stochastic noise field, and $\langle\!\langle ... \rangle\!\rangle$ denoting an average over the noise. For a heavy particle the Gaussian nature follows from the central limit theorem and the slow time scale of its dynamics, while the auto-correlator $\kappa_{\mathrm{cl}} = \int_{-\infty}^{\infty} \mathrm{d}t\, \langle\!\langle \xi_i(t) \xi_i(0) \rangle\!\rangle$ can be chosen such as to match that of the underlying theory, Eq. (5.5). It is easy to verify that within this dynamics, for a distribution with density $T\chi^{00}$ of heavy quarks, the equilibrium correlator is exactly Eq. (5.4).

Appendix B: Calculation of next-to-leading thermal masses

In this Appendix we evaluate the next-to-leading order ($\mathcal{O}(g)$) corrections (6.3) to the condensates (6.2), which are related to thermal masses. The corrections originate from the difference between using bare and HTL-resummed propagators, Eqs. (2.21).

For the scalar condensate we use the fact that the scalar HTL self-energy is simply a constant mass shift (see [30]). The calculation of $Z_S = 2\Phi^*\Phi$ can be done in Euclidean space, where only the zero Matsubara mode contributes to the $\mathcal{O}(g)$ correction:

$$\delta Z_S = 2T \int_q \left[\frac{1}{q^2 + m_{\infty,S}^2} - \frac{1}{q^2} \right] = \frac{-T m_{\infty,S}}{2\pi}. \tag{7.8}$$

A quick way to evaluate the shift to the gluon condensate is to use the fact that $-m_D^2 d_A/4$ times the angular average of Z_g is precisely the HTL effective action [29, 30], so $\langle Z_g \rangle = -4\langle \Gamma_{\mathrm{HTL}} \rangle / m_D^2 d_A$. Given the physical significance of this effective action, it should be possible to evaluate it in Euclidean space, where it reduces to a constant mass shift $\Gamma_{\mathrm{HTL}}^{\mathrm{Euclidean}} = -m_D^2 A_4 A_4/2$ for the zero Matsubara mode of the temporal gauge field (see, for instance, Chapter 5 of the review [16]), plus negligible corrections to the other modes. Thus,

$$\begin{aligned} \delta Z_g &= \frac{2}{d_A} \delta \langle A_4 A_4 \rangle \\ &= 2T \int_q \left[\frac{1}{q^2 + m_D^2} - \frac{1}{q^2} \right] = \frac{-T m_D}{2\pi}, \end{aligned} \tag{7.9}$$

which reproduces Eq. (6.3)(a) upon using $m_D = m_{\infty,g}\sqrt{2}$.

The only seemingly weak point of the preceding paragraph is the appeal to Euclidean techniques. This can be rigorously justified using the techniques developed in chapter 3: real-time expectation values localized on the lightcone in configuration space, such as Z_g, can always be cast to Matsubara sums, which reduce in the classical approximation ($n_B(\omega) = T/\omega$, which is justified for the NLO correction) to the $\omega_E = 0$ contribution in Eq. (7.9). This proves the first line of Eq. (7.9). Of course, it is always possible to verify Eq. (7.9) directly by numerically integrating the Minkowski-signature operator Z_g in Eqs. (6.2), evaluated with HTL-resummed propagators (and with bare propagators subtracted); we have done this.

REFERENCES

[1] D. J. Gross and F. Wilczek, Phys. Rev. Lett. **30**, 1343 (1973).

[2] H. D. Politzer, Phys. Rev. Lett. **30**, 1346 (1973).

[3] J. C. Collins and M. J. Perry, Phys. Rev. Lett. **34**, 1353 (1975).

[4] E.V.Shuryak, Phys. Reports 61 (1980) 71.

[5] I. Arsene *et al.* [BRAHMS Collaboration], Nucl. Phys. A **757**, 1 (2005) [arXiv:nucl-ex/0410020].

[6] K. Adcox *et al.* [PHENIX Collaboration], Nucl. Phys. A **757**, 184 (2005) [arXiv:nucl-ex/0410003].

[7] B. B. Back *et al.* [PHOBOS Collaboration], Nucl. Phys. A **757**, 28 (2005) [arXiv:nucl-ex/0410022].

[8] J. Adams *et al.* [STAR Collaboration], Nucl. Phys. A **757**, 102 (2005) [arXiv:nucl-ex/0501009].

[9] J. D. Bjorken, Phys. Rev. D **27**, 140 (1983).

[10] M. Luzum and P. Romatschke, Phys. Rev. C **78**, 034915 (2008) [Erratum-ibid. C **79**, 039903 (2009)] [arXiv:0804.4015 [nucl-th]]; U. W. Heinz, arXiv:0901.4355 [nucl-th]; D. Teaney, Phys. Rev. C **68**, 034913 (2003) [arXiv:nucl-th/0301099].

[11] M. E. Peskin and D. V. Schroeder, "An Introduction To Quantum Field Theory," Reading, USA: Addison-Wesley (1995).

[12] C. Itzykson and J. B. Zuber, "Quantum Field Theory," New York, USA: Mcgraw-hill (1980) (International Series In Pure and Applied Physics).

[13] J. I. Kapusta and C. Gale, "Finite-temperature field theory: Principles and applications," *Cambridge, UK: Univ. Pr. (2006) 428 p.*

[14] M. Le Bellac, "Thermal Field Theory", Cambridge 1996.

[15] P. Arnold, G. D. Moore and L. G. Yaffe, JHEP **0301**, 030 (2003) [arXiv:hep-ph/0209353].

[16] J. P. Blaizot and E. Iancu, Phys. Rept. **359**, 355 (2002) [arXiv:hep-ph/0101103].

[17] J. Schwinger, J. Math. Phys. 2, 407 (1961), L. V. Keldysh, Sov. Phys. JETP 20, 1018 (1964).

[18] T. S. Evans and A. C. Pearson, Phys. Rev. D **52**, 4652 (1995) [arXiv:hep-ph/9412217]; A. Niegawa, Phys. Rev. D **40**, 1199 (1989).

[19] A. Niegawa, Phys. Rev. D **40**, 1199 (1989); F. Gelis, Phys. Lett. B **455**, 205 (1999) [arXiv:hep-ph/9901263].

[20] K. C. Chou, Z. B. Su, B. L. Hao and L. Yu, Phys. Rept. **118**, 1 (1985). See also, M. v. Eijck, R. Kobes, Ch. v. Weert, Phys. Rev. D **50**, 4097 (1994).

[21] S. Caron-Huot, JHEP **0904**, 004 (2009) [arXiv:0710.5726 [hep-ph]].

[22] K. Osterwalder and R. Schrader, Commun. Math. Phys. **42**, 281 (1975); K. Osterwalder and R. Schrader, Commun. Math. Phys. **31**, 83 (1973).

[23] L. P. Kadanoff and G. Baym, "Quantum statistical mechanics: Green's function methods in equilibrium and non-equilibrium problems", New York: W. A. Benjamin 203 p., 1964.

[24] T. S. Evans, Nucl. Phys. B **374**, 340 (1992).

[25] F. Guerin, Nucl. Phys. B **432**, 281 (1994) [arXiv:hep-ph/9306210].

[26] E. M. Lifshitz and L. P. Pitaevskiĩ, "Physical kinetics", Oxford; New York: Pergamon Press 452 p., 1981.

[27] S. Ichimaru, "Statistical plasma physics", Redwood City, Calif.: Addison-Wesley Pub. Co., 1992.

[28] E. Braaten and R. D. Pisarski, Nucl. Phys. B **337**, 569 (1990).

[29] J. Frenkel and J. C. Taylor, Nucl. Phys. B **334**, 199 (1990).

[30] E. Braaten and R. D. Pisarski, Phys. Rev. D **45**, 1827 (1992).

[31] J. C. Taylor and S. M. H. Wong, Nucl. Phys. B **346**, 115 (1990).

[32] P. F. Kelly, Q. Liu, C. Lucchesi and C. Manuel, Phys. Rev. D **50**, 4209 (1994)

[33] T. Appelquist and R. D. Pisarski, Phys. Rev. D **23**, 2305 (1981).

[34] K. Farakos, K. Kajantie, K. Rummukainen and M. E. Shaposhnikov, Nucl. Phys. B **425**, 67 (1994) [hep-ph/9404201].

[35] M. Laine and Y. Schroder, JHEP **0503**, 067 (2005) [arXiv:hep-ph/0503061].

[36] D. J. Gross, R. D. Pisarski and L. G. Yaffe, Rev. Mod. Phys. **53**, 43 (1981).

[37] F. Di Renzo, M. Laine, V. Miccio, Y. Schroder and C. Torrero, JHEP **0607**, 026 (2006) [arXiv:hep-ph/0605042].

[38] P. Arnold and C. Zhai, Phys. Rev. D **51**, 1906 (1995) [arXiv:hep-ph/9410360].

[39] E. Braaten and A. Nieto, Phys. Rev. Lett. **76**, 1417 (1996) [arXiv:hep-ph/9508406].

[40] K. Kajantie, M. Laine, K. Rummukainen and Y. Schroder, Phys. Rev. D **67**, 105008 (2003) [arXiv:hep-ph/0211321]; F. Di Renzo, M. Laine, V. Miccio, Y. Schroder and C. Torrero, JHEP **0607**, 026 (2006) [arXiv:hep-ph/0605042].

[41] P. Arnold, G. D. Moore and L. G. Yaffe, JHEP **0206**, 030 (2002) [arXiv:hep-ph/0204343].

[42] P. Aurenche, F. Gelis and H. Zaraket, JHEP **0205**, 043 (2002) [arXiv:hep-ph/0204146].

[43] M. Gyulassy and X. n. Wang, Nucl. Phys. B **420**, 583 (1994) [arXiv:nucl-th/9306003].

[44] R. Baier, Y. L. Dokshitzer, S. Peigne and D. Schiff, Phys. Lett. B **345**, 277 (1995) [arXiv:hep-ph/9411409]. R. Baier, Y. L. Dokshitzer, A. H. Mueller, S. Peigne and D. Schiff, Nucl. Phys. B **483**, 291 (1997) [arXiv:hep-ph/9607355].

[45] B. G. Zakharov, JETP Lett. **65**, 615 (1997) [hep-ph/9704255]; **63** 952 (1996) [hep-ph/9607440].

[46] I. Vitev and M. Gyulassy, Phys. Rev. Lett. **89**, 252301 (2002) [arXiv:hep-ph/0209161].

[47] S. A. Bass, C. Gale, A. Majumder, C. Nonaka, G. Y. Qin, T. Renk and J. Ruppert, arXiv:0808.0908 [nucl-th].

[48] H. Schulz, Nucl. Phys. B **413** 353 (1993).

[49] M. E. Carrington, A. Gynther and D. Pickering, Phys. Rev. D **78**, 045018 (2008) [arXiv:0805.0170 [hep-ph]].

[50] J. P. Blaizot, E. Iancu and A. Rebhan, Phys. Rev. D **63**, 065003 (2001) [arXiv:hep-ph/0005003]; J. P. Blaizot, E. Iancu, U. Kraemmer and A. Rebhan, JHEP **0706**, 035 (2007) [arXiv:hep-ph/0611393].

[51] S. Caron-Huot and G. D. Moore, Phys. Rev. Lett. **100**, 052301 (2008) [arXiv:0708.4232 [hep-ph]]; S. Caron-Huot and G. D. Moore, JHEP **0802**, 081 (2008) [arXiv:0801.2173 [hep-ph]].

[52] J. P. Blaizot, E. Iancu and A. Rebhan, Phys. Rev. D **68**, 025011 (2003) [arXiv:hep-ph/0303045].

[53] K. Kajantie, M. Laine, K. Rummukainen and Y. Schroder, Phys. Rev. Lett. **86**, 10 (2001) [arXiv:hep-ph/0007109].

[54] E. Braaten and M. H. Thoma, Phys. Rev. D **44**, R2625 (1991); Phys. Rev. D **44**, 1298 (1991).

[55] J. Casalderrey-Solana and D. Teaney, JHEP **0704**, 039 (2007) [arXiv:hep-th/0701123].

[56] S. S. Gubser, Nucl. Phys. B **790**, 175 (2008) [arXiv:hep-th/0612143].

[57] H. Liu, K. Rajagopal and U. A. Wiedemann, Phys. Rev. Lett. **97**, 182301 (2006) [arXiv:hep-ph/0605178].

[58] H. Liu, K. Rajagopal and Y. Shi, JHEP **0808**, 048 (2008) [arXiv:0803.3214 [hep-ph]].

[59] Y. Hatta, E. Iancu and A. H. Mueller, JHEP **0805**, 037 (2008) [arXiv:0803.2481 [hep-th]].

[60] S. S. Gubser, D. R. Gulotta, S. S. Pufu and F. D. Rocha, arXiv:0803.1470 [hep-th].

[61] P. M. Chesler, K. Jensen, A. Karch and L. G. Yaffe, arXiv:0810.1985 [hep-th].

[62] P. Arnold and W. Xiao, Phys. Rev. D **78**, 125008 (2008) [arXiv:0810.1026 [hep-ph]].

[63] G. Y. Qin, J. Ruppert, C. Gale, S. Jeon, G. D. Moore and M. G. Mustafa, Phys. Rev. Lett. **100**, 072301 (2008) [arXiv:0710.0605 [hep-ph]].

[64] M. Gyulassy, P. Levai and I. Vitev, Nucl. Phys. B **594**, 371 (2001) [arXiv:nucl-th/0006010]; M. Gyulassy, P. Levai and I. Vitev, Phys. Rev. Lett. **85**, 5535 (2000) [arXiv:nucl-th/0005032].

[65] L. D. Landau and I. Pomeranchuk, Dokl. Akad. Nauk Ser. Fiz. **92** (1953) 535; L. D. Landau and I. Pomeranchuk, Dokl. Akad. Nauk Ser. Fiz. **92** (1953) 735; A. B. Migdal, Dokl. Akad. Nauk S.S.S.R. **105**, 77 (1955); A. B. Migdal, Phys. Rev. **103**, 1811 (1956).

[66] V. N. Gribov and L. N. Lipatov, Sov. J. Nucl. Phys. **15** (1972) 438; V. N. Gribov and L. N. Lipatov, Sov. J. Nucl. Phys. **15** (1972) 675; L. N. Lipatov, Sov. J. Nucl. Phys. **20** (1975) 94; G. Altarelli and G. Parisi, Nucl. Phys. **B126** (1977) 298; Yu. L. Dokshitzer, Sov. Phys. JETP **46** (1977) 641.

[67] S. Jeon and G. D. Moore, Phys. Rev. C **71**, 034901 (2005) [arXiv:hep-ph/0309332].

[68] P. Arnold and C. Dogan, Phys. Rev. D **78**, 065008 (2008) [arXiv:0804.3359 [hep-ph]].

[69] A. Majumder, arXiv:0810.1367 [nucl-th].

[70] C. A. Salgado and U. A. Wiedemann, Phys. Rev. D **68**, 014008 (2003) [arXiv:hep-ph/0302184].

[71] P. Arnold, arXiv:0903.1081 [nucl-th].

[72] B. G. Zakharov, JETP Lett. **73**, 49 (2001) [Pisma Zh. Eksp. Teor. Fiz. **73**, 55 (2001)] [arXiv:hep-ph/0012360].

[73] Z. T. Liang, X. N. Wang and J. Zhou, Phys. Rev. D **77**, 125010 (2008) [arXiv:0801.0434 [hep-ph]].

[74] L. S. Brown, Phys. Rev. D **62**, 045026 (2000) [arXiv:physics/9911056].

[75] N. Armesto, M. Cacciari, T. Hirano, J. L. Nagle and C. A. Salgado, arXiv:0907.0667 [hep-ph].

[76] P. Arnold, arXiv:0903.1081 [nucl-th].

[77] K. J. Eskola, H. Honkanen, C. A. Salgado and U. A. Wiedemann, Nucl. Phys. A **747**, 511 (2005) [arXiv:hep-ph/0406319]; A. Dainese, C. Loizides and G. Paic, Acta Phys. Hung. A **27**, 245 (2006) [arXiv:hep-ph/0511045]; A. Dainese, C. Loizides and G. Paic, Eur. Phys. J. C **38**, 461 (2005) [arXiv:hep-ph/0406201].

[78] W. Horowitz, Nucl. Phys. A **783**, 543 (2007) [arXiv:nucl-th/0610024].

[79] R. Rapp and H. van Hees, arXiv:0903.1096 [hep-ph].

[80] B.I. Abelev *et al.* [STAR Collaboration], Phys. Rev. Lett. 98 (2007) 192301 [nucl-ex/0607012]; A. Adare *et al.* [PHENIX Collaboration], Phys. Rev. Lett. 98 (2007) 172301 [nucl-ex/0611018].

[81] E. Braaten and M.H. Thoma, Phys. Rev. D 44 (1991) 1298; Phys. Rev. D 44 (1991) 2625.

[82] B. Svetitsky, Phys. Rev. D 37 (1988) 2484.

[83] G.D. Moore and D. Teaney, Phys. Rev. C 71 (2005) 064904 [hep-ph/0412346].

[84] R. Baier, Yu.L. Dokshitzer, S. Peigné and D. Schiff, Phys. Lett. B 345 (1995) 277 [hep-ph/9411409].

[85] P. Petreczky and D. Teaney, Phys. Rev. D 73 (2006) 014508 [hep-ph/0507318].

[86] C.P. Herzog, A. Karch, P. Kovtun, C. Kozcaz and L.G. Yaffe, JHEP 07 (2006) 013 [hep-th/0605158]; S.S. Gubser, Phys. Rev. D 74 (2006) 126005 [hep-th/0605182].

[87] J. Casalderrey-Solana and D. Teaney, Phys. Rev. D 74 (2006) 085012 [hep-ph/0605199].

[88] H. van Hees, V. Greco and R. Rapp, Phys. Rev. C 73 (2006) 034913 [nucl-th/0508055]; H. van Hees, M. Mannarelli, V. Greco and R. Rapp, Phys. Rev. Lett. 100 (2008) 192301 [0709.2884].

[89] S. Caron-Huot and G.D. Moore, Phys. Rev. Lett. 100 (2008) 052301 [0708.4232]; JHEP 02 (2008) 081 [0801.2173].

[90] E. Eichten, Nucl. Phys. Proc. Suppl. 4 (1988) 170; N. Isgur and M.B. Wise, Phys. Lett. B 232 (1989) 113; E. Eichten and B.R. Hill, Phys. Lett. B 234

(1990) 511; B. Grinstein, Nucl. Phys. B 339 (1990) 253; H. Georgi, Phys. Lett. B 240 (1990) 447.

[91] J.G. Körner and G. Thompson, Phys. Lett. B 264 (1991) 185.

[92] G. Aarts, C. Allton, J. Foley, S. Hands and S. Kim, Phys. Rev. Lett. 99 (2007) 022002 [hep-lat/0703008]; H.B. Meyer, Phys. Rev. D 76 (2007) 101701 [0704.1801].

[93] E. Braaten and R.D. Pisarski, Phys. Rev. D 42 (1990) 2156.

[94] M. Laine, G.D. Moore, O. Philipsen and M. Tassler, JHEP **0905**, 014 (2009) [arXiv:0902.2856 [hep-ph]].

[95] S.S. Gubser, Nucl. Phys. B 790 (2008) 175 [hep-th/0612143].

[96] Y. Koma, M. Koma and H. Wittig, Phys. Rev. Lett. 97 (2006) 122003 [hep-lat/0607009].

[97] A. Huntley and C. Michael, Nucl. Phys. B 286 (1987) 211.

[98] D. Guazzini, H.B. Meyer and R. Sommer [ALPHA Collaboration], JHEP 10 (2007) 081 [0705.1809].

[99] J. Heitger and R. Sommer [ALPHA Collaboration], JHEP 02 (2004) 022 [hep-lat/0310035]; R. Sommer, hep-lat/0611020.

[100] M. Beneke and V.M. Braun, Nucl. Phys. B 426 (1994) 301 [hep-ph/9402364].

[101] S. J. Gates, M. T. Grisaru, M. Rocek and W. Siegel, Front. Phys. **58**, 1 (1983) [arXiv:hep-th/0108200].

[102] S. Weinberg, "The quantum theory of fields. Vol. 3: Supersymmetry," *Cambridge, UK: Univ. Pr. (2000) 419 p*

[103] N. Seiberg and E. Witten, Nucl. Phys. B **426**, 19 (1994) [Erratum-ibid. B **430**, 485 (1994)] [arXiv:hep-th/9407087]; N. Seiberg and E. Witten, Nucl. Phys. B **431**, 484 (1994) [arXiv:hep-th/9408099].

[104] N. Arkani-Hamed, F. Cachazo and J. Kaplan, arXiv:0808.1446 [hep-th].

[105] J. M. Drummond and J. M. Henn, JHEP **0904**, 018 (2009) [arXiv:0808.2475 [hep-th]].

[106] Z. Bern, L. J. Dixon and V. A. Smirnov, Phys. Rev. D **72**, 085001 (2005) [arXiv:hep-th/0505205]; L. F. Alday and J. Maldacena, JHEP **0711**, 068 (2007) [arXiv:0710.1060 [hep-th]].

[107] M. F. Sohnius, Phys. Rept. **128** (1985) 39.

[108] S. P. Martin, arXiv:hep-ph/9709356.

[109] L. Girardello, M. T. Grisaru and P. Salomonson, Nucl. Phys. B **178**, 331 (1981).

[110] V. V. Lebedev and A. V. Smilga, Nucl. Phys. **B** 318 (1989) 669; P. Kovtun and L. G. Yaffe, Phys. Rev. D **68**, 025007 (2003) [arXiv:hep-th/0303010].

[111] H. A. Weldon, Phys. Rev. D **26**, 2789 (1982); H. A. Weldon, Phys. Rev. D **26**, 1394 (1982).

[112] R. D. Pisarski, Nucl. Phys. A **498** 423 (1989); U. Kraemmer, M. Kreuzer and A. Rebhan, Annals Phys. **201**, 223 (1990) [Appendix]. D. Comelli and J. R. Espinosa, Phys. Rev. D **55**, 6253 (1997) [arXiv:hep-ph/9606438].

[113] V. S. Rychkov and A. Strumia, Phys. Rev. D **75**, 075011 (2007) [arXiv:hep-ph/0701104].

[114] N. Brambilla, J. Ghiglieri, A. Vairo and P. Petreczky, Phys. Rev. D **78**, 014017 (2008) [arXiv:0804.0993 [hep-ph]].

[115] J. P. Blaizot, A. Ipp, A. Rebhan and U. Reinosa, Phys. Rev. D **72**, 125005 (2005) [arXiv:hep-ph/0509052].

[116] P. Arnold, G. D. Moore and L. G. Yaffe, JHEP **0111**, 057 (2001) [arXiv:hep-ph/0109064].

[117] Y. L. Dokshitzer, Sov. Phys. JETP **46** (1977) 641 [Zh. Eksp. Teor. Fiz. **73** (1977) 1216].

[118] A. P. Bukhvostov, E. A. Kuraev, L. N. Lipatov and G. V. Frolov, JETP Lett. **41** (1985) 92 [Pisma Zh. Eksp. Teor. Fiz. **41** (1985) 77].

[119] L. V. Gribov, E. M. Levin and M. G. Ryskin, Phys. Rept. **100**, 1 (1983). See also, L. D. McLerran and R. Venugopalan, Phys. Rev. D **59**, 094002 (1999) [arXiv:hep-ph/9809427].

[120] R. D. Pisarski, Phys. Rev. D **47** (1993) 5589.

[121] J. M. Maldacena, Adv. Theor. Math. Phys. **2**, 231 (1998) [Int. J. Theor. Phys. **38**, 1113 (1999)] [arXiv:hep-th/9711200]; S. S. Gubser, I. R. Klebanov and A. M. Polyakov, Phys. Lett. B **428**, 105 (1998) [arXiv:hep-th/9802109]; E. Witten, Adv. Theor. Math. Phys. **2**, 253 (1998) [arXiv:hep-th/9802150].

[122] S. Caron-Huot, P. Kovtun, G. D. Moore, A. Starinets and L. G. Yaffe, JHEP **0612**, 015 (2006) [arXiv:hep-th/0607237].

[123] G. E. Arutyunov and S. A. Frolov, Nucl. Phys. B **544**, 576 (1999) [arXiv:hep-th/9806216].

[124] D. T. Son and A. O. Starinets, JHEP **0209**, 042 (2002) [arXiv:hep-th/0205051].

[125] Y. Hatta, E. Iancu and A. H. Mueller, JHEP **0801**, 063 (2008) [arXiv:0710.5297 [hep-th]].

[126] K. G. Wilson, Phys. Rev. **179**, 1499 (1969); K. G. Wilson and W. Zimmermann, Commun. Math. Phys. **24** (1972) 87.

[127] M. A. Shifman, arXiv:hep-ph/0009131.

[128] O. Aharony, S. S. Gubser, J. M. Maldacena, H. Ooguri and Y. Oz, Phys. Rept. **323**, 183 (2000) [arXiv:hep-th/9905111].

[129] I. R. Klebanov and E. Witten, Nucl. Phys. B **536**, 199 (1998) [arXiv:hep-th/9807080].

[130] A. Ceresole, G. Dall'Agata, R. D'Auria and S. Ferrara, Phys. Rev. D **61**, 066001 (2000) [arXiv:hep-th/9905226].

[131] L.D. Landau and E.M. Lifshitz, *Statistical Physics*, Part 1, 3rd Edition (Pergamon Press, Oxford, 1993).

[132] S. Caron-Huot, Phys. Rev. D **79**, 065039 (2009) arXiv:0811.1603 [hep-ph].

[133] S. Caron-Huot, M. Laine and G. D. Moore, JHEP **0904**, 053 (2009) [arXiv:0901.1195 [hep-lat]].

[134] S. Caron-Huot, Phys. Rev. D **79**, 125002 (2009) [arXiv:0808.0155 [hep-th]].